Non-parametric kinetic modeling of gas-solid reactions for thermochemical energy storage

by Felix Birkelbach

A thesis for the degree of
Doctor technicae

In the
Doctoral Program in Engineering Sciences – Mechanical Engineering

At the
Faculty of Mechanical and Industrial Engineering, TU Wien

Under the supervision of
Andreas Werner, TU Wien

Reviewed by
Luisa Cabeza, Universitat de Lleida

and
Franz Winter, TU Wien

Author
Felix Birkelbach
Matr. Nr.: 01026754
felix.birkelbach@gmx.at

Supervisor
Andreas Werner
TU Wien
Institute for Energy Systems and Thermodynamics
Getreidemarkt 9/E302
1060 Wien

Reviewers
Luisa F. Cabeza
Universitat de Lleida
Departement of Computer and Industrial Engineering
Carrer de Pere de Cabrera
25003 Lleida

Franz Winter
TU Wien
Institute of Chemical, Environmental and Bioscience Engineering
Getreidemarkt 9/E166
1060 Wien

Funding
This work was supported by Austrian Research Promotion Agency (FFG) within the framework of the projects Tes4seT (#845020), SolidHeat Kinetics (#848876) and SolidHeat Pressure (#853593).

Going to press
I confirm that going to press of this thesis needs the confirmation of the examination committee.

Affidavit
I declare in lieu of oath, that I wrote this thesis and performed the associated research myself, using only literature cited in this volume. If text passages from sources are used literally, they are marked as such.
I confirm that this work is original and has not been submitted elsewhere for any examination, nor is it currently under consideration for a thesis elsewhere.

Vienna, August 2020

Felix Birkelbach

Abstract

This thesis investigates modeling methods for the kinetics of gas-solid reactions in the context of thermochemical energy storage (TCES). Established modeling methods require either strong assumptions about the reaction under consideration, which can introduce modeling bias, or are limited to only two independent variables, which does not reflect the complexity of gas-solid reactions. In this thesis, a data-driven modeling method is developed: the TensorNPK (non-parametric kinetics) method. It does require no assumption besides the General Kinetic Equation and it can derive models in any number of variables from experimental data.

Through a literature study, a gap in the theory of gas-solid reaction kinetics is identified: the lack of validated models for the behavior in close proximity to the reaction equilibrium. The near-equilibrium kinetics are highly relevant for TCES because these processes need to operate as close to the equilibrium as possible to maximize efficiency. With the TensorNPK method, insights in the relevant kinetics can be gained without explicit models for near-equilibrium effects.

In collaboration with colleagues, the TensorNPK method was applied in kinetic studies of various materials relevant for thermochemical energy storage. The performance of the TensorNPK method in these studies is evaluated and implications for kinetic modeling are highlighted.

Kurzfassung

Diese Doktorarbeit befasst sich mit der Untersuchung von Modellierungsmethoden für die Kinetik von Gas-Feststoffreaktionen im Kontext von thermochemischer Energiespeicherung. Etablierte Modellierungsmethoden beruhen entweder auf starken Annahmen über die untersuchte Reaktion, was das Ergebnis verzerren kann, oder sie sind auf zwei unabhängige Variablen beschränkt, was die Komplexität von Gas-Feststoffreaktionen nicht abbilden kann. In dieser Arbeit wird eine datengetriebene Modellierungsmethode entwickelt: die TensorNPK (non-parametric kinetics) Methode. Sie benötigt keine Annahme abgesehen von der General Kinetic Equation und sie kann Modelle mit beliebig vielen unabhängigen Variablen aus experimentellen Daten generieren.

Mit einer Literaturstudie wird ein blinder Fleck in der Theorie zu Gas-Feststoffreaktionen identifiziert: Das Fehlen validierter Modelle, die das Verhalten der Reaktionen in der Nähe des Reaktionsgleichgewichtes beschreiben. Dieses Verhalten ist von großer Relevanz für thermochemische Speicherprozesse, weil sie so nahe am Gleichgewicht wie möglich arbeiten müssen um höchstmögliche Effizenz zu erreichen. Mit der TensorNPK Methode können Erkenntnisse über die Kinetik gewonnen werden, auch wenn keine expliziten Modelle für Effekte in der Nähe des Reaktionsgleichgewichts verfügbar sind.

In Zusammenarbeit mit Kollegen wurde die TensorNPK Methode in kinetischen Studien von mehreren Materialien, die für thermochemische Energiespeicherung relevant sind, eingesetzt. Die Performance der TensorNPK Methode in diesen Studien wird evaluiert und Implikationen für kinetische Studien werden hervorgehoben.

Acknowledgments

A lot of time, effort and energy goes into writing a doctoral thesis, so naturally I am very proud of *my* thesis. Though, a thesis is not thought up and then written in complete solitariness. On the contrary: Writing a doctoral thesis is a process that involves a lot of interaction with many people, all of whom having their share in the completion of the thesis. I count myself lucky that so many people accompanied me in this academic endeavor.

First and foremost, thanks are due to my supervisor Andreas Werner for his support during the last three years and for trusting me to pursue my own ideas. Also to Markus Deutsch, whose work served as a stepping stone for my thesis in many ways, for putting me on track with my research.

I would also like to thank the whole SolidHeat team Peter Weinberger, Franz Winter, Michael Harasek, Georg Gravogl, Christian Jordan, Saman Setoodeh Jahromy, Christian Knoll, Danny Müller and Clemens Huber for the collaboration in our joint research projects.

Meeting Henk Huinink and Leyla Söğütoğlu from the Technical University of Eindhoven was a stroke of luck. From you, I learned an awful lot about the physics behind the models that I had been using, and working with you has just generally been a delight.

A very special thank you to Eva, Georg, Veri and Florian for proof-reading this thesis. Your feedback helped me straighten out some muddled passages and smooth over some rough edges of my writing. Thank you also for all the enlightening discussions and for sharing my enthusiasm for nerdy stuff that most others would only frown upon.

The last three years at the institute would have been dire, if it wasn't for my amazing colleagues Stelio, Viktoria, Stefan, Paul, Verena, Gregor, Lukas, Nina and Johannes. Be it joking during coffee breaks or letting off steam while enjoying an after-work beer. Your companionship has made my pre-doc years a time that I will look back at with nostalgia.

Last, though maybe most importantly: A big thank you to my family for your unconditional support that I can always count on; and to all my friends, room mates, climbing partners and fellow activists for all the encouragement and for sometimes just listening patiently while I ramble on about my research.

Kinetic models are like weather forecasts.
We need them but they are just wrong
too often to really rely on them.

Contents

List of Figures

Nomenclature

Acronyms

CFD	computational fluid dynamics
DSC	differential scanning calorimetry
GC	gas chromatography
GKE	General Kinetic Equation
ICTAC	International Confederation for Thermal Analysis and Calorimetry
IEA	International Energy Agency
IPCC	Intergovernmental Panel on Climate Change
NPK	non-parametric kinetics
TCES	thermochemical energy storage
TES	thermal energy storage
TGA	thermo-gravimetric analysis
REDOX	reduction-oxidation
TRL	technology readiness level
XRD	X-ray diffraction

Greek symbols

α	conversion	
$\boldsymbol{\gamma}_{k,i}$	interpolation vector	
γ_{k,i,j_i}	element of $\boldsymbol{\gamma}_{k,i}$	
$\mathrm{d}\alpha/\mathrm{d}t$	conversion rate	1/s

Subscripts

i	index for dimensions

j	index for elements	
j_i	index of an element in dimension i	
$j_i^\ddagger$	index of the first interpolation element in dimension i	
j_i^*	index of the reference element in dimension i	
k	index for data points	

Roman symbols

Cov	covariance	
D	number of dimensions	
$f(\alpha)$	effect of conversion, reaction model	
$\boldsymbol{f}_i$	effect vector containing the values of $f_i(v_i)$	
f_{i,j_i}	element of $\boldsymbol{f}_i$	
f_{i,j_i^*}	reference element of dimension i	
$f_i(v_i)$	effect of v_i	
$\hat{f}_{k,i}$	conversion rate of data point k projected in dimension i	
$h(\dots)$	effect of driving force	
$\boldsymbol{J}$	Jacobian	
K	scaling factor of reduced model	
$k(T)$	effect of temperature	1/s
MSE	mean square error	
p	partial pressure of gas	Pa
p_{eq}	equilibrium partial pressure of gas	Pa
$\boldsymbol{r}$	vector of residuals	
R_k	conversion rate of data point k	
$\hat{R}_k$	conversion rate estimate for data point k	
$\hat{R}_k^{\setminus i}$	conversion rate estimate for data point k excluding the effect of dimension i	
r_k	residual of data point k	
T	temperature	K

t	time	s
$\mathcal{T}$	model tensor	
Var	variance	
$\boldsymbol{v}_i$	variable vector containing the values of v_i	
v_i	independent variable	
v_{i,j_i}	element of $\boldsymbol{v}_i$	

Research summary

This chapter provides the backdrop for the publications that are at the heart of this thesis by publications. It starts out with the big picture, pointing out the global challenges that we are facing, and then narrows in on the more specific context of this thesis. Key concepts, like thermochemical energy storage and reaction kinetics, are introduced and the state of the art is discussed. Based on this discussion, the motivation for this thesis is presented, and the problem statement is formulated.

In Section 4, I describe the research that ultimately led to the publications that constitute the main part of this thesis. The links between the papers are discussed and the most important findings are highlighted.

Finally, the findings of my research are synthesized in Section 5. Conclusions are drawn and areas where further research is needed are identified.

1 Introduction

We are living in the beginning of a new geological epoch: the Anthropocene. It is the epoch, where human activity started having a profound impact on our planet. The anterior epoch, the Holocene, has been a relatively stable epoch of about 11 700 years. In this epoch humanity developed, and as such it is the only state of earth that we know for certain can support human society as we know it. Now human activity is threatening to destabilize the earth system and the consequences are unforeseeable (Steffen et al. 2015). While this might sound devastating, there is no need for defeatism. Even though it seems we are currently threatening our own basis of life, we also do have the power to turn things around by taking the necessary actions.

The intensity with which we are pushing at earths boundaries is maybe best illustrated by the World Overshoot Day. It marks the day at which we consumed earth's biocapacity for a year. For the EU it has been calculated to be May 10th in 2019 (WWF 2019). This means that we are depleting the ecosystem at a much faster rate than it can be renewed. With our current mode of production, we are consuming an equivalent of 2.8 earths each year.

Another significant marker for human activity is energy consumption, which is rising exponentially since the industrial revolution. Western countries are responsible for most of this increase, and emerging countries seem to be determined to follow a similar trajectory. Today, our main energy sources are non-renewable sources, specifically coal, crude oil and natural gas, which amount to over 80 % of total energy supply (IEA 2019). This puts massive strain on earth's resources and has been causing irreparable environmental destruction for decades (Meadows 1974). Not only are we depleting resources on a never before scale — the emission of CO_2 and other greenhouse gases is also driving global warming, which will have disastrous consequences (IPCC 2018). Some consequences are already manifesting, like increased frequency and intensity of droughts and floodings (IPCC 2012); many more are expected to manifest during the next decades. Ironically, developing countries that consume comparably little energy, are the ones most affected by global warming.

The only way to mitigate more disastrous consequences of climate change is to reduce the consumption of non-renewable energy drastically. The Intergovernmental Panel on Climate Change (IPCC) projected that only by keeping global warming below 1.5 °C, dangerous tipping points can be avoided (IPCC 2018). Reaching the 1.5 °C-goal would imply to approach net-zero greenhouse-gas emissions by 2040, according to the International Energy Agency (IEA 2016b). Yet, the IEA's prediction of future energy consumption (IEA 2016b) shows deeply distressing trends: even if all planned climate protection policies were adopted (*new policies* scenario), the CO_2 emissions would continue to rise. Given these predictions, reaching net-zero emissions ever seems to be utopian.

It is evident that to curb global warming and prevent disastrous consequences of climate change, we need to abandon our current reckless energy system that is rooted in unsustainable exploitation of earths resources. In its stead, we need to implement an energy system that is not only sustainable, but also more democratic and just — both globally and regarding future generations (Greenpeace 2015).

This radical change of our energy system will require a joint effort on all levels, including governments, industry and the people. Science will have to analyze the situation critically and provide solutions to the technological challenges ahead.

From the point of view of technology, there are three main levers to change our energy system:

Reducing the overall energy consumption. Especially in industrialized countries, which have the highest per-capita energy consumption today, this will without doubt be necessary, even if it means to restructure our economic system and maybe do without some conveniences that we got used to. In countries with very low per-capita consumption and low standard of living the energy consumption will have to continue rising, until they catch up in standard of living with the developed nations. For these countries the goal must be to transition to renewables directly, without repeating the mistakes of today's industrialized nations. This is often referred to as "leap frogging" (Watson et al. 2011). To manage this transition in industrialized, emerging and developing countries alike, effective regulations will be required (Abdmouleh et al. 2015). For example, certain unsustainable energy sources and technologies could be prohibited or an adequate price could be put on externalities such as pollution and resource consumption so that it reflects the true cost (IEA 2016a).

Increasing the share of renewable sources. The capacity of renewable sources must be increased rapidly, as their fossil counterparts are decommissioned. The International Renewable Energy Agency (IRENA 2019b) estimates that the total share of renewable energy would need to increase from 14 % today to 65 % by 2050 to keep global warming well below 2 °C. The main challenge with most renewable sources is their volatility. Unlike fossil energy carriers like coal, oil and natural gas, the precursors for renewable sources, such as sunlight and wind, cannot be buffered to provide energy on demand. To match volatile supply with demand, energy storage solutions are required. Also, the availability of renewable energy sources varies widely by region, so that tailored, decentralized solutions need to be employed (IRENA 2019a).

Increasing the efficiency of energy use/conversion. Or in other words: minimizing waste energy. This does not necessarily imply increasing the efficiency of one specific process, but can also mean taking a holistic approach to energy systems. By coupling energy flows to reuse the excess energy of one process as input to another process, the use of primary energy input can be reduced significantly. Just as with renewable energy sources, one of the main challenges is that waste energy sources and suitable energy sinks are often separated in time and/or space. To reuse excess energy, tailored energy storage and/or transfer solutions need to be implemented.

We need to act on all three of these levers quickly, in order to achieve the CO_2 reduction goal and to curb global warming. On the one hand, we need to change our unsustainable economic practices, and on the other hand, a wide range of new technologies will be required that supersede the fossil-fuel heavy technologies of today. For some applications, sustainable solutions are already available and can be deployed immediately. For many other applications new technologies still have to be developed, and innovative solutions to the technological challenges ahead have to be found.

2 Context

In the transition to a sustainable energy system, energy storage technologies will play a key role to enable both large-scale renewable power generation and to increase energy efficiency. Technically, energy can be stored in any form — be it electricity, mechanical work or heat. The best suited type of energy storage is determined by the excess energy source and the target energy sink. The goal is to provide the required storage capacity while minimizing conversion and storage losses.

The type of energy storage that we are most familiar with are electric batteries, as they are integrated in many devices that we use on a daily basis. Until recently, electric batteries could only be used for small devices like mobile phones and watches because battery capacity and power was limited. Recent advances in battery technology have enabled it for applications that require considerably larger storage capacity and power, such as electric vehicles or domestic photo voltaic installations. Ongoing research will allow battery storage to be applied on an even larger scale, for example the electricity grid. The IEA (2018) projects that battery storage will account for almost as much capacity as pumped hydro by 2040. In this way, batteries will contribute to grid stability and integration of renewables.

Another type of energy storage is thermal energy storage (TES). These devices are often referred to as heat batteries, in analogy to electric batteries. TES has a special role due to the limited convertibility of heat to other types of energy. The maximum conversion efficiency is determined by the temperature levels of the conversion process and is known as the Carnot efficiency. Due to this limitation, it is often more efficient to store heat directly instead of converting it to a more “pure” form of energy. Especially for applications that require a heat input, TES is often more efficient than other energy storage technologies.

An illustrative example for an application that requires TES is a concentrated solar power (CSP) plant (Liu et al. 2016; Pelay et al. 2017). Similarly to most other caloric power plants, CSP plants use a steam cycle to convert heat into mechanical work and then to electricity. Provided that there is sufficient irradiation (i.e. a lot of sunshine) to operate a CSP plant, it is a renewable alternative to coal, gas and nuclear power plants. The main implementation barrier is that its electricity production is coupled to the irradiation, i.e. electricity production peaks at noon and drops to zero at sunset. To decouple electricity production from sunshine, energy has to be buffered during the day. In principle, this can be done in two ways: either by using batteries to store electricity or by employing a TES system to store heat and drive the steam cycle during the night. One of the main challenges with electric batteries is the use of rare earths such as lithium. If no substitute for these rare resources can be found or highly efficient recycling strategies are developed, it might inhibit the deployment of electric batteries for large-scale applications such as power plants. TES on the other hand uses abundant materials to store heat and it scales very well for large-scale applications. For this reason, TES is already employed in CSP plants today. It is a key technology that enabled large-scale CSP plants as alternative to non-renewable power plants.

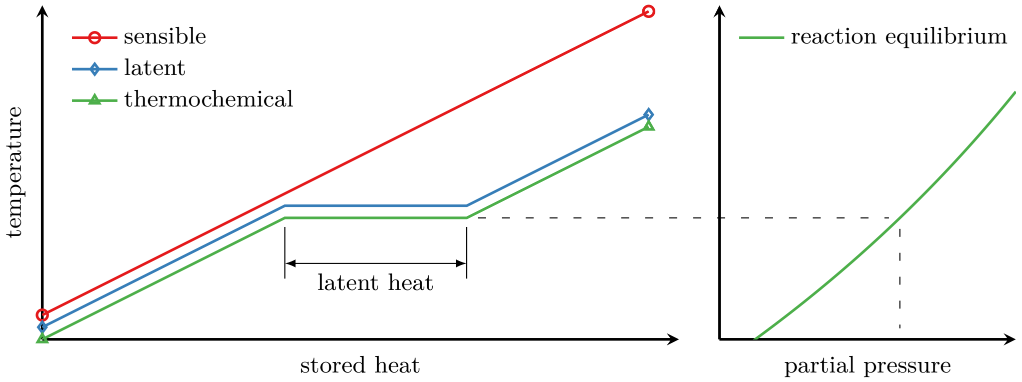

Figure 1: *Illustration of the thermal characteristic of sensible, latent and thermochemcial energy storage (left) and the effect of partial pressure on the reaction temperature for gas-solid reactions (right).*

Another example are industrial processes, where excess heat from a high temperature process is used to power a lower temperature process. By cascading processes that work on different temperature levels, a lot of primary energy input can be saved (Miró et al. 2016; Forman et al. 2016). If the two processes do not operate simultaneously, the excess heat has to be buffered in a TES system to match heat supply with demand. This TES application is especially relevant in energy intensive industries that employ batch processes like iron and steel.

Typical requirements for TES are high capacity/scalability, high energy density/ compact design, small storage losses, suitable operating temperature for the application at hand, high gradients to enable dynamic operation, no hazardous substances as well as economics of the device and the whole process (Sterner et al. 2018).

Three main types of TES are distinguished, based on the thermal characteristic of the storage material: sensible, latent and thermochemical energy storage. Their typical characteristics are illustrated in Figure 1.

Sensible energy storage utilizes the heat capacity of an inert substance to store heat. Commonly used materials are water, concrete, rock and sand. The stored heat is proportional to the temperature difference between the low and the high temperature level (red —○— line in Figure 1). To minimize storage losses, good insulation is required, since temperature differences between the storage and its surrounding are typically large. Widely used storage devices of this TES type are stratified storage tanks and concrete storage.

Latent energy storage exploits the phase change effect, typically solid-liquid or solid-solid, of certain materials. During the phase change, the material absorbs heat equal to its phase change enthalpy without changing its temperature (horizontal part of the blue —◇— line in Figure 1). In this way, a large quantity of heat can be stored in a very narrow temperature interval. The phase change temperature is a property of the material and usually fairly constant. With latent energy storage, heat can be absorbed and supplied at approximately constant temperature, which has many advantages for process design. A limiting factor is heat transfer in the solid phase, and dilatation is often a problem.

Thermochemical energy storage refers to all types of TES systems, where two substances interact with each other. The mechanisms range from physical adsorption to reversible chemical reactions. During the sorption process latent heat is released, equal to the enthalpy of the underlying process (horizontal part of the green —△— line in Figure 1). This allows to store a large quantity of heat in a narrow temperature interval, similarly to latent heat storage. In contrast to latent heat storage, the reaction temperature is not a material property, but depends on the reaction conditions. In the right-hand diagram in Figure 1 this is illustrated for a thermochemical process based on gas-solid reactions, where the temperature of heat release/uptake depends on the pressure of the reactant gas. Controlling the reaction conditions allows for more flexibility of the process and opens up the possibility of using different temperature levels for charging, storing and discharging. The specific characteristics vary greatly between different substances. Thus, individual processes have to be developed for each application and reaction system. Typical issues are low cycle stability and complex process design. Its main advantages are the high storage density and nearly loss-less long-term storage at ambient conditions.

It is evident that each TES type has its advantages and disadvantages. While sensible energy storage is the most straight forward TES solution, the added flexibility of thermochemical energy storage could make TES viable for more complex applications.

In our effort to make our energy system more sustainable, energy storage demand will rise significantly in the next couple of years. Even though the IEA (2018) projects that most of this storage demand will be covered by electric batteries, there are a multitude of applications where TES would be the better match. The main advantages of TES are that it requires mostly abundant materials, that it can be built at large scale and that conversion losses can be kept at a minimum if heat is required as input. Doubtlessly, TES will play an important role in our future energy system — even more so, if the implementation barriers of thermochemical energy storage can be overcome and its potential is realized.

2.1 Thermochemical energy storage

The term thermochemical energy storage (TCES) encompasses storages based on all types of sorption processes, from physisorption (e.g. zeolites) to chemisorption with various kinds of reversible reaction systems. In this work reversible gas-solid reactions are covered. They are in the focus of most research efforts because they enable high storage densities and because the two reactants can be separated easily.

Thermochemical storage reactions typically follow a reaction equation of the type

$$\mathrm{A(solid)} + \mathrm{B(gas)} \rightleftharpoons \mathrm{AB(solid)} + \mathrm{heat}\,. \qquad (1)$$

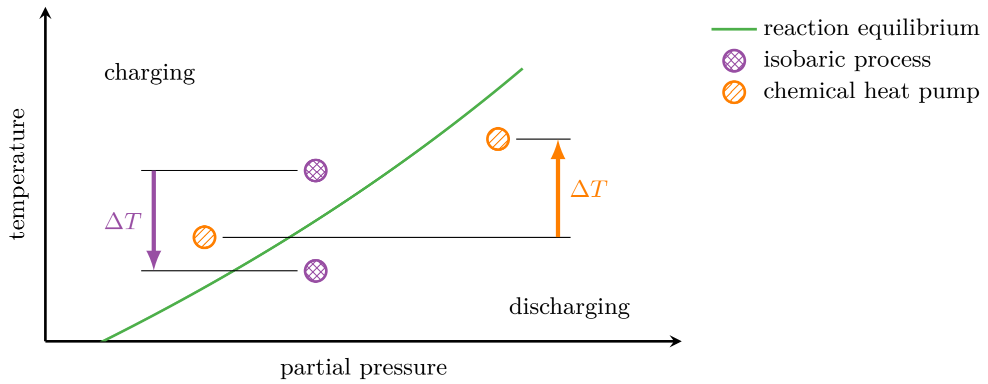

Figure 2: *Operating modes of a thermochemical energy storage.*

When the solid and the gas are brought into contact the reaction starts. The substances form a compound and heat equal to the reaction enthalpy, a property of each reaction system, is released. Since these enthalpies are typically quite large, the storage density of TCES is high. To revert the reaction, i.e. to separate the gas from the solid, the same amount of heat has to be supplied. By storing the two substances separately, the reaction can be inhibited and theoretically loss-less storage for unlimited time can be realized.

In reversible reactions both the forward and the reverse reaction take place at the same time. When the forward and the reverse reaction proceed at the same speed, the net conversion of molecules is zero and the system is said to be in equilibrium. The reaction equilibrium is a characteristic property of a reaction system. It determines the temperature range, in which the system can be used for TCES applications. By controlling the partial pressure in a TCES reactor, the temperature of heat uptake and release can be influenced. This is illustrated in the right-hand diagram in Figure 1. The higher the partial pressure, the higher the equilibrium temperature.

If the reaction conditions are such that the system is not in equilibrium, one reaction will proceed faster than the other. Conversion will occur and the reaction will proceed until all reactants are converted to products. At low temperatures and high partial pressures, the formation (discharging) reaction is favored and heat is released. At high temperatures and low partial pressures, the decomposition (charging) reaction is favored and heat is consumed.

In TCES, heat is released by mixing the two substances at a temperature below the equilibrium temperature. To charge the storage, the temperature has to be raised above the equilibrium temperature. Since the reaction rate is zero at the equilibrium, charging and discharging processes need to operate at a certain distance from the equilibrium to achieve sufficiently fast reaction rates (purple ⊗ markers in Figure 2). For this reason, the discharging temperature is generally lower than the charging temperature at constant pressure, which leads to a loss of “heat quality” in a storage cycle.

The temperature difference between the charging and the discharging process can be reduced by operating the discharging process at higher partial pressures than the charging process. If the pressure difference is sufficiently large, even positive temperature differences can be realized (orange ▨ markers in Figure 2). This concept is referred to as chemical heat pump.

Changing the partial pressure allows to operate the storage process in a way that would not be possible with sensible or latent thermal energy storage. On the other hand, the performance of TCES can deteriorate significantly if the partial pressure is not controlled. If reactant gas is not supplied fast enough during discharging, the partial pressure in the reactor might drop and the discharge temperature might decrease. During charging, if the gas is not removed efficiently from the reactor, the decomposition reaction might be very slow or even inhibited.

Even though the effect of temperature and partial pressure on the reaction is qualitatively the same for all gas-solid reaction systems, there are considerable differences among different reaction systems. Additionally, temperature and partial pressure in the reactor are also affected by mass and heat transport. For this reason, reactors and processes have to be designed specifically for each reaction system and the application at hand.

The basic working principle of TCES has been known at least since the 9th century. In one of his books, the alchemist Rasis (also Rhazes, al-Razi) describes an experiment, where an egg is cooked by pouring water over quicklime (Thorndike 1923, p. 784). When the water gets into contact with quicklime, an exothermic reaction is triggered that heats the water and boils the egg. The first modern application of TCES dates back to the 1880s, when some vehicles that generated steam by dissolving NaOH (sodium hydroxide) were operated in Germany: a river boat on the Spree, a street car in Berlin and Charlottenburg as well as a railway locomotive on the track between Jülich and Aachen (Beckmann et al. 1984, p. 17). Though, the technology did not catch on and TCES with NaOH fell out of use.

Today, TCES technology is considered to be on a fairly low technology readiness level (TRL) compared to sensible and latent TES. No thermochemical heat storages are currently in operation. Most research efforts are being made on TRL 3 (experimental proof of concept) and TRL 4 (validation in lab). At the time of writing of this thesis, there are two projects that are trying to push their TCES systems to TRL 6: the CREATE project[1], which aims to develop and demonstrate a heat battery based on salt hydrates for seasonal storage in buildings, and the SCORES project[2], which focuses on a Power-to-Heat concept based on a REDOX (reduction-oxidation) system; also for domestic applications.

Some research projects are currently testing components in the lab, such as solar kilns with Cu_2O/CuO (cuprous oxide/cupric oxide) for application in concentrated solar power plants (Neises et al. 2012), a fixed bed reactor with $SrBr_2/SrBr_2 \cdot H_2O$ (strontium bromide/strontium bromide mono hydrate) for industrial waste heat management (Stengler et al. 2020) and a fluidized bed reactor with $CaO/Ca(OH)_2$ (calcium oxide/calcium hydroxide) also for industrial waste heat management (Angerer et al. 2018).

$CaO/Ca(OH)_2$ is probably to most extensively studied reaction system today. Starting

---

[1] EU Horizon 2020 grant No. 680450, `www.createproject.eu`

[2] EU Horizon 2020 grant No. 766464, `www.scores-project.eu`

from detailed kinetic identification (Schaube et al. 2012), over concepts for improving the thermal conductivity and mass transport in packed beds through honey comb support structures (Funayama et al. 2020) and semi-permeable encapsulation of particles (Afflerbach et al. 2017), to system level simulations (Risthaus et al. 2020).

Most research efforts in TCES still focus on the detailed identification of prospective substances, such as the cycle stability of $CaC_2O_4/CaC_2O_4 \cdot H_2O$ (calcium oxalate/calcium oxalate mono hydrate) at a milligram scale (Knoll et al. 2017), near-equilibrium effects of various salt hydrates (Söğütoğlu et al. 2019) and high pressure carbonation of metal oxides (Gravogl et al. 2019) — to name just a few. Important characteristics include the heat of reaction, viable temperature intervals, cycle stability and the kinetics at process conditions. An overview over experimental characterization methods for thermochemical materials can be found in (Kato et al. 2019).

A considerable amount of research effort has also been dedicated to identifying potential applications for TCES. Typical low-temperature applications ($< 100\,°C$) include tap water and room heating (Scapino et al. 2017), industrial waste heat recovery applications are situated across the whole temperature range (Miró et al. 2016) and high-temperature applications ($> 800\,°C$) include concentrated solar power (Prieto et al. 2016). Even tough the temperature levels and other requirements of these applications vary widely, there is a plethora of potential reaction systems that could meet the demands of almost any application (Deutsch et al. 2016). The most relevant groups include salt hydrates with a typical temperature range between 40 and 300 °C (Donkers et al. 2017), metal hydroxides between 150 and 900 °C, carbonates between 600 and 1200 °C and REDOX systems between 800 and 1500 °C (Bulfin et al. 2017).

Bottom line, TCES systems are available for virtually any temperature level and application. The main advantages are high energy densities, almost loss-less long-term storage and that the reaction temperature can be controlled by changing the partial pressure of the gas. Challenges include the low TRL, i.e. the lack of off-the-shelf components and mature reactor and process concepts as well as our crude understandig of the effects on the material scale. If the existing implementation barriers can be overcome, TCES could be a key technology to facilitate large-scale use of renewable energy and to reduce the primary energy demand in domestic heating and industry.

2.2 Reaction kinetics of gas-solid reactions

Chemical kinetics is the study of the reaction rate and how it is influenced by reaction conditions. Generally, chemical kinetics are divided into micro- and macro-kinetics. The latter include heat and mass transport, while the former do not. The micro-kinetics are considered to be more universal, because they do not depend on the macroscopic configuration of the reaction system. The goal of a kinetic study of a specific reaction is to identify and understand its micro-kinetics, but unfortunately they are notoriously elusive. For reactions involving solids, they might even be non-existent because the chemical kinetics can not be fully separated from the physical effects at the gas-solid interface.

In gas-solid reactions, the reactants cannot mix indefinitely. The reaction takes place on a reaction interface in the solid, and the advancement of the reaction front as well as mass transfer between the phases has to be considered. Additionally, the particle morphology and the lattice configuration of the solid will also affect the reaction rate. Because of the multitude of processes that take place during a gas-solid reaction, kinetic studies of gas-solid reactions are very empirical with little first-principle theory to rely on.

Interest in chemical kinetics is twofold: First, the kinetics provide insight into the reaction mechanism and, thus, further our fundamental understanding of the reaction. Second, the kinetics have to be known for reactor and process design to estimate reaction rate under process conditions. The viability of a reaction system for a given application with a given temperature range is not only determined by the reaction equilibrium as discussed in the previous section. Even if the reaction is thermodynamically favored, i.e. if the thermodynamic conditions are such that the reaction can proceed, the reaction rate might be so slow that no noticable conversion can be achieved in a reasonable amount of time. In that case the reaction is said to be kinetically inhibited. To evaluate the potential of a reaction system, detailed knowledge of the kinetics under process conditions is required.

As a frame to describe and interpret chemical kinetics, kinetic models are employed. They define how we see the processes of chemical conversion. Without kinetic models, the kinetics could not be grasped because of the multitude of processes taking place simultaneously. By casting experimental data into models, we can check for systematic relationships between variables and identify underlying mechanisms or just represent the kinetic information in a systematic manner.

Some kinetic models describe the most relevant processes that determine the reaction kinetics separately. Typically, the reaction is assumed to consist of three consecutive steps: mass transfer through the boundary layer, diffusion through the particle and the chemical reaction itself. The overall rate is then the reciprocal sum of the individual rates of each process (Yagi et al. 1955). This class of models is frequently used in coal combustion. A characteristic feature of these models is that they seek to relate the rate to structural parameters of the reactants, like particle size, porosity and diffusion constants. Prominent models of this class include the Grain Model (Szekely et al. 1970) and the Random Pore Model (Bhatia et al. 1981). A review of solid-state phase transformation kinetics models and modeling recipes has been published by Liu et al. (2013).

Often it is not feasible, if even possible, to model the specific processes taking place during the reaction. Issues range from identifying the rate limiting processes and selecting appropriate models for each process to collecting sufficient data to calibrate these models. Then, a more simplistic approach should be employed. The most common simplification is the single-step approximation. It is based on the assumption that one of the processes is significantly slower than all the other ones. If the assumption holds, this process determines the overall rate of the reaction and is referred to as the rate limiting step.

The single-step approximation has its roots in homogeneous reaction kinetics. If only one elemental step is rate limiting, the analytically derived formulas for elementary reactions can be used to calculate the reaction rate of complex reactions. The single-step approximation formula for gas-solid reactions was designed in analogy to kinetic models of homogeneous reactions and extended by a term to take effects in the solid phase into account. The conversion rate $\mathrm{d}\alpha/\mathrm{d}t$ is typically modeled as the product of three independent effects:

$$\frac{\mathrm{d}\alpha}{\mathrm{d}t} = f(\alpha)\,k(T)\,h(p, p_{\mathrm{eq}})\,. \tag{2}$$

Here, $f(\alpha)$ is the effect of the conversion α, $k(T)$ the effect of temperature T and $h(p, p_{\mathrm{eq}})$ the effect of the driving force, usually expressed as a function of the partial pressure p and the equilibrium pressure p_{eq}. This formula is referred to as the General Kinetic Equation (GKE). It is by far the most commonly applied formula in kinetic modeling (Vyazovkin et al. 2011). Essentially, it is a synthesis of solid-state and homogeneous reaction rate models.

The effect of the advancement of the reaction front has been extensively studied in solid-state kinetics. Based on simplified geometric considerations, the effect of the advancement of the reaction front f can been derived as a function of the reaction progress α (Brown et al. 1980, p. 6). These models can be divided into nucleation, interface and diffusion models (Khawam et al. 2006). Sometimes "reaction order" models are employed, which imply that the concentration of the solid affects the reaction rate. This has no physical foundation and reaction order models are thus purely empirical. The main assumption behind $f(\alpha)$ models is that the reaction path does not depend on either reaction conditions or time. Some researchers argue that this is too much of a simplification and have developed more sophisticated reaction models for use with the GKE (Pijolat et al. 2011; Pijolat et al. 2018).

The functional form of $k(T)$ is usually assumed to be of Arrhenius type, even though it has been shown, that the assumptions that the Arrhenius equation is based on do not hold for reactions involving solids (Galwey et al. 2002; Galwey 2003a). Regardless, the Arrhenius equation tends to describe gas-solid reactions very well. For this reason it is widely used despite the lack of theoretical justification (Brown 1997). It has been suggested that, since the Arrhenius equation has to be regarded empirical, one might as well resort to completely empirical equations for $k(T)$, which are easier to handle mathematically (Flynn 1997). Also, an alternative theory to the Arrhenius approach, the "Congruent Dissociative Evaporaton", has been proposed (L'vov et al. 2013), but neither of these two suggestions did catch on.[3] At the moment, the Arrhenius equation seems to be firmly established in the field.

Very little literature is dedicated to the driving force term, and as a consequence it is used very inconsistently. The most common form is $h(p, p_{\mathrm{eq}}) = 1 - p/p_{\mathrm{eq}}$, which seems to have been developed in analogy to the concentration term in homogeneous reaction models and was introduced to modern day kinetics via the work of Šesták (2005). It

---

[3] There is a strange dispute going on between L'vov and the mainstream kinetic community represented by the ICTAC (International Confederation for Thermal Analysis and Calorimetry). While the ICTAC encourages the use of the Arrhenius equation despite its lack of theoretical justification, L'vov published his Congruent Dissociative Evaporation theory in the late 80s and continues to publish frequently on the topic. The ICTAC seems to neither approve nor reject his theory. They simply ignore it — very much to the frustration of L'vov (L'vov 2017).

functions as an accommodation term to incorporate the effect of the reverse reaction into the kinetic model. In most kinetic studies the driving force term is simply omitted (Vyazovkin et al. 2011). The underlying assumption is that the reaction takes place “sufficiently far” from the equilibrium. For TCES accurate driving force terms are highly relevant since TCES processes usually operate in close proximity to the equilibrium for maximum efficiency.

If not the chemical reaction but one of the physical processes taking place during the reaction is rate limiting, the GKE could still be employed, but the terms would assume completely different forms (Goodell et al. 1983). Only little research has been dedicated to this topic in kinetic analysis. Though, kinetic models of gas-solid reactions could benefit from this broadening of the scope, since the chemical micro-kinetics cannot be fully separated from the physical processes taking place during the reaction.

When using models based on the GKE, one has to be aware of the underlying assumptions and its limitations, because there are a lot of them. These shortcomings have been discussed thoroughly (Šimon 2007; Brown 2005; Galwey 2004; Maciejewski et al. 1987). In the end, the GKE is not a law of nature, but an empirical formula. Even if its not completely accurate, it is a rather useful lens for looking at gas solid reactions. It is simple enough to make kinetic data interpretable while also allowing for enough complexity to capture manifold processes that take place and interact in a gas-solid reaction.

2.3 Modeling methods for gas-solid reaction kinetics

The task of kinetic modeling methods is to calibrate kinetic models with experimental data. However, kinetic modeling includes some additional preliminary steps: deciding on the model purpose, selecting a model, collecting experimental data and preparing the data for processing with the modeling method.

The very first step in modeling is to decide on the purpose of the model. Two main purposes can be distinguished in kinetic modeling: kinetic analysis and kinetic predictions. In kinetic analysis, the goal is to get fundamental insight into the reaction mechanism. For kinetic predictions, the prediction accuracy in the relevant parameter range is most important. Depending on the purpose, a suitable model has to be chosen. For kinetic analysis, models with a strong theoretical foundation are needed, so that they can be interpreted mechanistically. For kinetic predictions, the requirements on the model are less stringent. Empirical formulas, accommodation factors and other heuristic approaches can be used freely.

In the previous section various types of kinetic models were discussed. Here, I will cover only modeling methods that are based on the General Kinetic Equation (GKE), which has been described in detail in the previous section. The GKE strikes a good balance between a strong theoretical foundation and sufficient leeway for heuristic approaches. For this reason the GKE is well suited for both kinetic analysis and kinetic predictions. For kinetic analysis, the assumptions that the GKE is based on need to be kept in mind. Only then, the GKE can be interpreted mechanistically.[4]

The basis for all kinetic models is reliable kinetic data. The most relevant group of experimental methods for collecting kinetic data of thermally induced reactions is called thermal analysis. Data is obtained by monitoring the reaction of a substance sample under controlled conditions (Vyazovkin et al. 2014). Unfortunately the chemical reaction rate cannot be measured directly. Information on the reaction has to be distilled from quantities that are indicators for the reaction progress such as mass-change (thermogravimetric analysis, TGA), heat flow (differential scanning calorimetry, DSC) or product gases (gas-chromatography, GC). Another approach for some reactions is to monitor the lattice configuration of the solid (X-ray diffractometry, XRD).

Extensive pre-processing is necessary to extract kinetic information from the measured signal. An illustrative example is the measured heat flow during heating of a sample in a DSC instrument. The signal is a superposition of the heat of reaction and the sensible heat uptake of the sample and crucible. Consider XRD as another example: To determine the share of reacted solid from the XRD pattern, the measured pattern has to be compared to the patterns of pure substances in a database. An algorithm then determines the composition of the sample. In both cases, we rely on a set of assumptions and extensive computations to obtain the kinetic information. These computations are a critical step in the kinetic modeling process because they determine the accuracy of the kinetic data.

To standardize the treatment of kinetic data irrespective of the measurement method, the measured values are usually converted to conversion values by considering the stoichiometry of the reaction. The conversion is a measure for the reaction progress from 0 (all solid substance in initial configuration) to 1 (solid substance converted completely). For multi-step reactions the definition of conversion is challenging since the progress of each reaction step has to be taken into account.

Generally, the more detailed a kinetic model is, i.e. the more effects are included, the more experiments at different reaction conditions are required. Today, the consensus is that at least three experimental runs should be used and that kinetic studies based on only one experiment are unreliable (Vyazovkin et al. 2011; Burnham 2017).

A comprehensive review of modeling methods for single-step reactions has been compiled by the ICTAC (International Confederation for Thermal Analysis and Calorimetry) and published by Vyazovkin et al. (2011). Most methods for modeling gas-solid reactions according to the GKE have two things in common: they neglect the pressure/driving force term and they presuppose the validity of the Arrhenius equation (Vyazovkin et al. 2011). Then, the kinetic identification of the reactions boils down to the identification of the kinetic triplet: the reaction model, the pre-exponential factor and the apparent activation energy.

Historically, one of the first methods for modeling the kinetics of gas-solid reactions with the GKE was the Kissinger method (Kissinger 1956). Kissinger showed that the activation energy can be determined from a series of constant-heating-rate experiments by identifying the temperature where the conversion rate peaks. The main advantage of the method is that the activation energy can be determined without having to assume

---

[4] Some scientists have not been very rigorous in that respect, which is why there have been heated debates on that topic (Galwey 2004; Brown 2005; Šesták 2017).

a reaction model and that very few calculations are required. Today, the method has fallen out of use because it is very sensitive to shifts in the conversion rate peaks and consequently to experimental error. Also, the scope of the Kissinger method is limited because of the assumptions that it is based on (Vyazovkin et al. 2011).

Around the same time, "model-fitting" methods were developed. By assuming a reaction model, the Arrhenius plot can be constructed and the Arrhenius parameters can be determined by fitting a straight line. Whichever reaction model leads to the most linear Arrhenius plot, i.e. to the smallest error when fitting the regression line, is deemed to be the correct one. These model-fitting methods exist in differential and integral variants. Today, these methods have fallen out of use, due to their poor performance of discriminating different reaction models and the wide range of activation energy values they produce (Vyazovkin et al. 1999; Maciejewski 2000).

The largest group of modeling methods are the isoconversional methods. A recent review of isoconversional methods has been published by Vyazovkin (2018). The best known isoconversional methods are the Friedmann and Ozawa-Flynn-Wall methods. With isoconversional methods, the activation energy can be determined without interference of a reaction model choice. For this reason these methods are often labeled "model-free". However, this label is quite misleading because isoconversional methods are of course not free of models — they are based on the GKE and the Arrhenius equation.

The central idea behind isoconversional methods is to fit the Arrhenius equation at constant conversion to obtain the activation energy as a function of conversion. If the activation energy is constant over the whole conversion range, the single-step assumption holds. Then, the activation energy can be used to construct a master plot for determining the most likely reaction model (Vyazovkin et al. 2011). Using a masterplot for identifying the reaction model is deemed more reliable than the model-fitting approaches described in the previous paragraph, because the activation energy is determined independently from the conversion model. Another advantage of isoconversional methods is that deviations from the single step assumption can be detected easily by looking for a variation of activation energy with conversion.

The identification of the reaction model from a master plot is usually done by fitting candidate models from literature and selecting the one with the smallest error. Another way to interpret the masterplot is to fit the Šesták-Berggren equation (Šesták et al. 1971). It combines features of interface, nucleation and power laws with weight factors. After fitting the Šesták-Berggren equation, the resulting weight factors can be compared to theoretical ones. If they match accurately, conclusions on the reaction pathway can be drawn (Šimon 2011). If they do not, the Šesták-Berggren equation is only useful for kinetic predictions.

If the isoconversional method shows that activation energy is not constant over conversion, it is most likely a complex or multi-step reaction. Then, the isoconversional method produces a "variable activation energy" plot, which — according to advocates of isoconversional methods — can be used to infer something about the reaction (Vyazovkin 2016; Criado et al. 2008). This approach has been criticized harshly, because a variable activation energy is in contradiction with kinetic theory and cannot be interpreted seriously

(Galwey 2003b; Galwey 2003a). Also, it has been shown that the “variable activation energy” plot can only be interpreted for certain multi-step reactions (Opfermann et al. 2002; Moukhina 2012). Nevertheless, isoconversional methods can be useful for getting first insights into complex reactions. Some scientist take a quite pragmatic approach to isoconversional methods and use them to get starting values for non-linear model fitting (Šimon 2004; Opfermann et al. 2002).

Non-linear model fitting methods are probably the best established alternative to isoconversional methods. They are included in most commercial kinetic software packages because they can be used for single-step and complex multi-step reactions alike (Opfermann 2000). A complete kinetic model is selected and fitted to the data with non-linear fitting algorithms. The main challenge of course is to select an appropriate model, when very little information about the reaction is available. Deviations between data and model can easily go unnoticed because of the complexity of the modeling process. For this reason, non-linear model fitting depends heavily on a-priori knowledge about the reaction and the researcher’s experience.

In an attempt to reduce the burden of a-priori model selection, flexible model equations, such as the Šesták-Berggren equation (Šesták et al. 1971) are often used. By employing equations that can fit a wide range of different reaction types, interference of model choices by the researcher is reduced at the expense of a more complex fitting problem (Pérez-Maqueda et al. 2006). The burden then lies on the fitting algorithm to choose the correct parameters that define the shape of these flexible models. This approach is best suited to generate kinetic prediction models, because the resulting models can generally not be interpreted mechanistically.

The main advantage of non-linear model fitting is that these methods can also be used to model multi-step reactions. The only limitation is the increasing complexity of the model and consequently the effort for fitting the model. An approach to reduce the complexity of a multi-step data set is to decompose the multi-step data into single reaction steps by performing peak fitting on the differential data (Perejón et al. 2011). Then, each reaction step can be analyzed with single step methods. Even though this approach is very convenient because established single-step models can be used, this approach has been shown to produce unreliable results for strongly overlapping reaction steps (Muravyev et al. 2019). Since multi-step reactions are out of the scope of this thesis, I will not go into more detail and conclude this topic with a reference to a recent review article on multi-step modeling methods: Vyazovkin 2020.

A completely different approach to modeling single-step kinetics according to the GKE is the non-parametric kinetics (NPK) method (Serra et al. 1998). By exploiting the mathematical structure of the GKE, the effects of conversion and temperature can be identified without having to assume a reaction model or relying on the Arrhenius equation. As input, the method needs a data set that covers the conversion and temperature range of interest and a conversion-temperature grid for the computation. The output are vectors that correspond to the effects of conversion and temperature on the selected grid without any restriction to their shape. The vectors can be interpreted in terms of the rate limiting step or used directly to predict the conversion rate. These vectors can also be used to identify the most likely reaction model and the apparent activation energy. Similarly to reaction model identification with isoconversional methods this yields reliable results because the identification of conversion and temperature effects is done independently. In contrast to isoconversional methods, the NPK method is not based on the Arrhenius equation. It only requires the GKE to identify the effects of temperature and conversion.

The available kinetic models and kinetic modeling methods have come a long way since the days when Peter Waage and Cato Guldberg introduced the law of mass action and Jacobus van't Hoff and Svante Arrhenius analyzed the effect of temperature on reaction rates in the late 19^{th} century. With computers complicated calculations are not a problem, and the methods have matured to a point, where leading scientists argue that the main bottleneck of kinetic modeling is collecting sufficient and above all reliable kinetic data. Specifically, Brown (2005) argues that existing modeling methods are sufficient, and improving the calculation procedures has little to no effect if no advancement in the experimental techniques and the interpretation of kinetic models is achieved. Brown touches on a critical point: The reliability of kinetic studies depends on the accuracy of all involved steps: underlying theory, experiments, data processing, modeling methods and interpretation. The more sophisticated modeling methods get, the more correct the results are often perceived. Regardless, if either one of the steps is inaccurate, it cannot be compensated by any of the other steps, and improvements to modeling methods would be for naught. While there is certainly a lot of truth to Brown's observation, there is still plenty of room for improvement of the available modeling methods.

In the context of thermochemical energy storage (TCES) all of the above mentioned methods have one significant shortcoming: There is no straight forward way to incorporate the effect of the pressure/driving force in the kinetic analysis of gas-solid reactions. Kinetic models for reactions in TCES must include the effect of driving force, because TCES processes typically operate in close vicinity to the equilibrium, where these effects cannot be neglected. Even though an extra term could easily be included in non-linear model fitting methods, the scarcity of theory on near-equilibrium effects complicates the extension of kinetic models. Clearly there is a need for a method that can be used in an explorative fashion, where knowledge about the reaction is discovered step by step from the kinetic data.

3 Motivation and problem statement

Thermochemical energy storage (TCES) has the potential to cover large parts of the future thermal energy storage demand for a multitude of applications. Its main advantages are the wide range of available materials that enable TCES for any temperature level and the high storage density in combination with virtually lossless storage for unlimited time. Yet, before TCES can be employed on a large scale, some implementation barriers have to be overcome.

Today, TCES is usually situated at the Technology Readiness Level (TRL) 4 "validation in lab". To increase the TRL, prototypes for relevant environments such as households or industry need to be developed and tested in the relevant environment. For many applications, suitable gas-solid reaction systems have been identified. Even though the potential of these reaction systems has been proven and they could readily be applied in prototypes, there is still a number of unanswered questions on the material level that are impeding the progress of TCES technology. One of the aspects that is not yet sufficiently well understood are the kinetics of gas-solid reactions, as is evident from the multitude of effects in experimental data that can not be readily explained or modeled accurately and the numerous disputes in the kinetic community.

As model for the kinetics of gas-solid reactions, the General Kinetic Equation (GKE) is firmly established, even though it clearly is an empirical formula and the possibility that the GKE could fall short of accurately describing the complexity of gas-solid reactions has to be kept in mind. Nevertheless, the GKE is a powerful tool to model kinetic data, because it is simple enough to make kinetic data interpretable while also allowing for enough complexity to capture manifold processes that take place and interact in a gas-solid reaction.

In the context of TCES the main shortcoming of kinetic theory around the GKE is that the effect of pressure/driving force is neglected more often than not. The reason might be the lack of suitable modeling methods that can deal with more than two terms in the GKE. The effects of conversion and temperature are generally considered more relevant and the driving force term is neglected based on the argument that the reaction takes place "sufficiently far from the equilibrium". For TCES this simplification is not viable, because processes typically operate in close proximity to the equilibrium, where the effect of the driving force cannot be neglected. To investigate the effect of the driving force, modeling methods are needed that are capable of analyzing the effect of conversion, temperature and driving force simultaneously.

At the moment, only non-linear model fitting methods are capable of deriving models in more than two variables. These methods require an a-priori choice for the terms in the GKE, which means that an assumption about the shape of the effect of pressure/driving force has to be made. Choosing an appropriate model is a difficult task, considering that just like many other aspects in kinetic analysis the near-equilibrium effects not yet well understood and there is very little reliable literature on the topic. Also it is often hard to judge the viability of a model from just the goodness of fit and an independent verification of the model is usually not possible.

What would be useful is a kinetic modeling method, that can model the kinetics with very little a-priori assumptions, so that modeling can be done in an exploratory fashion and the data can “speak for itself”. Here, the data-driven NPK (non-parametric kinetics) method shows a way forward because it is only based on the GKE and does require no other a-priori assumptions about the reaction under consideration. Consequently, no reaction, temperature or driving force model has to be selected beforehand. Yet, just like most established modeling methods, the NPK method can only derive models in two variables. The effect of the driving force cannot be taken into account while also considering the effect of conversion and temperature. Also, the NPK method is not viable for most research teams, because it is quite complicated algorithmically.

To make progress in kinetic modeling of single-step reactions, a data-driven method is required that

- can derive models in any number of variables,
- requires only few a-priori assumptions about the reaction under consideration,
- can process large, arbitrarily distributed data sets,
- includes tools to assess the model quality and
- is robust, flexible and easy to use.

With such a method it would be possible to gain new insights into the reaction kinetics of gas-solid reactions and compute more accurate kinetic predictions for reactor and process design. Ultimately, better understanding of the processes that control the heat release of chemical reactions could enable TCES as a competitive alternative to other thermal storage methods.

4 Research approach

The starting point for this thesis was in large parts the thesis of my predecessor Markus Deutsch (Deutsch 2017) and our joint paper on the orthogonal extension of the NPK (non-parametric kinetics) method that was published under the title “An extension of the NPK method to include the pressure dependency of solid state reactions” in Thermochimica Acta (Paper 4). As the title suggests, the goal was to use the NPK method to derive a model that did not only incorporate conversion and temperature effects but also the effect of pressure. The central idea was to apply the NPK method twice: once on a temperature-conversion plane, once on a pressure-conversion plane. At the intersection of these two planes, the two sub-models had to be equal. With this condition, the two sub-models could be combined into one model, that included the effect of all three variables.

This approach allows for an analysis of the combined temperature and pressure dependency of gas-solid reactions, without the need to make assumptions about the shape of the temperature and pressure terms in the General Kinetic Equation (GKE). Yet, the restriction to two planes limits the type of experimental data, that can be used for the analysis and as a consequence the scope of the analysis. For example, with this method it would not be possible to use constant-heating-rate data at two different pressure levels or to use a $1 - p/p_{\mathrm{eq}}$ term with data from a p-T grid. This limitation is not acceptable, since the goal is to develop a method that can process arbitrarily distributed data.

The first approach to overcome the limitation of the orthogonal NPK method was to develop a full higher-order extension of the original NPK algorithm. For this, all steps of the algorithm had to be extended from two to an arbitrary number of dimensions. The extended NPK method was published under the title “A higher-order generalization of the NPK-method” in Thermochimica Acta (Paper 1). It can process arbitrarily distributed data points in any number of dimensions — albeit with one severe shortcoming: it is algorithmically even more complicated than the original NPK method.

The cause of the complexity of the algorithm is the underlying mathematical method, the Singular Value Decomposition (SVD). Because this method cannot deal with missing values, which occur in almost all kinetic data sets, an intricate calculation sequence is required to select regions where enough data is available, apply the SVD to each region and then combine the SVD outputs to get the final result. Because of its algorithmic complexity, the extended NPK method is complicated to use, and it is not possible to assess the model quality reliably. Even though the method presented a significant advancement compared to established modeling methods, it was unlikely that it would ever be used for actual kinetic studies.

It quickly became clear that, to overcome these shortcomings, a more general mathematical approach had to be found that can be solved with more efficient algorithms. After an intensive and cumbersome search I found the solution: tensor decomposition methods. These methods are closely related to the Singular Value Decomposition, albeit much more flexible. Most importantly, these methods can deal with missing values and extend seamlessly to a higher number of dimensions.

At this point, the NPK method was completely overhauled: “NPK 2.0: Introducing tensor decompositions to the kinetic analysis of gas-solid reactions” in the International Journal of Chemical Kinetics (Paper 2). The only thing that the TensorNPK method still shared with the original NPK method was the underlying mathematical insight that a discretization of the GKE always has a rank-1 structure. In contrast to the original NPK method, the TensorNPK method is based on a very straight-forward and efficient algorithm and it fulfills all our requirements: It can derive models in any number of variables, process arbitrarily distributed data points and it is robust and fairly easy to use. Additionally it can track the error from the data points to the solution values and compute uncertainty estimates for the solution values. These error estimates can be used to assess the model quality and to improve the accuracy of post-processing.

After about two years, we finally had developed a method that was not just theoretically capable of deriving complex models with many variables but also ready to be used in actual kinetic analysis. The TensorNPK method allowed us to analyze simultaneously the dependency of gas-solid reactions on conversion, temperature and partial pressure without any assumption about the form of these dependencies.

The first application was to analyze the kinetics of the oxidation of Cu_2O (cuprous oxide). The investigation was done by my colleague Saman Setoodeh Jahromy, I contributed the kinetic modeling part. The result was published under the title “Impact of Partial Pressure, Conversion, and Temperature on the Oxidation Reaction Kinetics of Cu_2O to CuO in Thermochemical Energy Storage” in Energies (Paper 5). For the kinetic modeling a data set of isothermal-isobaric experiments on a p-T grid was available, which had to be transformed to a $(1 - p/p_{\mathrm{eq}})$-T grid to take the effect of the driving force into account. With the new TensorNPK method we were able to derive a kinetic model with three variables from this unequally distributed data set, which would not have been possible with any other method. With this kinetic model, we gained useful insights into the kinetics of this oxidation reaction. An interesting discovery in this study was that the reaction rate of the oxidation of Cu_2O decreases much faster towards the equilibrium than theory would predict.

This study of the oxidation of Cu_2O was not only about understanding the reaction but also an opportunity to test the TensorNPK method and to gain more experience with non-parametric modeling. Overall the TensorNPK method performed very well: The kinetic model approximated the data accurately and the effects could be interpreted in terms of the oxidation reaction. Though, data points halfway in-between two grid points were approximated not as well as data points that were close to the grid points. This undesired behavior was caused by a data pre-processing step, the projection of the data onto the tensor. To improve the accuracy of the algorithm, this pre-processing step had to be eliminated and the following step had to be adapted to be able to process the data directly. This change turned out to be a considerable improvement and was promptly implemented and published with the next paper (Paper 3).

To model the kinetics of Cu_2O oxidation, we employed the standard modeling term for the pressure dependency $1 - p/p_{\mathrm{eq}}$. While working on the kinetic modeling, I noticed an inconsistency with the values of the pressure term: It assumed large negative values, when a value between 0 and 1 would have been expected. It turned out that many other researchers were struggling with the same issue. After an in-depth literature study it became clear that the $1 - p/p_{\mathrm{eq}}$ term is only applicable for decomposition reactions — a fact that has been overlooked by many researchers. The finding was presented at the EuroTherm seminar and later published in the Journal of Renewable Energy under the title “The effect of the reaction equilibrium on the kinetics of gas-solid reactions — A non-parametric modeling study” (Papers 3 and 8).

In Paper 3, we also systematically tested different driving force term formulations to determine which one was the best match for non-parametric modeling. As test case for the different driving force terms, the hydration of CaC_2O_4 (calcium oxalate) was used. For this reaction, we found the same behavior that we had also noticed in the oxidation of Cu_2O: The rate decreases much faster towards the equilibrium than kinetic theory would predict. During my presentation at the EuroTherm conference, I raised the question whether anyone else had encountered similar effects. There was: A team from the TU Eindhoven led by Henk Huinink had observed the same effect in the hydration of salts and they were determined to find an explanation for it. They had collected a lot of high quality kinetic data but still needed a method to interpret it. We decided to team up to investigate this effect.

The team from the TU Eindhoven had identified nucleation limitation as the cause for the unexpectedly slow kinetics in the vicinity of the equilibrium. Yet, this could not explain the acceleration of kinetics at larger distances from the equilibrium. To get more insight into this effect, Leyla Söğütoğlu had collected large data sets of both isothermal and constant-cooling experiments at various partial pressures of water vapor. With this large amount of data, the TensorNPK method could demonstrate its strengths: We used the method to derive models with different driving forces, split the data sets and derived models for different reaction conditions. This explorative approach proved successful: we were able to show that the rate controlling step changed from nucleation to diffusion towards the reacting layer at a certain distance from the equilibrium. This finding was published in a joint paper in Thermochimica Acta under the title “Hydration of salts as a two-step process: Water adsorption and hydrate precipitation” (Paper 7).

During the salt hydration study, I noticed that the models were sensitive to the placement of the grid points that the TensorNPK method uses for the computations. On some data sets, shifting certain grid points could distort the result. This problem could be avoided by simply placing more grid points but this can deteriorate the model quality as it can lead to overfitting. When working with the TensorNPK method, scientists should not have to worry about the placement of grid points. As a remedy, ridge regression with a curvature penalty was implemented to counteract overfitting. With this modification, grid points can be placed generously and a cross-validation algorithm automatically selects appropriate penalty values to counteract overfitting when necessary. This modification solved the issue with grid point positioning and was applied in the study of salt hydration where it led to good results.

In the salt hydration study the TensorNPK method was used as a tool to dig into large datasets, test hypothesis on the data and reveal systematic effects in complex data sets.

This is one way, in which the data-driven modeling capabilities of the TensorNPK method can be exploited. The other very promising application is the data-driven modeling of reactions for kinetic predictions with little knowledge about the reaction. In Paper 3 we showed that NPK models can be used to predict the reaction rate despite obvious deviations from theoretical models in literature. Predicting the reaction kinetics without doing an in-depth kinetic study could be very useful for simulations of TCES systems or for reactor and process design. Unfortunately, I did not yet get around to investigate this in greater detail.

To give other scientists easy access to the TensorNPK method, a Matlab implementation of the algorithm has been made available in the supplementary material of Paper 3.

5 Conclusions and outlook

In the course of this thesis, the TensorNPK (non-parametric kinetics) method was developed. It is a data-driven method to derive kinetic models of gas-solid reactions from experimental reaction rate data. The method is based on the General Kinetic Equation (GKE), which implies that the reaction can be approximated by one single step and that the effects of all variables on the conversion rate are independent. The TensorNPK method identifies the effect of each variable by exploiting the mathematical structure of the GKE. The output are vectors that correspond to the unknown terms in the GKE. These vectors can either be used to predict the conversion rate or they can be interpreted in terms of the rate limiting step to get more insight into the reaction mechanism.

Applying the TensorNPK method to study the kinetics of materials relevant for thermochemical energy storage (TCES) allowed us to assess the method's performance and gave insights into the requirements of researchers and certain analyses. Based on these insights, two notable improvements were made after the method's publication. One, the way that the residuals are calculated was changed to improve the accuracy on sparse, unevenly distributed data sets. Two, penalized regression was introduced to counteract over-fitting and to make choosing the model grid easier.

Like the original NPK method, the TensorNPK method does not require models for the individual terms in the GKE beforehand. In contrast to the original NPK method, the TensorNPK method can derive models in any number of variables, it puts less restrictions on the data set and it is easier to use because the underlying algorithm is more straightforward. Additionally, it can produce error estimates of the solution values, which can be used to assess the model quality and to improve the accuracy of post processing.

Because the TensorNPK method derives the effect of each variable from the experimental data, model selection is much less an issue as it is with other kinetic modeling methods, and the likelihood that the scientist's expectations are affecting the modeling outcome is reduced. The TensorNPK method can even be used, when no information about the effect of a certain variable on the reaction rate is available. This flexibility comes at a price, of course: the TensorNPK method requires more data to derive a kinetic model. The more effects are included in the model, the more data is required. The cost and effort of collecting high quality kinetic data usually put a cap on the maximum complexity of NPK models.

Because of the data-driven approach in the TensorNPK method, there are some differences to other kinetic modeling methods. Instead of explicit models for the terms in the GKE, variables have to be chosen for the TensorNPK method. Using conversion and temperature is standard procedure, but selecting a meaningful variable for the driving force is not always straightforward. The choice of the driving force implies an assumption about which step is rate limiting. Often the assumption is that the chemical reaction itself is rate limiting, but for some reaction system it has been shown that the chemical reaction proceeds so fast that a physical process becomes rate limiting. In that case, completely different driving force formulations are required.

For each variable that is selected for the NPK model, a grid has to be defined that the TensorNPK method uses for its computation. In the first version of the algorithm, the number and position of grid points had to be chosen carefully because they could affect the model quality. This issue was eliminated fairly well through the implementation of penalized regression. Though, there are still some issues on very sparse data sets, and strategies for the automated selection of optimal penalty parameters could be improved to make the application of the TensorNPK method easier.

An obvious limitation of the TensorNPK method is that it can only be applied to reactions with one single rate-limiting step. Presented with any kinetic data set, the TensorNPK method will always produce the best single-step approximation — regardless of the actual number of reaction steps involved. If more than one reaction step is rate limiting, the result will become unreliable. The single-step assumption should be verified carefully beforehand, because it might be hard to judge from just the output of the TensorNPK method whether the single-step assumption has been violated or not. The TensorNPK method also inherited other limitations from the GKE, such as that the effects of all variables are independent and that particle effects are a function of conversion alone. These limitations need to be kept in mind when applying the TensorNPK method.

Compared to kinetic modeling approaches that seek to model all effects in great detail, the GKE might seem like a crude simplification. Indeed it might not be applicable to all reactions, but for a wide range of reactions it has been shown to perform very well. For these reactions the best justification for the GKE is maybe Occam's razor[5]: For models that are calibrated with experimental data, there is no need for the model to be more complex than the quality and quantity of available data permits. Having in mind that kinetic models are usually derived from thermogravimetric or calorimetric data, where the kinetic information is a superposition of various simultaneous processes that can only be separated by making many assumptions about these processes, the superiority of very detailed models is debatable.

In light of these considerations, models based on the GKE seem to be a good choice in the trade-off simplification vs. speculation. The GKE is a viable approximation for many reactions, as long as its limitations are kept in mind. Even though it might fall short of giving a perfectly accurate description of the underlying processes, it provides a useful frame to interpret the behavior of many reaction systems.

Compared to isoconversional methods the TensorNPK method does not even rely on the Arrhenius equation. More importantly, the TensorNPK method can model the effect of pressure directly and does not require the effect to be interpreted as an "apparent variation of activation energy with pressure". Interpreting the effect of pressure/driving force directly instead of taking the detour over the activation energy is not only more convenient, but also more meaningful from a theoretical perspective. For this reason, the TensorNPK method is better suited to obtain kinetic models that include more than the effects of just conversion and temperature.

---

[5] Occam's razor is a philosophical concept that says that when presented with competing hypotheses that make the same predictions, one should select the solution with the fewest assumptions. It is sometimes paraphrased by a statement like "the simplest solution is most likely the right one".

The main advantage of the TensorNPK method over non-linear model fitting methods is that it does require much less a-priori model assumptions. For mechanistic analyses, the problem of model selection is, so to say, postponed until after the effect of each variable has been identified. With the TensorNPK method, model fitting is done independently for each variable and when more information about the effect of each considered variable is available. In this way, model bias through the incorrect choice of models is reduced. On the other hand, non-linear model fitting can be used with any kind of model, while the TensorNPK method is limited to models based on the GKE.

In conclusion, what sets the TensorNPK method apart from established kinetic modeling methods is that it can derive models with more than two terms in the GKE without additional modeling assumptions. In the context of TCES this means that a driving force (and consequently the position of the equilibrium) can be included in the kinetic model without knowing exactly the shape of the effect of the driving force. As discussed in Paper 3, the inability of other modeling methods to take the driving force correctly into account led to the identification of negative apparent activation energies in some cases. For this reason the TensorNPK method is highly relevant for TCES research.

The TensorNPK method allows for various interesting analyses that were not yet possible in this way. Two main branches of analysis can be distinguished: kinetic predictions, where the goal is to derive an empirical model with high prediction accuracy, and kinetic analysis, where the goal is to get additional insight into the reaction mechanism.

For *kinetic predictions* only the accuracy of the prediction is relevant. Physical accuracy is not a priority, even though physically correct models can be expected to perform better when extrapolated. In Paper 3, it was demonstrated, that NPK models can be used as a generic prediction method for the kinetics of gas-solid reactions. While other kinetic modeling methods require explicit models for each relevant effect, the TensorNPK method requires only the variables that the effects are correlated with. The algorithm then identifies the effects from the experimental data. This allows to compute accurate kinetic predictions for a wide range of reaction systems with little modeling effort and without the need for an in-depth kinetic study. Possible applications for these models include computational fluid dynamics simulations as well as reactor and process design.

Even though such empirical models are convenient because of the comparably low effort of setting them up, they have to be used with care. Especially effects in the solid such as fractioning/agglomeration of particles, change of active surface or passivation due to side reactions are not included in these models, but they might become an issue during scale-up and long-term operation of a TCES reactor. For this reason, such empirical models have to be treated as contingent on the reaction conditions and the solid configuration in the experiments. To get accurate kinetic predictions, the experiments have to be conducted under conditions as close to the target ones as possible. If these requirements are met, the resulting models should be capable of giving a detailed description of the effect of reaction conditions on reaction rate and providing an accurate estimate of the operating behavior of a TCES reactor with that reaction system.

In *kinetic analysis* the goal is to get additional insight into the reaction mechanism. Even though the TensorNPK method is based on the GKE, which is a strong simplification, it can be used to analyze the effect of the most relevant variables. In that sense, NPK models can be used as a lens to interpret complex kinetic data. For this type of analysis, the main advantage of the TensorNPK method is that is does not require an assumption about the shape of each effect. This is especially relevant if no theoretical models are available and even if they are, such an assumption might introduce a significant bias into the modeling. The TensorNPK method avoids this bias and allows to explore complex data sets with very few a-priori assumptions. The data can, so to say, speak for itself.

In collaboration with colleagues, the TensorNPK method was used to study reaction systems relevant for TCES. Specifically, the oxidation of Cu_2O (cuprous oxide), the dehydration of H_3BO_3 (boric acid) and the hydration of K_2CO_3 (potassium carbonate), LiCl (lithium chloride), $MgCl_2$ (magnesium chloride) and $CuCl_2$ (copper chloride) were analyzed with the TensorNPK method. Especially in the copper oxidation and the salt hydration study, the new capabilities of the TensorNPK method came in handy. To model the kinetics of these reactions, at least three variables had to be considered: conversion, temperature and a driving force. The main challenge was the scarcity of agreed upon theory on the shape of the effect of driving force. Here, the fact that the TensorNPK does not require models for the terms in the GKE allowed us to model the reaction rate accurately, even when the effect of the driving force did not match any of the models in literature. After the algorithm had extracted the shape of the effect of the driving force, we could make hypotheses about the rate limiting process. For salt hydrates, we were able to show that the rate limiting step changes from nucleation limitation to diffusion limitation at a certain distance to the equilibrium. Also the identification of the Arrhenius parameters was only done after it was confirmed that the effect of temperature matched the Arrhenius equation. Thus avoiding the identification of meaningless activation energies.

In our studies, the TensorNPK method proved a versatile tool to derive kinetic models and get additional insight into the reaction mechanism. Yet, there are four main areas, where the TensorNPK method could still be improved and/or extended:

- A standardized strategy for diagnosing NPK models would help scientists to asses the model quality and to identify errors in models. For this, additional meaningful statistical markers and new visualization methods will need to be developed.
- The procedures for the automated selection of meta parameters (such as grid point positioning and penalty parameters) should be improved. Even though the current procedures produce good results with most data sets, the meta parameters sometimes need to be adjusted by hand when results are unsatisfactory.
- Weighting of data points could improve the accuracy of NPK models. Because kinetic data is usually recorded with a constant sampling rate, there are usually fewer data points in regions where the reaction proceeds the fastest. If data points are weighted equally, the algorithm puts more emphasis on regions with slow reaction rates. An approach to resolve this issue would be using Generalized Least Squares, which can take the correlation of data points (i.e. their density) into account.
- If the limitation to single step reactions can be overcome, it would greatly increase

the scope of the TensorNPK method. The most obvious approach would be to separate reaction steps with peak fitting and analyze each step separately. Another approach, that would be less of a workaround, is to consider rank-N tensor decompositions. For parallel reactions, it can be shown fairly easily that the discretization of the kinetic equation results in a tensor with rank equal to the number of parallel reactions. If this statement can be generalized to consecutive or even more complex reactions, rank-N decompositions could be used to extract information on the reaction steps from experimental data. Though, information of the reaction steps will be convoluted in the sub-tensors and a special deconvolution procedure will have to be developed to separate the models for each reaction step.

Kinetic models for gas-solid reactions would profit greatly from a standardized way to take the configuration of the solid reactants into account that goes beyond one single conversion term. Today, kinetic models are usually derived from experimental data, where the solid underwent a specific pre-treatment to ensure that the crystal structure of the solid is in a specific configuration. These models would not be capable of predicting the performance of a TCES reactor where the material is used for multiple cycles, even less if partial cycles are used. What would be needed are measures for describing the state of the solid, measurement methods for determining this state and models to predict the change of state. Modeling the solid with more detail would not just be interesting from a theoretical perspective, but also highly relevant for practical TCES applications as they could enable reliable kinetic predictions in later stages of the life cycle of the termochemical material. A lot more research needs to be dedicated to elucidating the effects in the solid in kinetic analysis. The TensorNPK method might prove useful for deriving models that include more detailed effects in the solid because additional terms can be added easily, provided that enough experimental data is available.

Even though there are countless unanswered questions on a material level and our understanding of the processes taking place during a gas-solid reaction is still rather rudimentary, TCES research would also profit greatly from more applied research that simply sets aside these blind spots for now. Some viable thermochemical materials have been identified for specific applications and the potential of these materials has been proven in the lab. Testing on a component level is already underway and the first tests in relevant environments have started recently. Successful demonstrations would prove the viability of TCES and could spur more fundamental research in the long run.

In the big picture, much is on the line. Global warming will have disastrous consequences, if we do not act quickly and adopt a more sustainable mode of production. Even though TCES will not solve the problem of global warming on its own, it could be an important building stone towards a more sustainable energy system.

References

Abdmouleh, Z., R. A. Alammari, and A. Gastli (2015). “Review of policies encouraging renewable energy integration & best practices”. In: *Renewable and Sustainable Energy Reviews* 45, pp. 249–262. ISSN: 13640321.
DOI: `10.1016/j.rser.2015.01.035`

Afflerbach, S., M. Kappes, A. Gipperich, R. Trettin, and W. Krumm (2017). “Semipermeable encapsulation of calcium hydroxide for thermochemical heat storage solutions”. In: *Solar Energy* 148, pp. 1–11. ISSN: 0038092X.
DOI: `10.1016/j.solener.2017.03.074`

Angerer, M., M. Becker, S. Härzschel, K. Kröper, S. Gleis, A. Vandersickel, and H. Spliethoff (2018). “Design of a MW-scale thermo-chemical energy storage reactor”. In: *Energy Reports* 4, pp. 507–519. ISSN: 23524847.
DOI: `10.1016/j.egyr.2018.07.005`

Beckmann, G. and P. V. Gilli (1984). *Thermal energy storage: Basics, design, applications to power generation and heat supply.* Topics in Energy. Wien: Springer. ISBN: 3-211-81764-6.

Bhatia, S. K. and D. D. Perlmutter (1981). “A random pore model for fluid-solid reactions: II. Diffusion and transport effects”. In: *AIChE Journal* 27.2, pp. 247–254. ISSN: 00011541.
DOI: `10.1002/aic.690270211`

Birkelbach, F., M. Deutsch, S. Flegkas, W. Franz, and A. Werner (2018). “A higher-order generalization of the NPK-method”. In: *Thermochimica Acta* 661, pp. 27–33. ISSN: 00406031.
DOI: `10.1016/j.tca.2018.01.005`

Birkelbach, F., M. Deutsch, S. Flegkas, F. Winter, and A. Werner (2019a). “NPK 2.0: Introducing tensor decompositions to the kinetic analysis of gas-solid reactions”. In: *International Journal of Chemical Kinetics* 51.4, pp. 280–290. ISSN: 05388066.
DOI: `10.1002/kin.21251`

Birkelbach, F., M. Deutsch, and A. Werner (2019b). “The effect of the reaction equilibrium on the kinetics of gas-solid reactions — A non-parametric modeling study”. In: *Advances in Thermal Energy Storage*. Ed. by Universitat de Lleida. Edicions de la Universitat de Lleida, pp. 161–171. ISBN: 978-84-9144-155-7.

– (2020). “The effect of the reaction equilibrium on the kinetics of gas-solid reactions — A non-parametric modeling study”. In: *Renewable Energy* 152, pp. 300–307. ISSN: 09601481.
DOI: `10.1016/j.renene.2020.01.033`

Brown, M. E. (1997). “Steps in a minefield”. In: *Journal of thermal analysis* 49.1, pp. 17–32. ISSN: 0022-5215.
DOI: `10.1007/BF01987418`

Brown, M. E. (2005). “Stocktaking in the kinetics cupboard”. In: *Journal of Thermal Analysis and Calorimetry* 82.3, pp. 665–669. ISSN: 1388-6150.
DOI: `10.1007/s10973-005-0947-4`

Brown, M. E., D. Dollimore, A. K. Galwey, C. H. Bamford, and C. F. H. Tipper, eds. (1980). *Reactions in the solid state.* Vol. v. 22. Comprehensive chemical kinetics. New York, Amsterdam, and New York: Elsevier Scientific Pub. Co. ISBN: 978-0-444-41807-4.

Bulfin, B., J. Vieten, C. Agrafiotis, M. Roeb, and C. Sattler (2017). "Applications and limitations of two step metal oxide thermochemical redox cycles; a review". In: *Journal of Materials Chemistry A* 5.36, pp. 18951–18966. ISSN: 2050-7488.
DOI: `10.1039/C7TA05025A`

Burnham, A. K. (2017). "Use and misuse of logistic equations for modeling chemical kinetics". In: *Journal of Thermal Analysis and Calorimetry* 127.1, pp. 1107–1116. ISSN: 1388-6150.
DOI: `10.1007/s10973-015-4879-3`

Criado, J. M., P. E. Sánchez-Jiménez, and L. A. Pérez-Maqueda (2008). "Critical study of the isoconversional methods of kinetic analysis". In: *Journal of Thermal Analysis and Calorimetry* 92.1, pp. 199–203. ISSN: 1388-6150.
DOI: `10.1007/s10973-007-8763-7`

Deutsch, M. (2017). "A systematic approach to identify new thermochemical energy storage systems". Doctoral thesis. Vienna: TU Wien.
URL: `http://katalog.ub.tuwien.ac.at/AC13698112`

Deutsch, M., F. Birkelbach, C. Knoll, M. Harasek, A. Werner, and F. Winter (2017). "An extension of the NPK method to include the pressure dependency of solid state reactions". In: *Thermochimica Acta* 654, pp. 168–178. ISSN: 00406031.
DOI: `10.1016/j.tca.2017.05.019`

Deutsch, M., D. Müller, C. Aumeyer, C. Jordan, C. Gierl-Mayer, P. Weinberger, F. Winter, and A. Werner (2016). "Systematic search algorithm for potential thermochemical energy storage systems". In: *Applied Energy* 183, pp. 113–120. ISSN: 03062619.
DOI: `10.1016/j.apenergy.2016.08.142`

Donkers, P., L. C. Söğütoğlu, H. P. Huinink, H. R. Fischer, and O. Adan (2017). "A review of salt hydrates for seasonal heat storage in domestic applications". In: *Applied Energy* 199, pp. 45–68. ISSN: 03062619.
DOI: `10.1016/j.apenergy.2017.04.080`

Flynn, J. H. (1997). "The 'Temperature Integral' — Its use and abuse". In: *Thermochimica Acta* 300.1-2, pp. 83–92. ISSN: 00406031.
DOI: `10.1016/S0040-6031(97)00046-4`

Forman, C., I. K. Muritala, R. Pardemann, and B. Meyer (2016). "Estimating the global waste heat potential". In: *Renewable and Sustainable Energy Reviews* 57, pp. 1568–1579. ISSN: 13640321.
DOI: `10.1016/j.rser.2015.12.192`

Funayama, S., H. Takasu, S. T. Kim, and Y. Kato (2020). "Thermochemical storage performance of a packed bed of calcium hydroxide composite with a silicon-based ceramic honeycomb support". In: *Energy* 201, p. 117673. ISSN: 03605442.
DOI: `10.1016/j.energy.2020.117673`

Galwey, A. K. (2003a). "Eradicating erroneous Arrhenius arithmetic". In: *Thermochimica Acta* 399.1-2, pp. 1–29. ISSN: 00406031.

DOI: `10.1016/S0040-6031(02)00465-3`

Galwey, A. K. (2003b). “What is meant by the term ‘variable activation energy’ when applied in the kinetic analyses of solid state decompositions (crystolysis reactions)?” In: *Thermochimica Acta* 397.1-2, pp. 249–268. ISSN: 00406031.
DOI: `10.1016/S0040-6031(02)00271-X`

– (2004). “Is the science of thermal analysis kinetics based on solid foundations?” In: *Thermochimica Acta* 413.1-2, pp. 139–183. ISSN: 00406031.
DOI: `10.1016/j.tca.2003.10.013`

Galwey, A. and M. Brown (2002). “Application of the Arrhenius equation to solid state kinetics: can this be justified?” In: *Thermochimica Acta* 386, pp. 91–98. ISSN: 00406031.

Goodell, P. D. and P. S. Rudman (1983). “Hydriding and dehydriding rates of the $LaNi_5$-H system”. In: *Journal of the Less Common Metals* 89.1, pp. 117–125. ISSN: 00225088.
DOI: `10.1016/0022-5088(83)90255-2`

Gravogl, G., C. Knoll, W. Artner, J. M. Welch, E. Eitenberger, G. Friedbacher, M. Harasek, K. Hradil, A. Werner, P. Weinberger, D. Müller, and R. Miletich (2019). “Pressure effects on the carbonation of MeO (Me = Co, Mn, Pb, Zn) for thermochemical energy storage”. In: *Applied Energy* 252, p. 113451. ISSN: 03062619.
DOI: `10.1016/j.apenergy.2019.113451`

Greenpeace (2015). *Energy [r]evolution: A sustainable world energy outlook 2015.*
URL: `https://www.greenpeace.de/presse/publikationen/energy-revolution`

Huber, C., S. S. Jahromy, F. Birkelbach, J. Weber, C. Jordan, M. Schreiner, M. Harasek, and F. Winter (2020). “The multistep decomposition of boric acid”. In: *Energy Science & Engineering* 35, p. 143. ISSN: 2050-0505.
DOI: `10.1002/ese3.622`

IEA (2016a). *Energy, Climate Change and Environment 2016 Insights.* Paris.
URL: `https://webstore.iea.org/energy-climate-change-and-environment-2016-insights`

– (2016b). *World Energy Outlook 2016.* Paris.
URL: `https://www.iea.org/reports/world-energy-outlook-2016`

– (2018). *World Energy Outlook 2018.*
URL: `https://www.iea.org/reports/world-energy-outlook-2018`

– (2019). *Key World Energy Statistics 2019.*
URL: `https://webstore.iea.org/key-world-energy-statistics-2019`

IPCC, ed. (2012). *Managing the risks of extreme events and disasters to advance climate change adaption: A Special Report of Working Groups I and II of the Intergovernmental Panel on Climate Change.* Cambridge: Cambridge University Press. ISBN: 9781107607804.
DOI: `10.1017/CBO9781139177245.`
URL: `https://doi.org/10.1017/CBO9781139177245`

– ed. (2018). *Global Warming of 1.5°C. An IPCC Special Report on the impacts of global warming of 1.5°C above pre-industrial levels and related global greenhouse gas emission pathways, in the context of strengthening the global response to the threat of climate change, sustainable development, and efforts to eradicate poverty.* Geneva, Switzerland.

IRENA (2019a). *Climate Change and Renewable Energy: National Policies and the role of communities, cities and regions: (Report to the G20 Climate Sustainability Working Group (CSWG)).* Abu Dhabi.
URL: `https://www.irena.org/publications/2019/Jun/Climate-change-and-renewable-energy`

– (2019b). *Global energy transformation: A roadmap to 2050.* Abu Dhabi.

Kato, Y., S. Funayama, E. Piperopoulos, and C. Milone (2019). "Experimental Methods for the Characterization of Materials for Thermal Energy Storage with Chemical Reactions". In: *Recent Advancements in Materials and Systems for Thermal Energy Storage*. Ed. by A. Frazzica and L. F. Cabeza. Green Energy and Technology. Cham: Springer International Publishing. ISBN: 9783319966410.
DOI: `10.1007/978-3-319-96640-3{\textunderscore}8`

Khawam, A. and D. R. Flanagan (2006). "Solid-state kinetic models: basics and mathematical fundamentals". In: *The journal of physical chemistry. B* 110.35, pp. 17315–17328. ISSN: 1520-6106.
DOI: `10.1021/jp062746a`

Kissinger, H. E. (1956). "Variation of Peak Temperature With Heating Rate in Differential Thermal Analysis". In: *Journal of Research of the National Bureau of Standards* 57.4.

Knoll, C., D. Müller, W. Artner, J. Welch, A. Werner, M. Harasek, and P. Weinberger (2017). "Probing cycle stability and reversibility in thermochemical energy storage - $CaC_2O_4 \cdot H_2O$ as perfect match?" In: *Applied Energy* 187, pp. 1–9. ISSN: 03062619.
DOI: `10.1016/j.apenergy.2016.11.053`

L'vov, B. V. (2017). "Ups and downs in the theory of thermal decomposition of solids for 130 years". In: *Journal of Thermal Analysis and Calorimetry* 128.1, pp. 593–600. ISSN: 1388-6150.
DOI: `10.1007/s10973-017-6200-0`

L'vov, B. V. and A. K. Galwey (2013). "Toward a general theory of heterogeneous reactions". In: *Journal of Thermal Analysis and Calorimetry* 113.2, pp. 561–568. ISSN: 1388-6150.
DOI: `10.1007/s10973-012-2754-z`

Liu, F., F. Sommer, C. Bos, and E. J. Mittemeijer (2013). "Analysis of solid state phase transformation kinetics: Models and recipes". In: *International Materials Reviews* 52.4, pp. 193–212. ISSN: 0950-6608.
DOI: `10.1179/174328007X160308`

Liu, M., N. H. Steven Tay, S. Bell, M. Belusko, R. Jacob, G. Will, W. Saman, and F. Bruno (2016). "Review on concentrating solar power plants and new developments in high temperature thermal energy storage technologies". In: *Renewable and Sustainable Energy Reviews* 53, pp. 1411–1432. ISSN: 13640321.
DOI: `10.1016/j.rser.2015.09.026`

Maciejewski, M. (2000). "Computational aspects of kinetic analysis - Part B: The ICTAC Kinetics Project - the decomposition kinetics of calcium carbonate revisited, or some tips on survival in the kinetic minefield". In: *Thermochimica Acta* 355.1-2, pp. 145–154. ISSN: 00406031.

DOI: `10.1016/S0040-6031(00)00444-5`

Maciejewski, M. and A. Reller (1987). “How (UN)reliable are kinetic data of reversible solid-state decomposition processes?” In: *Thermochimica Acta* 110, pp. 145–152. ISSN: 00406031.
DOI: `10.1016/0040-6031(87)88221-7`

Meadows, D. H. (1974). *The limits to growth: A report for the Club of Rome’s Project on the Predicament of Mankind*. 2. ed. New York: Universe Books. ISBN: 0-87663-165-0.

Miró, L., J. Gasia, and L. F. Cabeza (2016). “Thermal energy storage (TES) for industrial waste heat (IWH) recovery: A review”. In: *Applied Energy* 179, pp. 284–301. ISSN: 03062619.
DOI: `10.1016/j.apenergy.2016.06.147`

Moukhina, E. (2012). “Determination of kinetic mechanisms for reactions measured with thermoanalytical instruments”. In: *Journal of Thermal Analysis and Calorimetry* 109.3, pp. 1203–1214. ISSN: 1388-6150.
DOI: `10.1007/s10973-012-2406-3`

Muravyev, N. V., A. N. Pivkina, and N. Koga (2019). “Critical Appraisal of Kinetic Calculation Methods Applied to Overlapping Multistep Reactions”. In: *Molecules (Basel, Switzerland)* 24.12.
DOI: `10.3390/molecules24122298`

Neises, M., S. Tescari, L. de Oliveira, M. Roeb, C. Sattler, and B. Wong (2012). “Solar-heated rotary kiln for thermochemical energy storage”. In: *Solar Energy* 86.10, pp. 3040–3048. ISSN: 0038092X.
DOI: `10.1016/j.solener.2012.07.012`

Opfermann, J. (2000). “Kinetic Analysis Using Multivariate Non-linear Regression. I. Basic concepts”. In: *Journal of Thermal Analysis and Calorimetry* 60.2, pp. 641–658.
DOI: `10.1023/A:1010167626551`

Opfermann, J. R., E. Kaisersberger, and H. J. Flammersheim (2002). “Model-free analysis of thermoanalytical data-advantages and limitations”. In: *Thermochimica Acta* 391.1-2, pp. 119–127. ISSN: 00406031.
DOI: `10.1016/S0040-6031(02)00169-7`

Pelay, U., L. Luo, Y. Fan, D. Stitou, and M. Rood (2017). “Thermal energy storage systems for concentrated solar power plants”. In: *Renewable and Sustainable Energy Reviews* 79, pp. 82–100. ISSN: 13640321.
DOI: `10.1016/j.rser.2017.03.139`

Perejón, A., P. E. Sánchez-Jiménez, J. M. Criado, and L. A. Pérez-Maqueda (2011). “Kinetic analysis of complex solid-state reactions. A new deconvolution procedure”. In: *The journal of physical chemistry. B* 115.8, pp. 1780–1791. ISSN: 1520-6106.
DOI: `10.1021/jp110895z`

Pérez-Maqueda, L. A., J. M. Criado, and P. E. Sanchez-Jiménez (2006). “Combined kinetic analysis of solid-state reactions: A powerful tool for the simultaneous determination of kinetic parameters and the kinetic model without previous assumptions on the reaction mechanism”. In: *The journal of physical chemistry. A* 110.45, pp. 12456–12462. ISSN: 1089-5639.

DOI: `10.1021/jp064792g`

Pijolat, M. and L. Favergeon (2018). “Chapter 5 - Kinetics and Mechanisms of Solid-Gas Reactions”. In: *Handbook of Thermal Analysis and Calorimetry : Recent Advances, Techniques and Applications*. Ed. by S. Vyazovkin, N. Koga, and C. Schick. Vol. 6. Elsevier Science B.V, pp. 173–212. ISBN: 978-0-444-64062-8.
DOI: `10.1016/B978-0-444-64062-8.00011-5`

Pijolat, M., L. Favergeon, and M. Soustelle (2011). “From the drawbacks of the Arrhenius-f(α) rate equation towards a more general formalism and new models for the kinetic analysis of solid–gas reactions”. In: *Thermochimica Acta* 525.1-2, pp. 93–102. ISSN: 00406031.
DOI: `10.1016/j.tca.2011.07.026`

Prieto, C., P. Cooper, A. I. Fernández, and L. F. Cabeza (2016). “Review of technology: Thermochemical energy storage for concentrated solar power plants”. In: *Renewable and Sustainable Energy Reviews* 60, pp. 909–929. ISSN: 13640321.
DOI: `10.1016/j.rser.2015.12.364`

Risthaus, K., I. Bürger, M. Linder, and M. Schmidt (2020). “Numerical analysis of the hydration of calcium oxide in a fixed bed reactor based on lab-scale experiments”. In: *Applied Energy* 261, p. 114351. ISSN: 03062619.
DOI: `10.1016/j.apenergy.2019.114351`

Scapino, L., H. A. Zondag, J. van Bael, J. Diriken, and C. C. Rindt (2017). “Sorption heat storage for long-term low-temperature applications: A review on the advancements at material and prototype scale”. In: *Applied Energy* 190, pp. 920–948. ISSN: 03062619.
DOI: `10.1016/j.apenergy.2016.12.148`

Schaube, F., L. Koch, A. Wörner, and H. Müller-Steinhagen (2012). “A thermodynamic and kinetic study of the de- and rehydration of $Ca(OH)_2$ at high H_2O partial pressures for thermo-chemical heat storage”. In: *Thermochimica Acta* 538, pp. 9–20. ISSN: 00406031.
DOI: `10.1016/j.tca.2012.03.003`

Serra, R., J. Sempere, and R. Nomen (1998). “A new method for the kinetic study of thermoanalytical data”. In: *Thermochimica Acta* 316.1, pp. 37–45. ISSN: 00406031.
DOI: `10.1016/S0040-6031(98)00295-0`

Šesták, J., ed. (2005). *Science of Heat and Thermophysical Studies: A Generalized Approach to Thermal Analysis*. 1st ed. Elsevier Science. ISBN: 9780444519542.

– (2017). “Šesták–Berggren equation: Now questioned but formerly celebrated—what is right”. In: *Journal of Thermal Analysis and Calorimetry* 127.1, pp. 1117–1123. ISSN: 1388-6150.
DOI: `10.1007/s10973-015-4998-x`

Šesták, J. and G. Berggren (1971). “Study of the kinetics of the mechanism of solid-state reactions at increasing temperatures”. In: *Thermochimica Acta* 3.1, pp. 1–12. ISSN: 00406031.
DOI: `10.1016/0040-6031(71)85051-7`

Setoodeh Jahromy, S., F. Birkelbach, C. Jordan, C. Huber, M. Harasek, A. Werner, and F. Winter (2019). “Impact of Partial Pressure, Conversion, and Temperature on the

Oxidation Reaction Kinetics of Cu_2O to CuO in Thermochemical Energy Storage". In: *Energies* 12.3, p. 508. ISSN: 1996-1073.
DOI: `10.3390/en12030508`

Šimon, P. (2004). "Isoconversional methods". In: *Journal of Thermal Analysis and Calorimetry* 76.1, pp. 123–132.
DOI: `10.1023/B:JTAN.0000027811.80036.6c`

– (2007). "The single-step approximation". In: *Journal of Thermal Analysis and Calorimetry* 88.3, pp. 709–715. ISSN: 1388-6150.
DOI: `10.1007/s10973-006-8140-y`

Šimon, P. (2011). "Fourty years of the Šesták–Berggren equation". In: *Thermochimica Acta* 520.1-2, pp. 156–157. ISSN: 00406031.
DOI: `10.1016/j.tca.2011.03.030`

Söğütoğlu, L.-C., M. Steiger, J. Houben, D. Biemans, H. R. Fischer, P. Donkers, H. Huinink, and O. C. G. Adan (2019). "Understanding the Hydration Process of Salts: The Impact of a Nucleation Barrier". In: *Crystal Growth & Design* 19.4, pp. 2279–2288. ISSN: 1528-7483.
DOI: `10.1021/acs.cgd.8b01908`

Steffen, W., K. Richardson, J. Rockström, S. E. Cornell, I. Fetzer, E. M. Bennett, R. Biggs, S. R. Carpenter, W. de Vries, C. A. de Wit, C. Folke, D. Gerten, J. Heinke, G. M. Mace, L. M. Persson, V. Ramanathan, B. Reyers, and S. Sörlin (2015). "Planetary boundaries: guiding human development on a changing planet". In: *Science (New York, N.Y.)* 347.6223, p. 1259855.
DOI: `10.1126/science.1259855`

Stengler, J. and M. Linder (2020). "Thermal energy storage combined with a temperature boost: An underestimated feature of thermochemical systems". In: *Applied Energy* 262, p. 114530. ISSN: 03062619.
DOI: `10.1016/j.apenergy.2020.114530`

Sterner, M. and I. Stadler (2018). *Handbook of Energy Storage: Demand, Technologies, Integration*. Berlin and s.l.: Springer Berlin. ISBN: 978-3-662-55503-3.

Szekely, J. and J. W. Evans (1970). "A structural model for gas—solid reactions with a moving boundary". In: *Chemical Engineering Science* 25.6, pp. 1091–1107.
DOI: `10.1016/0009-2509(70)85053-9`

Thorndike, L. (1923). *A history of magic and expermiental science*. Vol. 2. New York: Macmillan.

Vyazovkin, S. (2016). "A time to search: finding the meaning of variable activation energy". In: *Physical chemistry chemical physics : PCCP* 18.28, pp. 18643–18656. ISSN: 1463-9084.
DOI: `10.1039/C6CP02491B`

– (2018). "Chapter 4 - Modern Isoconversional Kinetics: From Misconceptions to Advances". In: *Handbook of Thermal Analysis and Calorimetry : Recent Advances, Techniques and Applications*. Ed. by S. Vyazovkin, N. Koga, and C. Schick. Vol. 6. Elsevier Science B.V, pp. 131–172. ISBN: 978-0-444-64062-8.
DOI: `10.1016/B978-0-444-64062-8.00008-5`

– (2020). “Kinetic effects of pressure on decomposition of solids”. In: *International Reviews in Physical Chemistry* 39.1, pp. 35–66.
DOI: `10.1080/0144235X.2019.1691319`

Vyazovkin, S., A. K. Burnham, J. M. Criado, L. A. Pérez-Maqueda, C. Popescu, and N. Sbirrazzuoli (2011). “ICTAC Kinetics Committee recommendations for performing kinetic computations on thermal analysis data”. In: *Thermochimica Acta* 520, pp. 1–19. ISSN: 00406031.
DOI: `10.1016/j.tca.2011.03.034`

Vyazovkin, S., K. Chrissafis, M. L. Di Lorenzo, N. Koga, M. Pijolat, B. Roduit, N. Sbirrazzuoli, and J. J. Suñol (2014). “ICTAC Kinetics Committee recommendations for collecting experimental thermal analysis data for kinetic computations”. In: *Thermochimica Acta* 590, pp. 1–23. ISSN: 00406031.
DOI: `10.1016/j.tca.2014.05.036`

Vyazovkin, S. and C. A. Wight (1999). “Model-free and model-fitting approaches to kinetic analysis of isothermal and nonisothermal data”. In: *Thermochimica Acta* 340-341, pp. 53–68. ISSN: 00406031.
DOI: `10.1016/S0040-6031(99)00253-1`

Watson, J. and R. Sauter (2011). “Sustainable innovation through leapfrogging: A review of the evidence”. In: *International Journal of Technology and Globalisation* 5.3/4, p. 170. ISSN: 1476-5667.
DOI: `10.1504/IJTG.2011.039763`

WWF (2019). *EU Overshot Day: Living Beyond Nature’s Limits*. Brussels.

Yagi, S. and D. Kunii (1955). “Studies on combustion of carbon particles in flames and fluidized beds”. In: *Symposium (International) on Combustion* 5.1, pp. 231–244. ISSN: 00820784.
DOI: `10.1016/S0082-0784(55)80033-1`

Publications

In this chapter all publications that are relevant for this thesis are presented. This includes the publications where I was the first author as well as publications that I wrote in collaboration with colleagues. A short summary that puts each publication into context for this thesis, my own contribution and the reference are provided.

For the core publications of this thesis, the full-length papers are included. For all other publications, the abstract is provided.

Papers included in this thesis

Paper 1

A higher-order generalization of the NPK-method

published in Thermochimica Acta in collaboration with Markus Deutsch, Stylianos Flegkas, Franz Winter and Andreas Werner.

This paper covers the first approach to develop an algorithm that can model the kinetics of gas-solid reactions in more than two variables based on arbitrarily distributed data. The starting point for the new algorithm was the original NPK algorithm, which could only model kinetic data in two dimensions.

To derive models in more than two variables, all parts of the original NPK algorithm had to be extended to an arbitrary number of dimensions. Just as with the original NPK method this lead to a complex sequence of processing steps because the underlying mathematical method, the Singular Value Decomposition (SVD), cannot deal with missing values directly. To avoid missing values, the data set had to be split into regions without missing data, which could be processed with the SVD. Then, the results had to be combined to obtain the full model. All steps are presented in this paper.

With this method, model-free analysis of kinetic data in more than two variables was possible for the first time. This allowed to analyze the effect of the driving force on kinetics in a whole new way. The main shortcoming of this approach is that it is algorithmically very complex. As a consequence, it is hard to assess the model quality and using the method is quite complicated.

My contribution: Development of the algorithm, implementing it in Matlab and testing it. Evaluation of the higher-order NPK method. Drawing up and writing the paper.

F. Birkelbach, M. Deutsch, S. Flegkas, W. Franz, and A. Werner (2018). "A higher-order generalization of the NPK-method". In: Thermochimica Acta *661, pp. 27–33.* ISSN*: 00406031.*
DOI*:* `10.1016/j.tca.2018.01.005`

Thermochimica Acta 661 (2018) 27–33

Contents lists available at ScienceDirect

Thermochimica Acta

journal homepage: www.elsevier.com/locate/tca

A higher-order generalization of the NPK-method

Felix Birkelbach[a,*], Markus Deutsch[b,c], Stylianos Flegkas[a], Winter Franz[b], Andreas Werner[a]

[a] TU Wien, Institute for Energy Systems and Thermodynamics, 1060 Vienna, Austria
[b] TU Wien, Institute of Chemical Engineering, 1060 Vienna, Austria
[c] BIOENERGY 2020+ GmbH, 8010 Graz, Austria

ARTICLE INFO

Keywords:
Solid state reactions
Heterogeneous kinetics
Model identification
Pressure dependency
NPK

ABSTRACT

A novel algorithm to identify the full kinetic model of solid state reactions according to the General Kinetic Equation is presented. It is a higher-order generalization of the Non-Parametric Kinetics method (NPK-method) and allows for the simultaneous identification of the conversion, temperature and pressure dependency from any combination of measurements. As a model-free identification method, it does not rely on a-priori assumptions about the kinetic model. The result vectors can be used to identify the kinetic parameters by means of model fitting for each variable independently.

The steps of the algorithm are described and its effectiveness is demonstrated by applying it to simulated datasets. The kinetic parameters could be recovered very accurately from the test data, also in the presence of noise.

Overall the higher order NPK-method is a very promising approach to derive kinetic models from experimental data with a minimum of a-priori assumptions about the reaction.

1. Introduction

For many technological applications the feasibility of solid state reactions is determined by the reaction kinetics. They directly influence important reaction parameters like the residence time and yield. Therefore, reliable kinetic models covering a wide range of process parameters are indispensable to determine the optimal reaction conditions for a given application.

The kinetics of simple solid state reactions that follow the equation

$$A(s) \rightleftharpoons B(s) + C(g) \tag{1}$$

are often modelled based on the reaction rate $\mathrm{d}\alpha/\mathrm{d}t$ as a product of the contributions of three independent variables:

$$\frac{\mathrm{d}\alpha}{\mathrm{d}t} = f(\alpha)k(T)h(p). \tag{2}$$

Here $f(\alpha)$ is the contribution of the conversion α, $k(T)$ is the contribution of the temperature T and $h(p)$ is the contribution of the partial pressure of the gaseous component p. This equation is commonly referred to as the General Kinetic Equation. It is based on the single-step approximation, which has been subject to some dispute [1,2]. Nevertheless it is a reasonable approximation for many solid state reactions and is widely used in the field of kinetic analysis.

Most publications on kinetic modelling only consider the first two terms of Eq. (2) and omit the pressure term [3]. These models are sufficient for applications with isobaric conditions, but for some reactor types, e.g. fluidized bed reactors, that feature high partial pressure gradients of the gaseous components [4] information about the pressure dependency is indispensable for reactor design. Also the modelling of batch processes, like the drying of goods, where concentration changes over time, requires the full kinetic model.

The first pressure dependency model was derived on theoretical grounds in 1968 by Barret [5] and later confirmed with different assumptions by Reading et al. [6] and Searcy et al. [7]. Most studies that have been dedicated to the systematic identification of the pressure dependency of solid state reactions, e.g. [8,9] or [10], employed a model fitting approach. The first model-free method was published by Deutsch et al. [11] as an extension of the Non-Parametric Kinetics method (NPK-method). The main advantage of this method is, that it requires no a-priori assumption about the kinetic model and that it utilizes all available data points for the identification.

The NPK-method was developed by Serra et al. [12,13]. The core insight that lead to the development of the NPK-method was that the General Kinetic Equation can be represented as a rank-1 matrix when the pressure term is neglected. The authors discretized the equation on an $(\alpha \times T)$-grid, used the Singular Value Decomposition (SVD) to compute the best rank-1 approximation of the data, which was then used to derive the kinetic model. Later, Deutsch et al. [11] introduced

---

[*] Corresponding author.
E-mail address: felix.birkelbach@tuwien.ac.at (F. Birkelbach).

https://doi.org/10.1016/j.tca.2018.01.005
Received 25 October 2017; Received in revised form 6 January 2018; Accepted 8 January 2018

Nomenclature

i	index for modes and dimensions	$\boldsymbol{M}$	matrix unfolding of a tensor
j	index for elements of a vector	N	number of dimensions/modes
k	index for sub-tensors	p	partial pressure, bar
A	pre-exponential factor, 1/s	s	singular value
c	scaling factor	T	temperature, K
E_a	activation energy, J/mol	$\boldsymbol{T}$	tensor corresponding to the General Kinetic Equation, 1/s
$f(\alpha)$	conversion dependency, 1	$\boldsymbol{t}$	generic vector
$h(p)$	pressure dependency, 1	t	time, s
I_i	number of elements in dimension i	$\boldsymbol{u}$	left singular vector
$k(T)$	temperature dependency, 1/s	$\boldsymbol{v}$	right singular vector
		α	conversion, 1
		ϵ	error parameter of the rank-1 approximation

an extension to the original method to also include the pressure dependency. They evaluated the function on an ($\alpha \times T$)-grid and on an ($\alpha \times p$)-grid. Then they used an intersection vector to combine the two results and obtain the full kinetic model.

Even though this method is capable of deriving the full kinetic model it has one considerable shortcoming: it can only process data on isobaric or isothermal planes, requiring a specific set of isobaric and isothermal measurements. This does not only limit the flexibility of the method, but can also lead to complications when data on more than two planes has to be taken into account. Then additional assumptions and deviations from the General Kinetic Equation can be necessary to incorporate the additional information into the model [11].

In this paper a general higher order, i.e. more than two variables, extension of the NPK-method is presented. It is capable of identifying the full kinetic model according to the General Kinetic Equation from any combination of measurements. With this method, it is possible to utilize a set of constant-heating-rate measurements at different partial pressures for the model identification to compute the kinetic model. This reduces the number of experiments needed to cover a wide temperature range at each pressure level.

2. Higher order rank-1 approximations

The mathematical method, which is used to compute the rank decomposition of the data matrix, in the NPK-method is the Singular Value Decomposition (SVD). If the assumption of the single step approximation holds, i.e. if the reaction follows Eq. (2), all but the first term of the SVD will be negligible and the decomposition can be truncated. The result is the best rank-1 approximation of the data matrix, consisting of two singular vectors and a singular value, that can be interpreted in terms of the general kinetic equation.

The main reason, why the NPK-method has not yet been extended to more than two variables, is that the SVD is only defined for matrices. In three (and more) variables the discretization of the general kinetic equation results in a tensor, which cannot readily be decomposed with the SVD.

In mathematics a tensor is a multidimensional array. This concept must not be confused with tensors in physics, such as stress tensors. An N-way or Nth-order tensor has N dimensions or modes. These terms are used interchangeably. An N-way tensor $\boldsymbol{T}$ is rank-1 if it can be written as the outer product of N vectors $\boldsymbol{t}$ [14]:

$$\boldsymbol{T} = \boldsymbol{t}^{(1)} \otimes \cdots \otimes \boldsymbol{t}^{(N)}. \tag{3}$$

For tensors no straight forward equivalent to the SVD to compute a low-rank approximation exists. Nevertheless, the SVD can be applied repeatedly to obtain the rank-1 approximations of a tensor, which can be interpreted as a simplification of the method published by Lathauwer et al. [15] for the special case of rank-1 approximations.

Given an N-way tensor $\boldsymbol{T} \in \mathbb{R}^{I_1 \times \cdots \times I_N}$ with I_i elements in each mode. In the first step the tensor $\boldsymbol{T}^{(1)} = \boldsymbol{T}$ is unfolded into a matrix $\boldsymbol{M}^{(1)} \in \mathbb{R}^{I_1 \times (I_2 \cdots I_N)}$ by rearranging the slices of the tensor side by side. Then the rows of the matrix correspond to the first mode of the tensor and the columns correspond to the remaining $N - 1$ modes. Fig. 1 shows the matrix unfolding of a three-way tensor.

The unfolded matrix $\boldsymbol{M}^{(1)}$ can then be decomposed with the SVD such that

$$\boldsymbol{M}^{(1)} = \sum_{j=1}^{I_1} \boldsymbol{u}_j^{(1)} s_j^{(1)} \boldsymbol{v}_j^{(1)T} \approx \boldsymbol{u}_1^{(1)} s_1^{(1)} \boldsymbol{v}_1^{(1)T}. \tag{4}$$

If the assumption of the single step approximation holds, the first singular value $s_1^{(1)}$ will be significantly larger than the following ones and the remaining terms can be neglected. Then the left singular vector $\boldsymbol{u}_1^{(1)}$ corresponds to the first mode of the tensor $\boldsymbol{T}$ and the right singular vector $\boldsymbol{v}_1^{(1)}$ to the remaining $N - 1$ modes. Its values are then rearranged in a $(N - 1)$-way tensor $\boldsymbol{T}^{(2)} \in \mathbb{R}^{I_2 \times \cdots \times I_N}$. This procedure is illustrated in Fig. 2.

This process is repeated $N - 1$ times. Each time the order of the tensor is reduced by one. At the last step the initial tensor $\boldsymbol{T}^{(1)}$ is reduced to a matrix $\boldsymbol{T}^{(N-1)} = \boldsymbol{M}^{(N-1)} \in \mathbb{R}^{I_{N-1} \times I_N}$ and the procedure is the same as for the original NPK-method. The left singular vector $\boldsymbol{u}_1^{(N-1)}$ of this matrix corresponds to the $N - 1$th mode of the tensor $\boldsymbol{T}$ and the right singular vector $\boldsymbol{v}_1^{(N-1)T} = \boldsymbol{u}_1^{(N)}$ to the Nth mode.

The rank-1 approximation of the N-way tensor $\boldsymbol{T}$ is comprised of the singular vectors $\boldsymbol{u}_1^{(1)}$ through $\boldsymbol{u}_1^{(N)}$ and the overall singular value s so

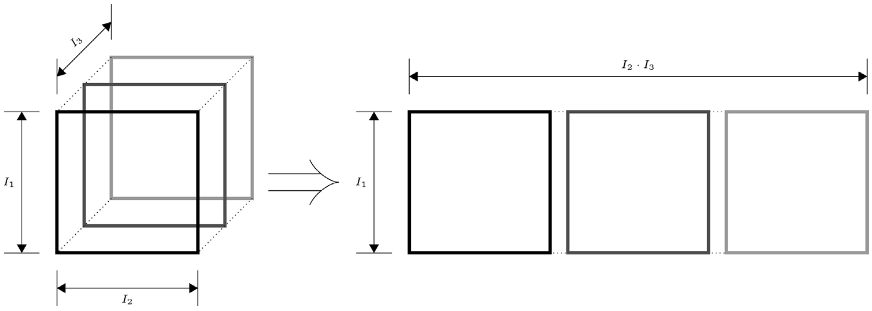

Fig. 1. Unfolding of a 3-way tensor into a matrix.

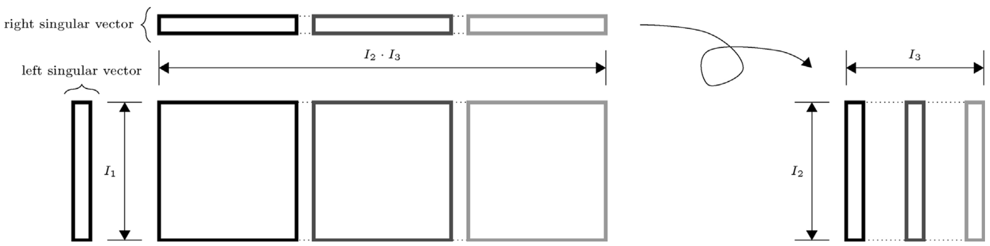

Fig. 2. SVD of the unfolded tensor and subsequent rearrangement of the right singular vector.

that

$$\boldsymbol{T} \approx s \cdot \boldsymbol{u}_1^{(1)} \otimes \cdots \otimes \boldsymbol{u}_1^{(N)} \quad \text{with} \quad s = \prod_{i=1}^{N} s_1^{(i)}. \tag{5}$$

Each singular vector corresponds to one term in the General Kinetic Equation and can be interpreted in terms of the kinetic model.

To assess the quality of the rank-1 approximation the singular value can be used. A property of the SVD is that the singular vectors are normalized. Thus, the the singular value is equal to the norm of the associated tensor/matrix. By comparing the overall singular value s to the norm of the initial tensor $\boldsymbol{T}$ a characteristic value can be computed:

$$\varepsilon = 1 - \frac{s}{\|\boldsymbol{T}\|}. \tag{6}$$

It is a measure for the amount of neglected information due to the rank-1 approximation compared to the available information. The closer this value to 0 the better the approximation.

3. Adapting the NPK-algorithm

Similarly to the SVD, the higher order rank-1 approximation can only be applied to fully occupied matrices and tensors. Since it is generally not feasible to collect enough experimental data to generate fully occupied matrices/tensors over a wide range of input variables, Serra et al. [12] developed a method to partition the data space into rectangular subspaces. These subspaces are placed in-between measured values, so that the corresponding matrices can be filled with data by interpolating between the measured values. The results of the rank-1 approximation of these matrices can then be combined to obtain the kinetic model over the full range of the input variables. The same can be done in three and more variables, but the complexity of the algorithm increases considerably.

In this section an outline of the required steps is presented to implement an automated higher order NPK analysis. The structure of the section is similar to [12] where the original NPK-method was published. There will be multiple references to this paper to avoid the repetition of concepts introduced there.

In practice, the starting point for the algorithm would be the reaction rate data at different values of α, T and p from experiments. Here a decomposition reaction following Eq. (2) was assumed to demonstrate the effectiveness of this method and to visualize the steps of the algorithm. Simulated datasets are well suited for the validation of the method, since the recovered kinetic parameters can be compared to the "true" values used in the simulation. The reaction kinetics are given by Eq. (7)–(9) and the dependency functions are shown in Fig. 3. In total 15 experiments were simulated at $p = 0.1, 0.15, 0.2, 0.3, 0.4$,bar with three heating rates each: 2, 10, 20,K/min. The data is visualized in Fig. 4 in the $(\alpha \times T \times p)$-space. The algorithm will extract the dependency functions and the corresponding kinetic parameters from the simulated data. To confirm the effectiveness of the algorithm the extracted parameters will be compared with the input parameters from Eq. (7)–(9).

$$f(\alpha) = 4(1-\alpha)[-\ln(1-\alpha)]^{3/4} \tag{7}$$

$$k(T) = 10^9 \exp\left(\frac{-6 \times 10^4}{8.314T}\right) \tag{8}$$

$$h(p) = (1-p)^4 \tag{9}$$

The algorithm is divided in four main steps: Projection onto the grid, partitioning into sub-tensors, rank-1 approximation and combination of result vectors.

In the first step the experimental data (Fig. 4) has to be projected onto a grid. This is done by interpolating between the data points under the assumption of local linearity.

First the Delaunay triangulation of the data points is computed to obtain the convex hull of the data points. The Delaunay triangulation was chosen because it has been extensively studied in Finite Elements and because it is included in most scientific computing softwares. If the

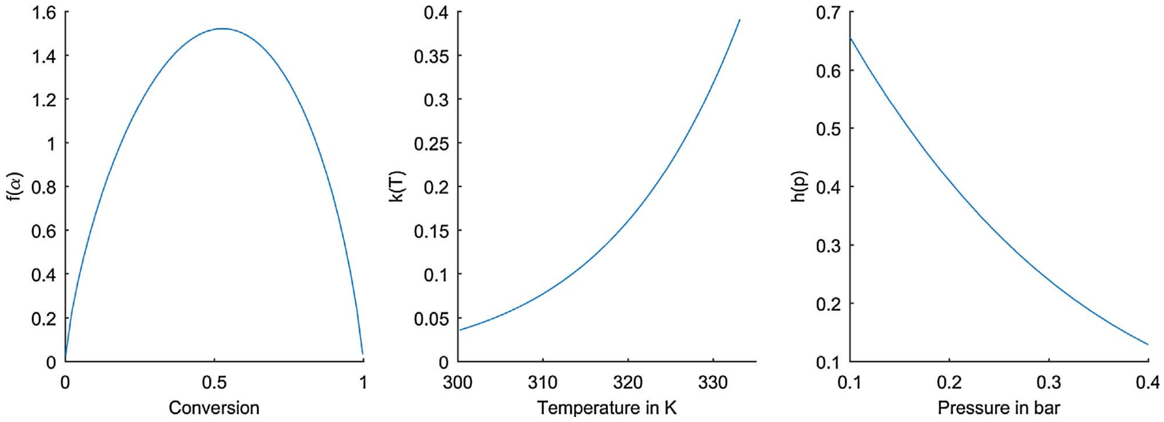

Fig. 3. The kinetic model used for the simulations.

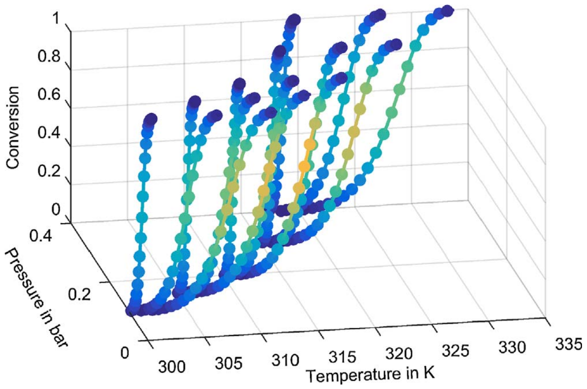

Fig. 4. Data from constant-heating-rate measurements.

data set is comprised of constant heating rate experiments (like in the example used here) the convex hull also covers grid points in the concave parts on the outside of the data space. Here interpolation is, even if it would be possible mathematically, not admissible, because these points lie outside of the data space (see [12]). These parts of the hull have to be excluded manually. Fig. 5 shows the triangulated concave hull of the data points in Fig. 4.

The triangulation is then used to project the reaction rate data onto the grid points inside the hull (see Fig. 6). Grid points, for which reaction rate data is available, will be referred to as applicable grid points.

In the second step the grid is partitioned into sub-tensors for the rank-1 approximation. These tensors have to

- contain only applicable grid points, so that they are fully occupied,
- contain as many grid points as possible to minimize the error of the rank-1 approximation and
- overlap partially so that the results of the rank-1 approximations can be combined afterwards.

Also, the union of all tensors should cover as many of the applicable grid points as possible to utilize the available information.

This step has been automated with a two-part greedy algorithm. In the first greedy part each candidate tensor is grown until it covers as many applicable grid points as possible, with the restriction that each tensor must overlap with its parent tensor. In the second part the candidate tensor covering the most not-yet-covered grid points is selected.

The algorithm is initialized with one candidate tensor in center of the applicable grid points. Then the greedy growing and selection algorithm is applied repeatedly until a sufficiently large portion of the applicable grid points is covered. Each time a tensor candidate is selected, additional candidate tensors are created on each side of the selected tensor. By establishing a hierarchical relationship between the tensors, where the selected tensor is the parent to the candidate tensors that are created on its sides, it can be ensured that the results of the the rank-1 approximations can be combined afterwards.

Even though it cannot be guaranteed that a greedy algorithm converges to an optimal solution, our tests have shown that this greedy algorithm performs very well in partitioning the applicable grid points into tensors that can be used in the following steps of the algorithm. Fig. 6 shows the first two tensors, that have been selected by the algorithm. To cover 90% of the grid in the example the decomposition algorithm created 174 tensors in total.

In the third step the higher-order rank-1 approximation described in the previous section is computed for all sub-tensors and the singular vectors and values are stored. In the final step these vectors have to be combined by computing scaling factors to arrive at the global model. For the comparably simple two-dimensional case Serra et al. [12] proposed an sequential alignment algorithm that utilizes the order of the sub-matrices. In the present multi-dimensional case no sequential algorithm can be applied, since there is no apparent order to the sub-tensors. The scaling factors have to be found for all tensors at once.

In principle this is a constrained non-linear optimization problem, but due to the large number of unknowns (number of sub-tensors times number of variables; 522 in this example) it would not be feasible to solve it directly. In the remainder of this section we will show, that the problem can be transformed to a constrained linear optimization problem, which can be solved efficiently for a large number of unknowns.

In the general case the global tensor $\boldsymbol{T}$ corresponding to the kinetic model can be expressed as

$$\boldsymbol{T} = \boldsymbol{t}^{(1)} \otimes \cdots \otimes \boldsymbol{t}^{(N)} \tag{10}$$

where each $\boldsymbol{t}^{(i)}$ corresponds to the unknown contribution of one variable. The rank-1 approximation of a sub-tensor $\boldsymbol{T}_k$, that has been computed in the previous step, can be expressed as

$$\boldsymbol{T}_k = s_k \cdot \boldsymbol{u}_k^{(1)} \otimes \cdots \otimes \boldsymbol{u}_k^{(N)} = c_k^{(1)} \boldsymbol{u}_k^{(1)} \otimes \cdots \otimes c_k^{(N)} \boldsymbol{u}_k^{(N)} \tag{11}$$

The values of each $\boldsymbol{u}_k^{(i)}$ correspond to the range of the global $\boldsymbol{t}^{(i)}$ where the tensor $\boldsymbol{T}_k$ is placed. The singular value s_k is divided into the scaling factors $c_k^{(i)}$.

All indices i refer to the modes of the tensors. The indices j refer to the elements of a vector. The indices k refer to sub-tensors. Consequently the elements of the global vectors $\boldsymbol{t}^{(i)}$ are referred to as $t_j^{(i)}$ and the elements of the singular vectors $\boldsymbol{u}_k^{(i)}$ are referred to as $u_{k,j}^{(i)}$.

The goal is to choose the scaling factors $c_k^{(i)}$ so that the deviation of each individual $u_{k,j}^{(i)}$ to the corresponding $t_j^{(i)}$ would ideally be zero

$$c_k^{(i)} u_{k,j}^{(i)} = t_j^{(i)} \quad \forall\ i, j, k \tag{12}$$

under the constraint that

$$s_k = \prod_{i=1}^{N} c_k^{(i)} \quad \forall\ k \tag{13}$$

Because the tensors are overlapping there are multiple $u_{k,j}^{(i)}$ for each unknown $t_j^{(i)}$. Let us define $t_j^{(i)}$ as the geometric mean of all corresponding $u_{k,j}^{(i)}$:

$$t_j^{(i)} = \left(\prod_{k=1}^{n} c_k^{(i)} u_{k,j}^{(i)} \right)^{\frac{1}{n}} \quad \forall\ i, j \tag{14}$$

where n is the number of tensors containing $t_j^{(i)}$.

Inserting Eq. (14) into Eq. (12) yields an overdetermined system of equations for the unknown scaling factors with the corresponding constraints from Eq. (13). Because of the choice of the geometric mean this equation system can be linearized by applying the logarithm. Then,

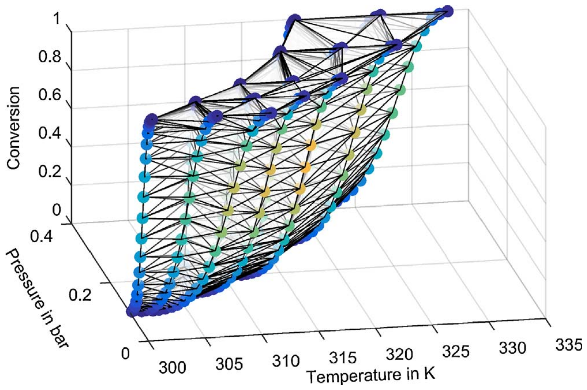

Fig. 5. Triangulation of the data points.

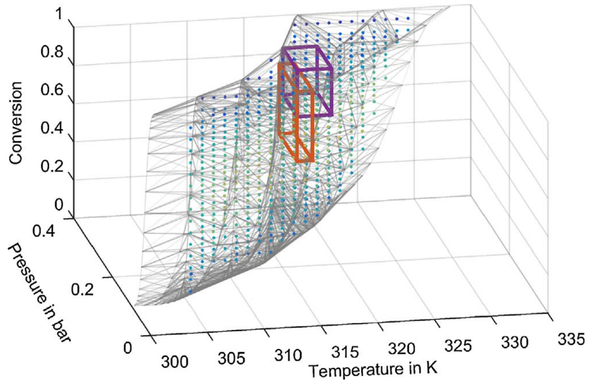

Fig. 6. Reaction rate data projected onto the grid with the first two sub-tensors.

the standard method for constrained linear least squares can be applied to find the scaling factors. Fig. 7 shows the aligned singular vectors of the sub-tensors.

Once the scaling factors have been computed, the global result vectors $\boldsymbol{t}^{(i)}$ can be calculated according to (14). Each of these vectors corresponds to one term of the General Kinetic Equation. Now the dependency of the reaction rate on the input variables can be analyzed for each variable independently.

4. Validation

In this section we will assess the effectiveness of the proposed method and take a closer look on the effect of noise on its capability to recover the model parameters.

For the noiseless case, the scaled singular vectors of the sub-tensors are displayed in Fig. 7. Since there is little deviation between the vectors, it can be concluded, that the algorithm performed as intended in partitioning the data space, decomposing the sub-tensors and aligning the partial vectors. The dashed lines in Fig. 7 represent the kinetic model from Eq. (7)–(9) that was used to simulate the data. It can be seen, that the result coincides with the input model. The recovered model parameters can therefore be expected to match the original values.

To recover the model parameters the fitting method described in [11] was used. Fitting of $f(\alpha)$ resulted in an R-value of 0.9998. The recovered Arrhenius parameters were $A = 9.99 \times 10^8\,1/\mathrm{s}$ and $E_a = 6.015 \times 10^4\,\mathrm{J/mol}$ with $R = 0.9881$. The confidence interval of these parameters was very large due to the kinetic compensation effect, though. The exponent of the pressure dependency $h(p)$ was identified as 3.937 with $R = 0.9998$. All recovered values match the input values from Eq. (7)–(9). It can therefore be concluded that the algorithm works as intended.

To assess the effect of noise on the algorithm different levels of random noise have been added to the simulated data. Then the higher order NPK method has been applied and the model parameters were recovered with the same fitting method as above. Normally distributed noise with a percentage of the peak reaction rate as standard deviation has been used. At each noise level 50 data sets were generated and processed. Fig. 8 shows the model identification diagrams of a dataset with 12% noise. The blue dots are the elements of the result vectors of the higher order NPK-method. In the conversion plot the two statistically significant reaction models are shown. In the temperature and the pressure plot the dashed black lines are the input functions for the simulation and the red lines are the fitted functions.

The identification of the reaction model was successful for all data sets. The correct model `A1` from Eq. (7) was always among the statistically significant. At higher noise levels this identification was not always unambiguous and other models, specifically `A3` and `B1`, were not rejected at a confidence level of $\alpha = 0.05$. With 8% noise 14% of the identifications were ambiguous; with 12% noise this number rose to 48%.

Fig. 9 shows the Activation Energy derived from the Arrhenius fit at different noise levels. In the noiseless case the value of the Activation Energy is extremely accurate. Yet, with increasing noise the calculated value of the Activation Energy decreases to about 95% of the true Activation Energy. At 12% noise the Arrhenius fit becomes rather unreliable, as can be seen by the big increase of the standard deviation.

The exponent of the pressure dependency model could be recovered very accurately across all noise levels with a deviation from the input value of less than 2%. This can be attributed to the large number of data points available at each pressure level.

Overall the algorithm performs well on the set of experiments used in this example, even in the presence of noise. The Arrhenius fit turned out to be the most sensitive to noise, which is not surprising considering numerical difficulties due to the strong correlation of the Activation Energy and the Arrhenius Parameter. For the Activation Energy the error remained within reasonable bounds up to a noise level of 2%. It should be kept in mind though, that these 2% are not the error of the measurements, but the residual error of the data points used as input for this algorithm (see Fig. 4). These data points are usually derived from experimental data with smoothing and regularization methods. Depending on the employed smoothing method the acceptable error of the measurements is considerably higher.

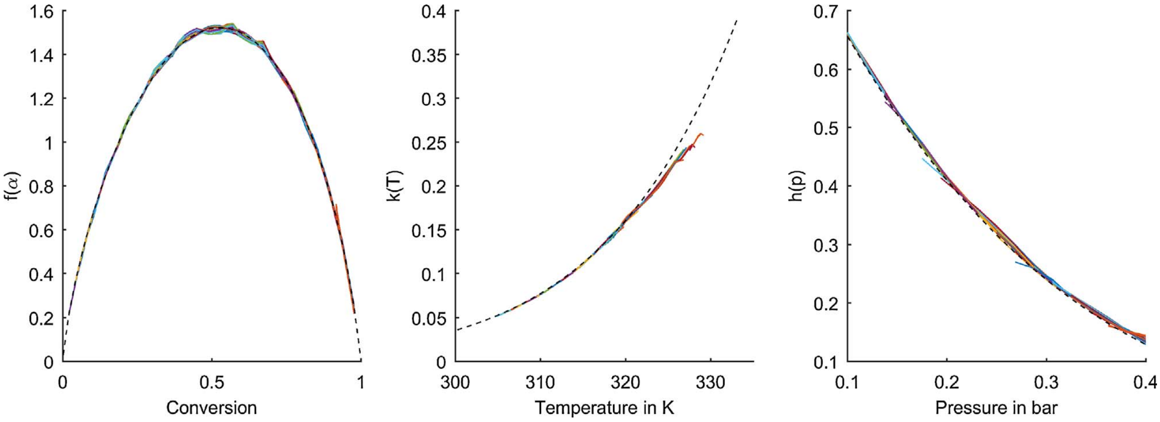

Fig. 7. The aligned partial vectors of the higher order NPK.

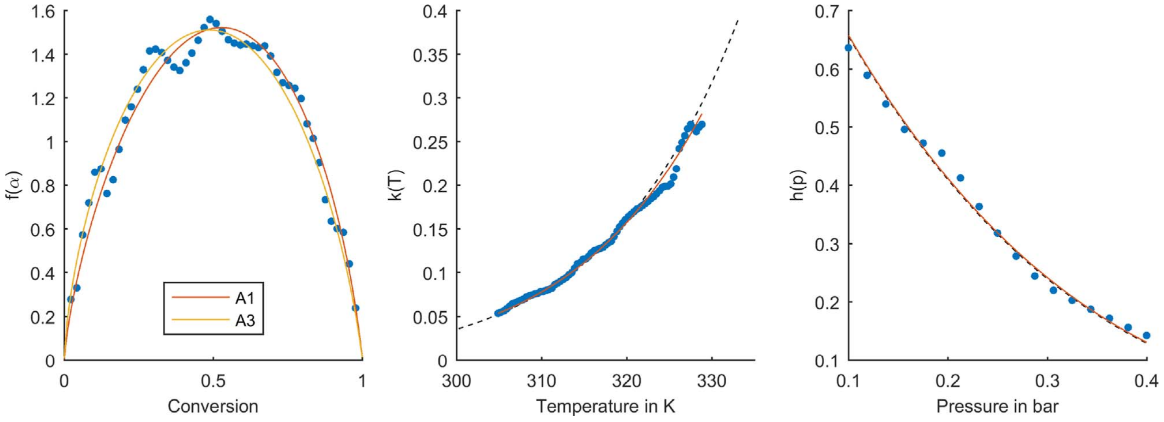

Fig. 8. Model identification of a dataset with 12% noise.

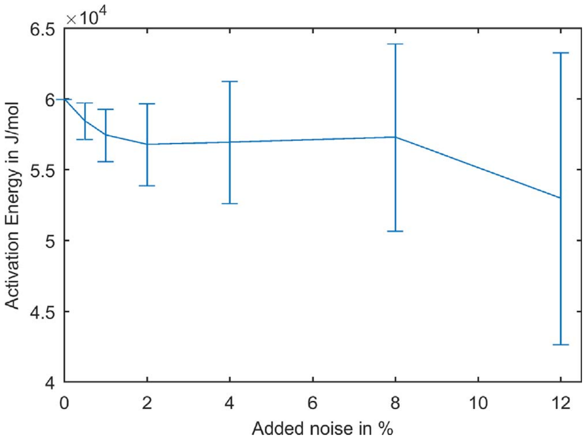

Fig. 9. Activation energy over added noise.

5. Discussion

In essence, the application of the higher order NPK-method achieved a complexity reduction for the model fitting step. Conventional model-fitting methods require the simultaneous fitting of the temperature, conversion and pressure model. Generally it is hard to select an appropriate combination of models for the fitting since there are many unforeseeable interaction effects. The higher order NPK-method decomposes the experimental data into dependency vectors according to the General Kinetic Equation. Then the model fitting can be performed for each variable independently, which is easier and generally less prone to error.

A downside of this algorithm is that the interpolation, partitioning and subsequent recombination of the data makes it impossible to provide a statistically sound error estimate of the calculated values. With this algorithm the quality of the decomposition can be assessed by considering either the overall lack-of-fit or the ε-values of each subtensor approximation. None of which can be interpreted quantitatively in terms of each individual $t_j^{(i)}$. Knowing the variance of each $t_j^{(i)}$ would be desirable to quantify the error introduced by the decomposition and to calculate weights for the model fitting steps.

A commonly voiced criticism of the NPK-method is that it involves a large amount of complex computations [16]. This also applies to the higher-order NPK-method. Especially the exclusion of invalid parts of the triangulation is complex in more than two dimensions. This is currently done manually, since attempts to automate this step yielded unreliable results. Further development is required to automate this step and make the algorithm widely applicable.

6. Conclusion

An algorithm extending the NPK-method to more than two dimensions has been presented. It can process data from experiments with arbitrary temperature and pressure profiles to derive the full kinetic model. The algorithm was applied to a set of simulated measurements with different levels of noise to verify the method. The performed tests show that the algorithm is capable of recovering the parameters of the full kinetic model accurately, also in the presence of noise.

As an extension of the NPK-method, it inherits all of its advantages and disadvantages. One major upside is that the application of the (higher order) NPK-method does not require any a-priori assumption about the reaction model, the temperature or the pressure dependency of the analyzed reaction. The only assumption is that the reaction can be approximated by a single step reaction. On the other hand, the higher order NPK-method involves a lot of complex calculations that require considerable programming and computational effort.

The main improvement of this higher order extension over the one published by Deutsch et al. is that any combination of measurements can be used for the derivation of the kinetic model, instead of a set of specific isothermal and isobaric measurements. For example it is possible to utilize a set of constant-heating-rate measurements at different partial pressures to compute the model, which reduces the number of experiments to cover a wide temperature range at each pressure level. The flexibility of this method allows to process many different sets of experiments. Extensive testing will be required to determine the most suitable combinations to derive reliable kinetic models.

The higher order NPK-method also opens up the possibility to include additional parameters in the kinetic model. The effect of any combination of variables can be investigated, since the algorithm can process arbitrarily distributed data points and does not require any a-priori assumptions about the model, besides the multiplicativity of each variable's contribution. Including different or additional parameters in the kinetic equation could be interesting for deriving more detailed kinetic models.

Overall the higher order NPK-method is a very promising approach to derive kinetic models from experimental data with a minimum of a-priori assumptions about the reaction. Research is on the way to improve the usability of the algorithm.

Acknowledgements

The authors would like to thank the Austrian Research Promotion Agency (FFG) for their financial support of the projects SolidHeat Kinetics (#848876) and SolidHeat Pressure (#853593).

References

[1] P. Simon, Considerations on the single-step kinetics approximation, J. Therm. Anal. Calorim. 82 (3) (2005) 651–657, http://dx.doi.org/10.1007/s10973-005-0945-6.

[2] M. Pijolat, L. Favergeon, M. Soustelle, From the drawbacks of the Arrhenius-f(α) rate equation towards a more general formalism and new models for the kinetic analysis of solid–gas reactions, Thermochim. Acta 525 (1–2) (2011) 93–102, http://dx.doi.org/10.1016/j.tca.2011.07.026.

[3] S. Vyazovkin, A.K. Burnham, J.M. Criado, L.A. Pérez-Maqueda, C. Popescu, N. Sbirrazzuoli, ICTAC Kinetics Committee recommendations for performing kinetic computations on thermal analysis data, Thermochim. Acta 520 (2011) 1–19, http://dx.doi.org/10.1016/j.tca.2011.03.034.

[4] S. Flegkas, F. Birkelbach, F. Winter, N. Freiberger, A. Werner, Fluidized bed reactors for solid–gas thermochemical energy storage concepts – modelling and process limitations, Energy 143 (2018) 615–623, http://dx.doi.org/10.1016/j.energy.2017.11.065.

[5] P.M. Barret, Expression théorique en fonction de la pression de la loi de vitesse de croissance d'une solide, Comp. R. hebd. séances Acad. Sci. Sér. C Sci. Chim. 266 (1968) 856–859.

[6] M. Reading, D. Dollimore, R. Whitehead, The measurement of meaningful kinetic parameters for solid state decomposition reactions, J. Therm. Anal. 37 (9) (1991) 2165–2188, http://dx.doi.org/10.1007/BF01905585.

[7] A.W. Searcy, D. Beruto, Kinetics of endothermic decomposition reactions: 2. Effects of the solid and gaseous products, J. Phys. Chem. 82 (2) (1978) 163–167, http://dx.doi.org/10.1021/j100491a008.

[8] J.M. Criado, M. González, J. Málek, A. Ortega, The effect of the CO_2 pressure on the thermal decomposition kinetics of calcium carbonate, Thermochim. Acta 254 (1995) 121–127, http://dx.doi.org/10.1016/0040-6031(94)01998-V.

[9] Y.A. Criado, M. Alonso, J.C. Abanades, Kinetics of the $CaO/Ca(OH)_2$ hydration/dehydration reaction for thermochemical energy storage applications, Ind. Eng. Chem. Res. 53 (32) (2014) 12594–12601, http://dx.doi.org/10.1021/ie404246p.

[10] F. Schaube, L. Koch, A. Wörner, H. Müller-Steinhagen, A thermodynamic and kinetic study of the de- and rehydration of $Ca(OH)_2$ at high H_2O partial pressures for thermo-chemical heat storage, Thermochim. Acta 538 (2012) 9–20, http://dx.doi.org/10.1016/j.tca.2012.03.003.

[11] M. Deutsch, F. Birkelbach, C. Knoll, M. Harasek, A. Werner, F. Winter, An extension of the NPK method to include the pressure dependency of solid state reactions, Thermochim. Acta 654 (2017) 168–178, http://dx.doi.org/10.1016/j.tca.2017.05.019.

[12] R. Serra, J. Sempere, R. Nomen, A new method for the kinetic study of thermoanalytical data, Thermochim. Acta 316 (1) (1998) 37–45, http://dx.doi.org/10.1016/S0040-6031(98)00295-0.

[13] R. Serra, R. Nomen, J. Sempere, The non-parametric kinetics a new method for the kinetic study of thermoanalytical data, J. Therm. Anal. Calorim. 52 (3) (1998) 933–943, http://dx.doi.org/10.1023/A:1010120203389.

[14] F.L. Hitchcock, The expression of a tensor or a polyadic as a sum of products, J. Math. Phys. 6 (1–4) (1927) 164–189, http://dx.doi.org/10.1002/sapm192761164.

[15] L.D. Lathauwer, B. de Moor, J. Vandewalle, A multilinear singular value decomposition, SIAM J. Matrix Anal. Appl. 21 (4) (2000) 1253–1278, http://dx.doi.org/10.1137/S0895479896305696.

[16] J.D. Sewry, M.E. Brown, "Model-free" kinetic analysis? Thermochim. Acta 390 (1–2) (2002) 217–225, http://dx.doi.org/10.1016/S0040-6031(02)00083-7.

Paper 2

NPK 2.0: Introducing tensor decompositions to the kinetic analysis of gas-solid reactions

published in the International Journal of Chemical Kinetics in collaboration with Markus Deutsch, Stylianos Flegkas, Franz Winter and Andreas Werner.

In this paper the TensorNPK method is presented and two algorithms for computing models are assessed.

Even though the higher-order generalization of the NPK method, which was presented in Paper 1, could technically model kinetic data the way we wanted it to, its stability and usability was unsatisfactory. To overcome the limitations of the higher-order generalization of the NPK method, the mathematical basis of the NPK method was revised. Tensor decomposition methods emerged as a powerful alternative to the Singular Value Decomposition, since they can deal with missing data points directly. Two algorithms to compute the tensor decomposition are presented and evaluated: Alternating Least Squares and Non-linear Least Squares. Even though both algorithms were able to recover the kinetic model from simulated data very accurately, the latter converged much faster.

The TensorNPK method fulfilled all our requirements: It can derive models in any number of variables, process arbitrarily distributed data sets and is robust. We had developed a modeling method that was fit to be applied in kinetic studies.

My contribution: Development of the tensor NPK method, implementing the algorithm in Matlab and testing it. Evaluation of the algorithm and the tensor NPK method. Drawing up and writing of the paper.

F. Birkelbach, M. Deutsch, S. Flegkas, F. Winter, and A. Werner (2019a). "NPK 2.0: Introducing tensor decompositions to the kinetic analysis of gas-solid reactions". In: International Journal of Chemical Kinetics *51.4, pp. 280–290.* ISSN*: 05388066.*
DOI*: `10.1002/kin.21251`*

Received: 2 July 2018 | Revised: 9 January 2019 | Accepted: 9 January 2019
DOI: 10.1002/kin.21251

ARTICLE

WILEY

NPK 2.0: Introducing tensor decompositions to the kinetic analysis of gas–solid reactions

Felix Birkelbach[1] | Markus Deutsch[2] | Stylianos Flegkas[1] | Franz Winter[3] | Andreas Werner[1]

[1]TU Wien, Institute for Energy Systems and Thermodynamics, Vienna, Austria

[2]BIOENERGY 2020+ GmbH, Graz, Austria

[3]TU Wien, Institute of Chemical, Environmental and Bioscience Engineering, Vienna, Austria

Correspondence
Felix Birkelbach, TU Wien, Institute for Energy Systems, and Thermodynamics, Getreidemarkt 9/E302, 1060 Vienna, Austria.
Email: felix.birkelbach@tuwien.ac.at

Funding information
Austrian Research Promotion Agency (FFG), SolidHeat Kinetics (#848876) and SolidHeat Pressure (#853593)

Abstract

A method for deriving kinetic models of gas–solid reactions for reactor and process design is presented. It is based on the nonparametric kinetics (NPK) method and resolves many of its shortcomings by applying tensor rank-1 approximation methods. With this method, it is possible to derive kinetic models based on the general kinetic equation from any combination of experiments without additional a priori assumptions. The most notable improvements over the original method are that it is computationally much simpler and that it is not limited to two variables. Two algorithms for computing the rank-1 approximation as well as a tailored initialization method are presented, and their performance is assessed. Formulae for the variance estimation of the solution values are derived to improve the accuracy of the model identification and to provide a tool for diagnosing the quality of the kinetic model. The methods effectiveness and performance are assessed by applying it to a simulated data set. A Matlab implementation is available as Supporting Information.

KEYWORDS

gas–solid reactions, heterogeneous kinetics, model identification, nonparametric kinetics, pressure dependency, tensor decomposition

---

Abbreviation: NPK, nonparametric kinetics; SVD, singular value decomposition

Nomenclature: Cov, covariance; $d_{j_1,\dots,j_D}$, element of the data tensor; D, number of dimensions; $d\alpha/dt$, reaction rate, 1/s; E, error function; $f(\alpha)$, conversion dependency, 1; $f_i(v_i)$, contribution of v_i; f_{i,j_i}, element of $\boldsymbol{f}_i$; $\boldsymbol{f}$, vector of unknowns of the full problem; $\boldsymbol{f}_i$, vector of values of $f_i(v_i)$; $\boldsymbol{f}'$, vector of unknowns of the reduced problem; $\boldsymbol{H}$, Hessian matrix; $h(p)$, pressure dependency, 1; i, index for dimensions; $\boldsymbol{J}$, Jacobian matrix; j, index for elements; j_i, index of an element in dimension i; $j_1, \dots, j_D$, index of an element of a D-dimensional tensor; K, scaling factor of the reduced problem; $k(T)$, temperature dependency, 1/s; MSE, mean square error; N_e, number of tensor elements; N_m, number of missing elements; N_p, number of unknown parameters; p, partial pressure, bar; $\boldsymbol{r}$, vector of residuals; $r_{j_1,\dots,j_D}$, element of the residual vector; SEE, standard error of estimate; T, temperature, K; t, time, s; $\widetilde{\mathcal{T}}$, model tensor; $\tilde{t}_{j_1,\dots,j_D}$, element of the model tensor; $\mathcal{T}$, data tensor; v_i, independent variable; $\boldsymbol{v}_i$, vector of values of v_i; v_{i,j_i}, element of $\boldsymbol{v}_i$; Var, variance; $\boldsymbol{W}$, weight matrix; $\mathcal{W}$, weight tensor; $w_{j_1,\dots,j_D}$, element of the weight tensor; α, conversion, 1; Δ, small difference; ∇, nabla operator

1 | INTRODUCTION

Gas–solid reactions are relevant to many technological applications such as thermochemical energy storage.[1,2] Kinetic models of these reactions are indispensable for process and reactor design, as the reaction rate influences important parameters like the residence time and yield. To determine optimal reaction conditions for a given application, reliable kinetic models over a wide range of relevant process parameters are required.

This paper will focus on reactions that follow the equation

$$\mathrm{A(s)} + \Delta H \rightleftharpoons \mathrm{B(s)} + \mathrm{C(g)}, \qquad (1)$$

where A and B are solid species and C is a gas.

Gas–solid reactions of this type are inherently complex, because the reactants cannot mix indefinitely. The reaction takes place at the reaction interface in the solid, and the advancement of the reaction front in the solid has to be considered. Gas–solid reactions feature an entangled interplay of various physical and chemical processes, such as mass transfer from the gas bulk to the solid surface, adsorption of the gas at the surface, nucleation, diffusion through the product layer, and the chemical reaction itself, which generally involves a series of elementary reactions. Often it is not practical, if even possible, to model all these processes in detail. An extensive discussion of the processes involved in a gas–solid reaction, as well as a critical assessment of the modeling assumptions commonly made, has been published by Brown et al.[3] Especially when computation time is an issue for simulations on a macro scale, such as of reactors, simple models that can predict the reaction with sufficient accuracy are required.

The most common simplification, the “single rate limiting step” assumption, is applicable if one process proceeds much slower than all the other ones. Then, the effect of the advancement of the reaction front on the reaction rate can be derived as a function of conversion, based on certain mechanistic assumptions about the reaction. These functions are usually referred to as reaction models. A comprehensive review has been published by Khawam and Flanagan.[4] To describe the effect of temperature[5,6] and the concentration of the gaseous reactant[7–9] on the reaction rate, two more terms are included in analogy to the theory of homogeneous reactions.

This leads to the general kinetic equation, which describes the reaction rate $d\alpha/dt$ as the product of the contributions of the conversion α, the temperature T and the partial pressure of the gaseous component p:

$$\frac{d\alpha}{dt} = f(\alpha)\,k(T)\,h(p). \qquad (2)$$

where $f(\alpha)$ is often referred to as conversion dependency or reaction model, $k(T)$ as temperature dependency or rate constant and $h(p)$ as pressure dependency. A key feature of this equation is that the contributions of all variables are independent of each other. The underlying assumption is that the overall reaction can be modeled as a single, rate-determining reaction step. Accordingly, applying this equation to model gas–solid reactions is referred to as the single-step approximation.

The numerous assumptions and simplifications involved in deriving the general kinetic equation have been criticized, and it has been questioned, whether the model parameters can be interpreted mechanistically.[10–12] Also, due to the many different processes involved in a gas–solid reaction, the rate-limiting step can change, depending on the reaction conditions. Then, the single-step approximation is only valid in the temperature and pressure interval, where one step is dominant. Since these intervals can generally only be determined by experiments, extrapolation of kinetic models has to be done with care. Nevertheless, the general kinetic equation is the most commonly applied formula to describe the reaction rate of gas–solid reactions.

A multitude of methods have been developed to derive kinetic models from experimental data according to the general kinetic equation. A summary of the most relevant methods has been published by Vyazovkin et al.[13] One of the more recent methods for the derivation of kinetic models is the nonparametric kinetics (NPK) method by Serra et al.[14] Its main advantage is that is does not require any modeling assumptions besides the general kinetic equation, but it has some shortcomings that limit its applicability.

In this paper, we first discuss the advantages and shortcomings of the original NPK method. Then, after introducing the mathematics of tensor rank-1 approximation methods with missing values, we present two implementations of the new NPK method. The first, alternating least squares (ALS), exploits the blockwise linearity of the problem. In the second, nonlinear least squares (NLS), established optimization methods in combination with analytically computed Jacobians are used to compute the approximation. Then, we describe a tailored initialization method and assess the performance of the algorithms. In the last section, we discuss the interpretation of the output of the new NPK method in the context of kinetic modeling and outline new possibilities opening up through the application of the proposed algorithm.

2 | THE NPK METHOD

The NPK method by Serra et al.[14] is a data-driven method, which is based on the observation that the discretization of the general kinetic equation on a $(\alpha \times T)$ grid results, by definition, in a rank-1 matrix. When experimental reaction rates are arranged in a matrix, the singular value decomposition (SVD) can be applied to compute the rank-1 approximation. Then the singular vectors will correspond to the contributions $k(T)$ and $f(\alpha)$.

The main advantage of the NPK method is that it allows the separation of the contributions $f(\alpha)$ and $k(T)$ without a priori assumptions about the reaction model or the temperature dependency. Models are selected and parameterized after the separation, independently for each variable, by fitting the contribution vectors. This is generally much easier and less prone to error, compared to direct model-fitting methods, where a combination of models is fitted directly to the experimental data.

However, there are three drawbacks that limit the applicability of the NPK method. The first drawback, its algorithmic complexity, has already been criticized as the most limiting factor of the NPK method.[15] It can be attributed to the fact that the SVD is restricted to fully occupied matrices. Yet, if constant heating rate experiments are used, it is usually infeasible to collect enough data to obtain fully occupied matrices. As a remedy, Serra et al.[14] devised a method to partition the data space into smaller subspaces, where matrices can be filled by linear interpolation. The solution can then be assembled from the singular vectors of the submatrices. However, as a result of this procedure, the algorithmic complexity of the NPK method is quite high. An efficient method for the model identification should therefore be able to deal with missing data directly.

Second, the NPK method is restricted to two independent variables, which is a shortcoming that it shares with many other established methods.[13] As a consequence, the pressure term in Equation 2 has to be omitted. The resulting models are adequate for processes, where the partial pressure of the gaseous component can be regarded constant. For applications, where the concentration changes over time (e.g., batch processes) or over the reactor height (e.g., in fluidized bed reactors[2]) the full kinetic model, including the pressure term, is required. Most studies that include a systematic identification of the pressure dependency of gas–solid reactions employed a model-fitting approach.[16–18] Recently model free approaches based on the NPK method have been proposed,[19,20] but their algorithmic complexity is even higher than of the original NPK method.

The third shortcoming is related to the model-fitting step: It is not possible to estimate the variance of the solution values. The implicit assumption is that all elements of the solution vectors have the same variance, even though there may be structural causes for unequal variance, like the distribution of data points or correlation of variables. If the variance is not taken into account in the model-fitting step by weighting the values accordingly, the result can be inaccurate.

In this paper, a reworked NPK method is presented that resolves the shortcomings described in the preceding paragraphs. It can derive the kinetic model in any number of variables from experimental data. Like the original NPK method, it is a model-free method that does not require any a priori assumptions about the model, but unlike its predecessors it can process missing values directly. This is achieved by switching from the SVD to tensor decomposition methods, which greatly reduces the algorithmic complexity and improves the methods' efficiency and robustness. Since the result vectors of the NPK method are often used to parameterize models by means of least squares fitting, formulae for estimating the variance of the solution values are derived, to calculate weights for the model-fitting step.

3 | TENSOR RANK-1 APPROXIMATION

In mathematics, a tensor is a multidimensional array, i.e. a higher dimensional generalization of matrices (matrices can be considered two-dimensional tensors). To compute the low-rank approximation of matrices the SVD can be used, but no single equivalent for tensors exists. Instead, a multitude of decompositions for different purposes have been developed. Many of these methods originated in psychometrics[21] and have become widely used in the field of chemometrics[22] among others. An extensive review has been published by Kolda and Bader,[23] a review with focus on applications of tensor decompositions in chemistry by Bro.[24]

The most relevant type of tensor decomposition for this paper is usually referred to as CANDECOMP (canonical decomposition) or PARAFAC (parallel factors). Methods based on this decomposition have not been applied for the kinetic analysis of gas–solid reactions to date, even though they do have many advantages over the SVD in the original NPK method by Serra et al.[14] and the higher order generalization by Birkelbach et al.[20] Most notably, some of these methods can deal with missing values and are therefore not limited to fully occupied matrices. This eliminates the need for the subspace decomposition and subsequent realignment of the result vectors, which in turn does not only decrease the computational cost and improve the robustness of the algorithm, but also allows to compute statistically sound variance estimates of the output values.

Throughout this paper, the following formalism is used: Vectors are written in bold lower-case letters $\boldsymbol{v}$, tensors in calligraphic letters $\mathcal{T}$. Throughout this paper, the index i is used to refer to dimensions and j is used to refer to elements of vectors or tensors. Consequently, j_i is the element index in dimension i and the index $j_1, \dots, j_D$ points to one specific element of a D-dimensional tensor.

The underlying assumption for this method regarding the chemistry is that the reaction rate of gas–solid reactions can be modeled as the multiplication of the contributions of D independent variables v_i:

$$\frac{d\alpha}{dt}(v_1, \dots, v_D) = \prod_{i=1}^{D} f_i(v_i). \tag{3}$$

Here, $f_i(v_i)$ are the unknown contributions of the variables v_i. Typically, these would be $f(\alpha)$, $k(T)$ and $h(p)$ from Equation 2. In other words: Equation 3 is a generalization of the general kinetic equation for an arbitrary number of contributions. The goal of the algorithm is to derive these contributions from experimental data.

First the interval of each variable v_i is discretized into N_i elements. The resulting vectors $\boldsymbol{v}_i = [v_{i,j_i}]^T$ with $j_i \in [1, N_i]$ span the data space $(\boldsymbol{v}_1 \times \cdots \times \boldsymbol{v}_D)$. Evaluating Equation 3 on the data space and arranging the values in the model tensor $\widetilde{\mathcal{T}}$ yields

$$\widetilde{\mathcal{T}} = \left.\frac{d\alpha}{dt}\right|_{\boldsymbol{v}_1\times\cdots\times\boldsymbol{v}_D} = \boldsymbol{f}_1 \otimes \cdots \otimes \boldsymbol{f}_D \tag{4}$$

where each tensor element can be expressed as

$$\tilde{t}_{j_1,\dots,j_D} = \prod_{i=1}^{D} f(v_{i,j_i}) = \prod_{i=1}^{D} f_{i,j_i}. \tag{5}$$

Here, $\boldsymbol{f}_i = [f_i(v_{i,j_i})]^T = [f_{i,j_i}]^T$ are the vectors corresponding to the unknown contributions of the variable v_i and $\otimes$ denotes the outer vector product.

A D-dimensional tensor is rank-1 if it can be written as the outer product of D vectors.[25] Thus, Equation 4 shows that the tensor $\widetilde{\mathcal{T}}$ is of rank 1, as a consequence of the multiplication of the contributions in Equation 3. This tensor has $N_e = \prod_{i=1}^{D} N_i$ elements, and the contribution vectors have $N_p = \sum_{i=1}^{D} N_i$ elements. These N_p elements are the unknowns of the rank-1 approximation problem.

To compute the contributions $f_i(v_i)$, the experimental data are arranged in the data tensor $\mathcal{T} = [d_{j_1,\dots,j_D}]$. This tensor also has N_e elements, of which some (N_m) may be missing. The goal of the rank-1 approximation is to find the rank-1 tensor $\widetilde{\mathcal{T}}$ that best resembles the data tensor $\mathcal{T}$. Then each of the vectors $\boldsymbol{f}_i$ can be interpreted in terms of the kinetic model.

In mathematical terms, the goal is to minimize the distance $\|\cdot\|$ between the two tensors.

$$\text{minimize } \|\widetilde{\mathcal{T}} - \mathcal{T}\| \quad \text{s.t.} \quad \widetilde{\mathcal{T}} = \boldsymbol{f}_1 \otimes \cdots \otimes \boldsymbol{f}_D. \tag{6}$$

The distance is calculated with the Frobenius, i.e. , the elementwise square, norm. To take missing values into account, this formalism is extended by a weight tensor $\mathcal{W}$ that contains the weights associated with each tensor element. The squared distance is then given by

$$\|\widetilde{\mathcal{T}} - \mathcal{T}\|^2_{\mathcal{W}} = \sum_{\forall[j_1,\dots,j_D]} w_{j_1,\dots,j_D}\left(\tilde{t}_{j_1,\dots,j_D} - d_{j_1,\dots,j_D}\right)^2. \tag{7}$$

The weights may be any positive number, determining the impact of the associated tensor element on the approximation. The weights of missing values must be zero, so that they do not affect the approximation. The weights of available tensor elements should reflect their uncertainty. Only if the weights are equal to the inverse of the variance, the result of the approximation will be optimal in the sense of minimum variance. If the variance is unknown, it is common to set the weights to 1, which amounts to the assumption of equal variance.

4 | ALTERNATING LEAST SQUARES

This algorithm was developed by Carroll and Chang[26] and Harshman.[27] Because of its simplicity, it is the most commonly applied algorithm, even though it generally takes many iterations to converge.

In the ALS algorithm, at each step all but one result vector $\boldsymbol{f}_i$ are held constant. Using this approach, the problem of finding the optimal values f_{i,j_i} is reduced to a series of linear least squares problems that can be solved with conventional methods:

$$\underset{f_{i,j_i}}{\arg\min}\ \|\mathcal{T}_{i,j_i} - f_{i,j_i}\mathcal{T}_i^*\|_{\mathcal{W}_{i,j_i}} \qquad \forall f_{i,j_i} \tag{8}$$

Here $\mathcal{T}_{i,j_i}$ denotes the j_ith slice of $\mathcal{T}$ in dimension i, i.e. the slice that corresponds to the unknown f_{i,j_i} and $\mathcal{T}_i^*$ is the tensor product of all constant $\boldsymbol{f}$, i.e., all but $\boldsymbol{f}_i$.

To use standard linear least squares formulae, the tensor values have to be arranged in column vectors. This is denoted with an arrow. Values corresponding to zero weights are omitted, to avoid matrix singularity.

$$f_{i,j_i} = \left[\overrightarrow{\mathcal{T}_i^*}^T \operatorname{diag}\left(\overrightarrow{\mathcal{W}}_{i,j_i}\right)\overrightarrow{\mathcal{T}_i^*}\right]^{-1}\overrightarrow{\mathcal{T}_i^*}^T \operatorname{diag}\left(\overrightarrow{\mathcal{W}}_{i,j_i}\right)\overrightarrow{\mathcal{T}}_{i,j_i} \tag{9}$$

Optimal values are computed in a circular fashion until a convergence criterion is met. No sophisticated optimization methods are required, but some have been suggested Ref. [30].

Once the rank-1 approximation has been computed, the mean square error (MSE) is given by

$$MSE = \frac{\|\widetilde{\mathcal{T}} - \mathcal{T}\|^2_{\mathcal{W}}}{N_e - N_m - N_p} \tag{10}$$

and the variance of the parameters can be estimated with

$$\operatorname{Var}(f_{i,j_i}) = MSE\left[\overrightarrow{\mathcal{T}_i^*}^T \operatorname{diag}\left(\overrightarrow{\mathcal{W}}_{i,j_i}\right)\overrightarrow{\mathcal{T}_i^*}\right]^{-1}. \tag{11}$$

5 | NONLINEAR LEAST SQUARES

The rank-1 approximation problem can also be interpreted as a general NLS optimization problem, where all unknown parameters are optimized simultaneously. This approach has been proposed by Paatero[28] and Tomasi and Bro.[29] Even though it is generally more memory and calculation expensive than the ALS algorithm, it tends to converge much faster. Depending on the optimization algorithm, even quadratic convergence rates can be achieved.

The goal is to minimize the error given by the objective function

$$E(\boldsymbol{f}) = \frac{1}{2}\|\tilde{\mathcal{T}} - \mathcal{T}\|^2_{\mathcal{W}} = \frac{1}{2}\boldsymbol{r}(\boldsymbol{f})^T \boldsymbol{W}\boldsymbol{r}(\boldsymbol{f}). \tag{12}$$

Here $\boldsymbol{f}$ is the column vectors of all unknown f_{i,j_i} with N_p elements, $\boldsymbol{r}$ is the vector of residuals

$$r_{j_1,\ldots,j_D}(\boldsymbol{f}) = \prod_{i=1}^{D} f_{i,j_i} - d_{j_1,\ldots,j_D} \qquad \forall d_{j_1,\ldots,j_D} \tag{13}$$

with one element per element in the data tensor $\mathcal{T}$, i.e., $N_e - N_m$, elements and $\boldsymbol{W}$ is the diagonal matrix of the weights of all available tensor elements.

Most optimization methods are based on a truncated tailor expansion of the objective function to find the optimum. They require the Jacobian of the problem to calculate the normal equations. For Equation 12, the problem is ill-posed: The scaling indeterminacy of the rank-1 approximation results in an infinite number of equivalent solutions, which causes the Hessian to be singular. Some authors, e.g., Paatero,[28] proposed to deal with this issue by introducing a regularization parameter. In the case of rank-1 approximations, the singularity can also easily be avoided by reformulating the objective function. Using this approach, the adapted NLS problem can be solved directly. No update strategy for the regularization terms has to be devised, and no distortion of the solution due to the regularization terms has to be accepted.

A D-dimensional rank-1 tensor approximation has $(D-1)$ surplus degrees of freedom, which need to be eliminated to avoid singularity of the normal equations. By choosing a reference point $(j_1^*, \ldots, j_D^*)$ and defining a global scaling factor $K = \prod_{i=1}^{D} f_{i,j_i^*}$, the residuals can be calculated with

$$r_{j_1,\ldots,j_D}(\boldsymbol{f}') = K\prod_{i=1}^{D} f'_{i,j_i} - d_{j_1,\ldots,j_D} \quad \text{with} \quad f'_{i,j_i} = \frac{f_{i,j_i}}{f_{i,j_i^*}}. \tag{14}$$

This will be referred to as the "reduced" problem $E(\boldsymbol{f}')$, since it only contains $N_p - D + 1$ unknown parameters $\boldsymbol{f}' = [f'_{i,j_i}, K]$ with $j_i \neq j_i^*$.

Using the nabla operator as a shorthand for the partial derivatives with respect to the unknown parameters, the Jacobian is then given by $\boldsymbol{J}(\boldsymbol{f}') = \nabla\boldsymbol{r}(\boldsymbol{f}')^T$ with

$$\frac{\partial r_{j_1,\ldots,j_D}(\boldsymbol{f}')}{\partial f'_{d,n}} = \begin{cases} 0 & \text{for } j_d \neq n \\ K\prod\limits_{\substack{i=1\\ i\neq d}}^{D} f'_{i,j_i} & \text{for } j_d = n \end{cases} \tag{15}$$

$$\frac{\partial r_{j_1,\ldots,j_D}(\boldsymbol{f}')}{\partial K} = \prod_{i=1}^{D} f'_{i,j_i}. \tag{16}$$

Two things can be noticed here: First, there will be many structural zero elements in the Jacobian (first line in Equation 15). Each line contains $N_p - D + 1$ elements but only $D + 1$ nonzero elements. Second, there are many repeated elements in the Jacobian (second line in Equation 15). Both properties can be exploited to compute the Jacobian more efficiently: Since there are so many repeated elements, it suffices to calculate a vector of unique Jacobian values that is then used to assemble the Jacobian. Also, the high number of structural zero values indicates sparse matrix storage. The positions of nonzero elements in the Jacobian does not change during the iteration, because they are determined by the availability of measured data. Therefore, the positions as well as the references to the associated unique Jacobian values can be computed beforehand. During the iteration, each unique value needs only be computed once and the Jacobian can be assembled from this vector of unique values with minimum computational effort. Since the Jacobian needs to be computed at every step of the optimization algorithm, this reduces the computational cost considerably. For more details about the implementation, we refer the interested reader to the code, that is included in the Supporting Information, specifically the functions `getJacobianSparseArgs` and `lsqnonlinFun`.

After computing the solution with any optimization algorithm, the variance-covariance matrix $\boldsymbol{D}$ of the parameters $\boldsymbol{f}'$ at the solution can be estimated with

$$MSE = \frac{\|\tilde{\mathcal{T}} - \mathcal{T}\|^2_{\mathcal{W}}}{N_e - N_m - N_p - D + 1} \tag{17}$$

and

$$\boldsymbol{D}(\boldsymbol{f}') = MSE\,\boldsymbol{H}(\boldsymbol{f}')^{-1} \approx MSE\left[\boldsymbol{J}(\boldsymbol{f}')^T \boldsymbol{W}\boldsymbol{J}(\boldsymbol{f}')\right]^{-1}. \tag{18}$$

Here, the Hessian $\boldsymbol{H}$ has been replaced with its first-order approximation. This approximation is reasonable if the residuals are small, since

$$\boldsymbol{H} = \boldsymbol{J}^T\boldsymbol{W}\boldsymbol{J} + \sum_{\forall [j_1,\ldots,j_D]} w_{j_1,\ldots,j_D} r_{j_1,\ldots,j_D} \nabla^2 r_{j_1,\ldots,j_D}. \tag{19}$$

This means that, if the model fits the data, the estimated variance will be accurate.

The main diagonal of $\boldsymbol{D}$ contains the variances of the parameters $\mathrm{Var}(f'_{i,j_i})$ and $\mathrm{Var}(K)$. The last column/row contains the covariances $\mathrm{Cov}(f'_{i,j_i}, K)$. These values can be used to estimate the variance of the parameters of the full model by assuming linear error propagation:

$$\frac{\mathrm{Var}(f_{i,j_i})}{f_{i,j_i}^2} = \begin{cases} \dfrac{\mathrm{Var}(K)}{K^2} & \text{for } j_i = j_i^* \\ \dfrac{\mathrm{Var}(K)}{K^2} + \dfrac{\mathrm{Var}(f'_{i,j_i})}{f'^2_{i,j_i}} + 2\dfrac{\mathrm{Cov}(f'_{i,j_i}, K)}{f'_{i,j_i} K} & \text{for } j_i \neq j_i^* \end{cases} \tag{20}$$

6 | INITIAL ESTIMATE

Both proposed algorithms require a starting value for the solution vectors $\boldsymbol{f}_i$. The closer the starting value is to the solution, the faster the algorithm will converge. If the starting value is far away from the solution, the algorithm might not converge at all. Therefore, it is paramount to provide an initial estimate of the rank-1 decomposition that is as close as possible to the solution.

The most common way to initialize the algorithm is to simply use random starting values. Of course, there is no guarantee that these values are anywhere near the solution. A method tailored to the specific problem at hand would be preferable. Kinetic models according to the general kinetic equation have an important property that can be exploited to calculate good starting values: Since always only one reaction direction is considered, the reaction rate $d\alpha/dt$, and as a consequence, the values of the contribution functions, are always greater or equal to zero.

The requirement that the model fit the experimental data can be formulated as an overdetermined system of nonlinear equations:

$$\prod_{i=1}^{D} f_{i,j_i} \overset{!}{=} d_{j_1,\dots,j_D} \qquad \forall [j_1, \dots, j_D]. \tag{21}$$

Since all values are greater than zero, the logarithm can be applied to convert Equation 21 into an overdetermined system of $N_e - N_m$ linear equations with N_p unknowns. Similarly to the NLS algorithm, the scaling indeterminacy results in $D - 1$ surplus degrees of freedom that will cause the system of equations to be singular. This can be avoided by fixing one element of all but the last solution vector $\boldsymbol{f}_i$. Then the solution can be computed with ordinary least squares.

This method allows to calculate an initial estimate to the rank-1 approximation problem very quickly and easily. The result may be distorted, though, because the logarithm causes values close to zero to be weighted more heavily than larger ones. This also results in an overproportional error amplification at values close to zero, since $\Delta \log(d) \approx \Delta d/d$. Therefore, values close to zero need to be excluded when calculating the initial estimate with this method.

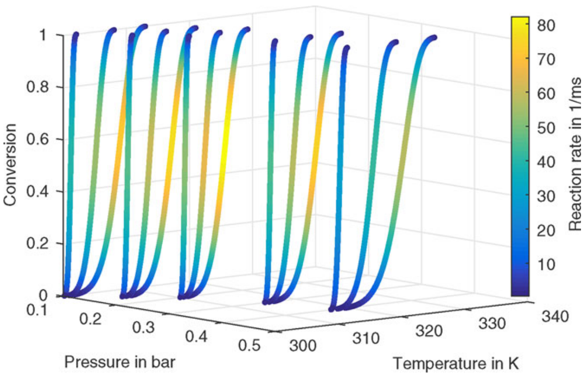

FIGURE 1 Test data set consisting of 15 constant heating rate measurements[19] [Color figure can be viewed at wileyonlinelibrary.com]

7 | PERFORMANCE OF ALGORITHMS

To compare the two algorithms and initialization methods, they were applied to a simulated data set[19] of five constant heating rate measurements at different partial pressures (Figure 1). Random noise in the range of 0–15% of the maximum reaction rate was added to simulate the effect of fluctuations in the mass signal or any other source of signal noise. Then the data were projected on a $(\alpha \times T \times p)$ grid with $(25 \times 50 \times 5)$ elements, and the rank-1 approximation of the resulting tensor was computed. The tensor had 6250 elements, of which 91.8% were missing. The goal of the algorithm is to reconstruct the kinetic model used for the simulation from the available data.

At each noise level, 50 data sets were generated and processed. The algorithms were initialized with random starting values as well as with the initial estimate of the log-method, described in the previous section. The results show that both algorithms were able to compute the correct rank-1 approximation up to numerical uncertainty, regardless of the initialization method. There is no difference regarding the accuracy of the two algorithms or initialization methods, but the performance differed considerably.

Figure 2 shows the mean elapsed time and the mean number of iterations over the noise level. Blue and red lines show the results of the two algorithms and initialization methods, whereas the yellow line shows the time it took to calculate the initial estimate with the log method. Error bars represent the standard deviation.

It can be seen that the noise level had very little to no impact on the computation time. Even though an iteration of the NLS algorithm is more than twice as expensive as an iteration of the ALS algorithm ($\approx 3.3\,ms$ vs. $\approx 1.4\,ms$), the improved convergence speed of the NLS algorithm far outweighs this disadvantage: Instead of around 90 iterations, the NLS algorithm

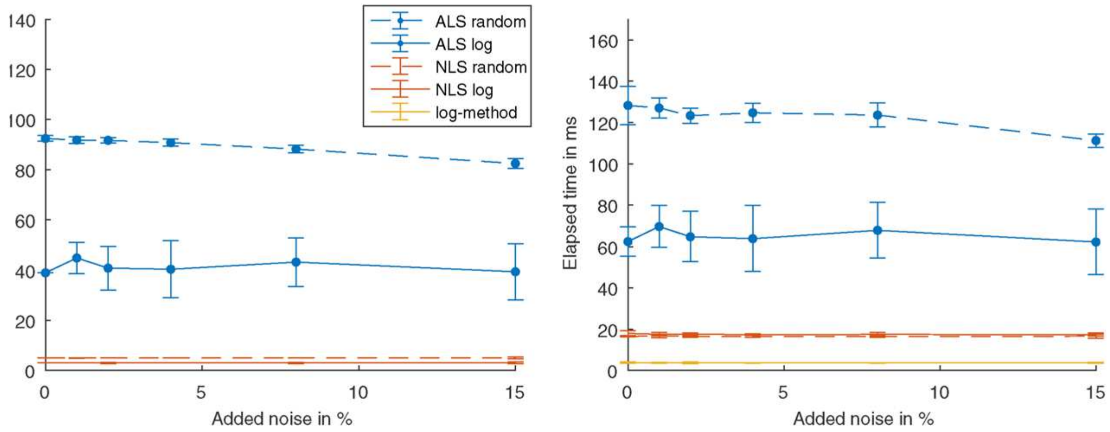

FIGURE 2 Performance of the two algorithms [Color figure can be viewed at wileyonlinelibrary.com]

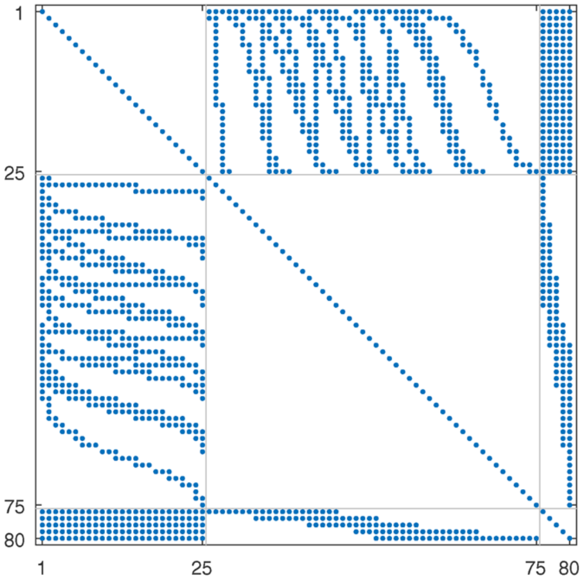

FIGURE 3 Nonzero pattern of the Hessian matrix [Color figure can be viewed at wileyonlinelibrary.com]

only requires five iterations in the case of random starting values.

The superior convergence properties of the NLS algorithm can be explained by viewing the ALS algorithm as a simplification of the NLS algorithm. The Hessian matrix of the least squares problem illustrates this nicely. Figure 3 shows the nonzero pattern of the Hessian associated with the rank-1 approximation of the test data set. Its block diagonal structure that is exploited by the ALS algorithm is clearly visible. The ALS algorithm omits the off diagonal elements to arrive at a series of linear problems. Algorithmic simplicity is traded at the cost of convergence speed. The NLS algorithm, on the other hand, takes the off diagonal elements into account, allowing the algorithm to take larger steps toward the solution and resulting in quadratic convergence speed close to the solution.

Tomasi and Bro[29] also compared an ALS-type algorithm with a derivative based one and found that the latter outperformed the former in the presence of a large amount of missing values. The ALS algorithm can be improved by including a Line Search,[30] which has been shown to increase the convergence speed considerably.

Using the result of the log-method instead of random starting values has a dramatic impact on the performance of the ALS algorithm: The number of iterations as well as the computation time decreased by about 50%. With the NLS algorithm, the number of iterations also decreased, but the impact on the computation time was negligible: The time saving due to the reduced number of iterations was offset by the time it took to compute the initial estimate.

In conclusion, from the two considered algorithms, the NLS algorithm seems to be more suitable than the ALS algorithm for the calculation of rank-1 approximations in kinetic analysis. Even though the quality of the solution is the same, the performance of the NLS algorithm is far superior. Even when starting values are calculated with the log-method, the NLS algorithm is about three times faster than the ALS algorithm.

8 | INTERPRETATION OF RESULT VECTORS

Up front, a quick reminder that the basis for a reliable model is reliable data. The NPK method requires that the experimental data have been collected and processed in a way that ensures that the input values to the NPK method are representative of the chemical process under consideration. For an extensive discussion of this topic, we refer to the ICTAC Kinetics Committee recommendations[31] and a critical assessment of them by Šesták.[32]

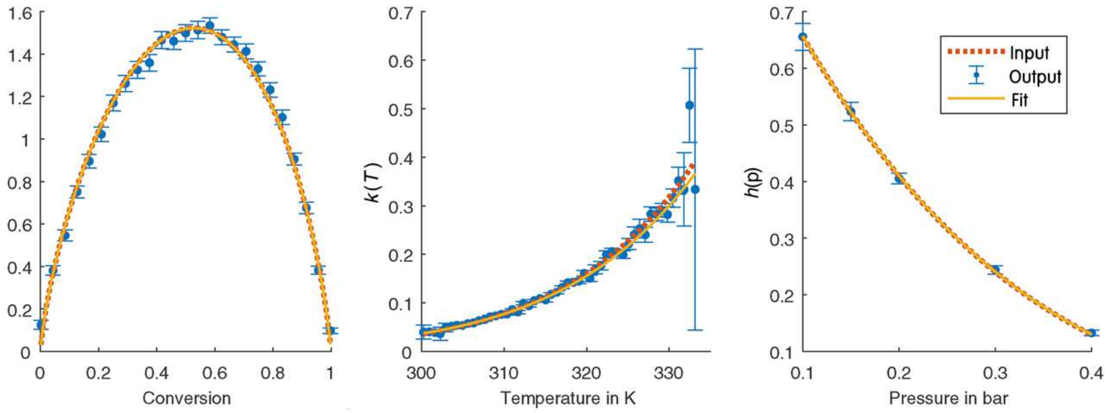

FIGURE 4 Output of the NLS algorithm alongside the input model used for the simulation and the fit result [Color figure can be viewed at wileyonlinelibrary.com]

Before interpreting the result vectors in detail, it must be confirmed that the goodness of fit is reasonable and that the single-step approximation is viable. Only then, the result vectors can be interpreted in terms of the general kinetic equation. For the simulated data set, this is straight forward: The result vectors can be compared to the input model. Figure 4 shows the result of the NLS algorithm applied to the test data set with 15%, noise. The blue bars represent the elements of the solution vectors with their standard deviation. It can be seen that the values are in good agreement with the input model (red dotted lines) and that the error bars are reasonably small. Thus, the algorithm managed to recover the kinetic model very well, even if 91.8% of the data tensor elements were missing.

If the input to the algorithm is experimental data, the assessment of the result is more complex and often ambiguous. There is no reliable method to legitimize the single-step approximation independently, based solely on chemical considerations. Usually it is assumed that the single-step approximation is viable if the model fits the data well. However, this does not present conclusive proof that the reaction is indeed limited by one single step. Thus, a lot of consideration and expert judgment is required when interpreting the result vectors.

One important metric for the goodness of fit is the standard error of the estimate (*SEE*), which can be calculated with

$$SEE = \sqrt{\frac{\|\widetilde{\mathcal{T}} - \mathcal{T}\|_{\mathcal{W}}^2}{N_e - N_m}}. \qquad (22)$$

It has the same unit as the reaction rate and can be interpreted as the average distance of the experimental values to the values predicted by the model. It is an overall measure of how well the model fits the experimental data and should be small compared to the reaction rate of the process. A related metric are the variances of the elements of the result vectors (blue bars in Figure 4), which can be calculated with Equations 11 and 20. The standard deviations should be small compared to the effect of the associated variable. If they are not, the associated value is unreliable. If all elements of a solution vector are unreliable, the corresponding variable does not have a significant effect or it may be superimposed by another effect.

In Figure 4, the variance of the elements of the conversion dependency and the pressure dependency are fairly constant, while the variance of the temperature dependency is much bigger at high- and low-temperature values. There are two reasons for this: First, there are fewer data points available at the beginning and the end of the temperature range than at the center, since the data set is made up of constant heating rate measurements. Second, since the conversion dependency approaches zero at both low and high conversion values (Figure 4, left) and low-/high-temperature values are correlated with low/high conversion values, the temperature dependency can not be estimated properly in these regions. Larger error bars reflect the uncertainty of the associated values. The information about the uncertainty of the dependency values is used later in the model-fitting step to weight the values accordingly.

With the help of the error bars, it should be possible to identify not only increased uncertainty of the result due to small data spread or correlation, but also deviations from the single-step approximation. Changes in the size of the error bars could indicate a change of the reaction mechanism or an interaction of the Arrhenius function with the reaction equilibrium. If this was the case, the data tensor could simply be split and models for the different regions could be derived, similar to what Schaube et al.[18] did with a direct model-fitting method.

In kinetic analysis, when the reaction is modeled according to the general kinetic equation, the aim is usually to find a reaction model and to determine the Arrhenius parameters, i.e. the aim is to identify the kinetic triplet. If the pressure is considered, a suitable pressure dependency model has to be found. Most established methods for kinetic analysis require an a priori assumptions about the models for each variable. Model fitting is either done for all variables at the same time or sequentially, so that the model choices influence each other. Finding the right combination of models is generally quite difficult, since there are many possible combinations and unforeseeable interactions between the models. The main advantage of the NPK method is that it can separate the contributions of the considered variables without any assumption about the models. Model identification is performed after the separation, independently for each variable, by fitting the solution vectors. In fact, from a modeling point of view, the result vectors could be used without any additional processing to predict the reaction rate, by simply interpolating each vector and multiplying the contributions.

However, there is one issue that needs to be addressed for the model identification with the NPK method: Some values of the result vectors will be more accurate than others due to structural reasons like the distribution of experimental data or correlation of variables. The accuracy of each value is reflected by its variance. Least squares fitting yields optimal results (in the sense of minimum variance) if all data points are weighted with the inverse of their variances. Omitting weights in the model-fitting step amounts to the assumption of homoscedasticity, which is generally not applicable and may cause the result to be inaccurate. Therefore, the variances of the solution values need to be taken into account in the model-fitting step to produce accurate results. This was not possible with the original NPK method, but with the method proposed in this paper it is possible to track the error propagation from the experimental values all the way to the estimated model parameters.

For the identification of the reaction model of the simulated data set, 43 reaction models from the literature were fitted to the conversion dependency vector (Figure 4, left) and a pairwise F-test was used to determine the most likely model (see Ref. [19] for more details on the models and the testing procedure). The correct model was identified unequivocally from all data sets at a confidence level of $\alpha = 0.95$.

To determine the activation energy, the Arrhenius function was fitted to the temperature dependency vector. The activation energy and the standard deviation at each noise level are shown in Figure 5. It can be seen that the estimated values from the weighted fit are very close to the value used for the simulation: 60 kJ/mol. The deviation was less than 3% across all noise levels and can be attributed to the collinearity of the activation energy and the Arrhenius parameter. Here the importance of accounting for unequal variances in the model-fitting step becomes especially apparent. Values at high and low temperatures, where outliers are common (Figure 4, middle), are weighted much less than values in the medium temperature range. Otherwise, they would have distorted the fit considerably (red dash–dotted line in Figure 5).

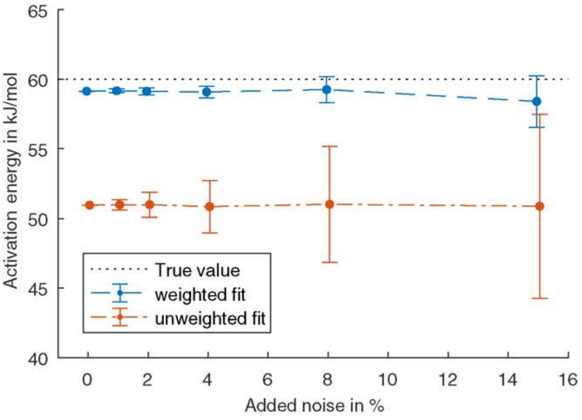

FIGURE 5 Estimated activation energy over added noise [Color figure can be viewed at wileyonlinelibrary.com]

9 | CONCLUSION

The NPK method has been reworked, and two algorithms for computing the solution have been presented. The new NPK method shares the advantages of the original one, while resolving many of its shortcomings. Like the original NPK method, it is model free and can process data from any combination of experiments, but in contrast to the original method it is algorithmically much simpler due to its ability to deal with missing values directly. Also, it can derive kinetic models in any number of variables. This was made possible by switching from the SVD to tensor low-rank decomposition methods. Additionally, formulae for estimating the variance of the output vectors have been derived to weight values in the model-fitting step correctly, else the fitting results might be distorted considerably.

From the two proposed algorithms, ALS and NLS, the latter is better suited for the computation of rank-1 approximations of kinetic data. Even though the two algorithms did not differ with respect to the quality of the solution, the performance of NLS was far superior.

Tests on a simulated data set show that the new NPK method is capable of recovering the full kinetic model, including the pressure dependency, very accurately, even in the presence of noise and missing values. A distortion of the model identification results, due to structural heteroescedasticity typical for data sets with constant heating rate measurements, is prevented by using variance estimates to calculate weights for the model-fitting step. The variance estimates also allow the detection of deviations from rank-1 structure of the data, i.e. a violation of the single-step assumption. Then models for different regions, e.g., at low and at high temperature, can be derived by simply splitting the data tensor.

Generally, the new NPK method opens up many possibilities for the identification of kinetic models. The improved usability, robustness, and diagnostic capabilities of the new NPK method have the potential to make it widely applicable.

The resulting models should be well suited to compute kinetic predictions, if the statistical errors are small and the results are consistent. A mechanistic interpretation of the kinetic triplet, on the other hand, should only be done with care, since the adequateness of the single-step approximation goes far beyond the goodness of fit. Gas–solid reactions are very complex processes, and the general kinetic equation has been derived based on a number of assumptions and simplifications that need to be considered when the goal is to draw conclusions about the reaction.

Since the new NPK method can process any number of variables, additional parameters besides conversion, temperature, and pressure could be included to derive more detailed kinetic models as suggested by Koga.[33] The main challenge will be collecting sufficient data for the parameterization of such a model.

Another promising topic for future investigations would be the application of rank > 1 approximations for the derivation of multistep models. Algorithms for computing low-rank approximations of tensors are available and well documented. Their application to kinetic analysis would greatly increase the scope of the NPK method by overcoming the limitation to single-step reactions.

ACKNOWLEDGMENTS

The authors would like to thank the Austrian Research Promotion Agency (FFG) for their financial support of the projects SolidHeat Kinetics (#848876) and SolidHeat Pressure (#853593).

CONFLICT OF INTEREST

The authors have declared no conflict of interest.

ORCID

Felix Birkelbach https://orcid.org/0000-0003-4928-6209

REFERENCES

1. Deutsch M, Müller D, Aumeyer C, et al. Systematic search algorithm for potential thermochemical energy storage systems. *Appl Energy*. 2016;183:113–120.
2. Flegkas S, Birkelbach F, Winter F, Freiberger N, Werner A. Fluidized bed reactors for solid-gas thermochemical energy storage concepts—Modelling and process limitations. *Energy*. 2018;143:615–623.
3. Brown ME, Dollimore, D, Galwey, AK, Bamford, CH, Tipper, CFH, eds. *Reactions in the Solid State*, vol. 22 of Comprehensive Chemical Kinetics. Amsterdam, the Netherlands: Elsevier Scientific Publishing Company; 1980.
4. Khawam A, Flanagan DR. Solid-state kinetic models: basics and mathematical fundamentals. *J Phys Chem B*. 2006;110(35):17315–17328.
5. Flynn JH. The 'Temperature Integral'—its use and abuse. *Thermochim Acta*. 1997;300(1-2):83–92.
6. Galwey A, Brown M. Application of the Arrhenius equation to solid state kinetics: can this be justified? *Thermochim Acta*. 2002;386:91–98.
7. Barret PM. Expression théorique en fonction de la pression de la loi de vitesse de croissance d'une solide. *C R Hebd Séances Acad Sci, Sér C*. 1968;266:856–859.
8. Reading M, Dollimore D, Whitehead R. The measurement of meaningful kinetic parameters for solid state decomposition reactions. *J Therm Anal*. 1991;37(9):2165–2188.
9. Searcy AW, Beruto D. Kinetics of endothermic decomposition reactions: 2. Effects of the solid and gaseous products. *J Phys Chem*. 1978;82(2):163–167.
10. Galwey AK. Is the science of thermal analysis kinetics based on solid foundations? *Thermochim Acta*. 2004;413(1-2):139–183.
11. Pijolat M, Favergeon L, Soustelle M. From the drawbacks of the Arrhenius-f(a) rate equation towards a more general formalism and new models for the kinetic analysis of solid–gas reactions. *Thermochim Acta*. 2011;525(1-2):93–102.
12. Šimon P. Considerations on the single-step kinetics approximation. *J Therm Anal Calorim*. 2005;82(3):651–657.
13. Vyazovkin S, Burnham AK, Criado JM, Pérez-Maqueda LA, Popescu C, Sbirrazzuoli N. ICTAC Kinetics Committee recommendations for performing kinetic computations on thermal analysis data. *Thermochim Acta*. 2011;520:1–19.
14. Serra R, Sempere J, Nomen R. A new method for the kinetic study of thermoanalytical data. *Thermochim Acta*. 1998;316(1):37–45.
15. Sewry JD, Brown ME. "Model-free" kinetic analysis? *Thermochim Acta*. 2002;390(1-2):217–225.
16. Criado JM, González M, Málek J, Ortega A. The effect of the CO_2 pressure on the thermal decomposition kinetics of calcium carbonate. *Thermochim Acta*. 1995;254:121–127.
17. Criado YA, Alonso M, Abanades JC. Kinetics of the $CaO/Ca(OH)_2$ hydration/dehydration reaction for thermochemical energy storage applications. *Ind Eng Chem Res*. 2014;53(32):12594–12601.
18. Schaube F, Koch L, Wörner A, Müller-Steinhagen H. A thermodynamic and kinetic study of the de- and rehydration of $Ca(OH)_2$ at high H_2O partial pressures for thermo-chemical heat storage. *Thermochim Acta*. 2012;538:9–20.
19. Deutsch M, Birkelbach F, Knoll C, Harasek M, Werner A, Winter F. An extension of the NPK method to include the pressure dependency of solid state reactions. *Thermochim Acta*. 2017;654:168–178.
20. Birkelbach F, Deutsch M, Flegkas S, Franz W, Werner A. A higher-order generalization of the NPK-method. *Thermochim Acta*. 2018;661:27–33.
21. Tucker LR. Some mathematical notes on three-mode factor analysis. *Psychometrika*. 1966;31(3):279–311.
22. Andersen CM, Bro R. Practical aspects of PARAFAC modeling of fluorescence excitation-emission data. *J Chemom*. 2003;17(4):200–215.

23. Kolda TG, Bader BW. Tensor decompositions and applications. *SIAM Rev*. 2009;51(3):455–500.
24. Bro R. Review on multiway analysis in chemistry—2000–2005. *Crit Rev Anal Chem*. 2006;36(3–4):279–293.
25. Hitchcock FL. The expression of a tensor or a polyadic as a sum of products. *J Math Phys*. 1927;6(1-4):164–189.
26. Carroll JD, Chang JJ. Analysis of individual differences in multidimensional scaling via an *n*-way generalization of "Eckart-Young" decomposition. *Psychometrika*. 1970;35(3):283–319.
27. Harshman RA. Foundations of the PARAFAC procedure: models and conditions for an "explanatory" multimodal factor analysis. *UCLA Work Pap Phonetics*. 1970;16:1–84.
28. Paatero P. A weighted non-negative least squares algorithm for three-way "PARAFAC" factor analysis. *Chemom Intell Lab Syst*. 1997;38(2):223–242.
29. Tomasi G, Bro R. PARAFAC and missing values. *Chemom Intell Lab Syst*. 2005;75(2):163–180.
30. Rajih M, Comon P, Harshman RA. Enhanced line search: a novel method to accelerate PARAFAC. *SIAM J Matrix Anal Appl*. 2008;30(3):1128–1147.
31. Vyazovkin S, Chrissafis K, Di Lorenzo ML, et al. ICTAC Kinetics Committee recommendations for collecting experimental thermal analysis data for kinetic computations. *Thermochimi Acta*. 2014;590:1–23.
32. Šesták J. The quandary aspects of non-isothermal kinetics beyond the ICTAC kinetic committee recommendations. *Thermochim Acta*. 2015;611:26–35.
33. Koga N. Ozawa's kinetic method for analyzing thermoanalytical curves. *J Ther Anal Calorim*. 2013;113(3):1527–1541.

SUPPORTING INFORMATION

Additional supporting information may be found online in the Supporting Information section at the end of the article.

How to cite this article: Birkelbach F, Deutsch M, Flegkas S, Winter F, Werner A. NPK 2.0: Introducing tensor decompositions to the kinetic analysis of gas–solid reactions. *Int J Chem Kinet*. 2019;51:280–290. https://doi.org/10.1002/kin.21251

Paper 3

The effect of the reaction equilibrium on the kinetics of gas-solid reactions — A non-parametric modeling study

published in Renewable Energy in collaboration with Markus Deutsch and Andreas Werner, based on Paper 8.

This paper presents a literature review on models for the effect of the equilibrium/driving force on the kinetics of reversible gas-solid reactions and implications for non-parametric modeling. These near-equilibrium effects are especially relevant to thermochemical energy storage, since these processes need to be operated in close vicinity of the equilibrium to maximize their efficiency.

What we found is that literature on the effect of the equilibrium on gas-solid reactions is scarce and that models are used very inconsistently. The only model that also pretended to be applicable to formation reactions was based on Transition State Theory. To evaluate this model and other more empirical models found in literature, the hydration of CaC_2O_4 (calcium oxalate) was modeled with our tensor NPK algorithm. The effect of the equilibrium could be identified, but it did not match theoretic predictions. It seems that all theories available today are falling short of describing the effect of the equilibrium/driving force on gas-solid reactions.

While this lack of accurate theory is disappointing, we were able to show that NPK models can be used to predict kinetics accurately regardless of the shortcoming of theory. To model the effect of the equilibrium/driving force, the TensorNPK method only requires a measure for the equilibrium distance. The reduced partial Gibbs enthalpy was identified as the most viable distance measure, and kinetic predictions were found to be in very good agreement with experimental data. In this way, the non-parametric modeling can be used as a generic kinetic prediction method.

My contribution: Literature review on pressure and equilibrium models. Kinetic modeling of the hydration of CaC_2O_4 and the reduction of CuO. Interpretation of results. Drawing up and writing of the paper.

F. Birkelbach, M. Deutsch, and A. Werner (2020). “The effect of the reaction equilibrium on the kinetics of gas-solid reactions — A non-parametric modeling study”. In: Renewable Energy *152, pp. 300–307.* ISSN*: 09601481.*
DOI*:* `10.1016/j.renene.2020.01.033`

Renewable Energy 152 (2020) 300–307

Contents lists available at ScienceDirect

Renewable Energy

journal homepage: www.elsevier.com/locate/renene

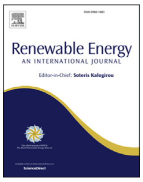

The effect of the reaction equilibrium on the kinetics of gas-solid reactions — A non-parametric modeling study

Felix Birkelbach [a], [*], Markus Deutsch [b], Andreas Werner [a]

[a] TU Wien, Institute for Energy Systems and Thermodynamics, Vienna, Austria
[b] BIOENERGY 2020+ GmbH, Graz, Austria

ARTICLE INFO

Article history:
Received 20 August 2019
Received in revised form
12 December 2019
Accepted 7 January 2020
Available online 13 January 2020

Keywords:
Thermochemical energy storage
Heterogeneous kinetics
Model identification
NPK
Pressure dependency
Reaction equilibrium

ABSTRACT

The viability of thermochemical energy storage for a given application is often determined by the reaction kinetics under process conditions. For high exergetic efficiency the process needs to operate in close proximity to the reaction equilibrium. Thus, accurate kinetic models that include the effect of the reaction equilibrium are required.

In the present work, different parametrization methods for the equilibrium term in the General Kinetic Equation are evaluated by modeling the kinetics of two reaction systems relevant for thermochemical energy storage (CaC_2O_4 and CuO) from experimental data. A non-parametric modeling method based on tensor decompositions is used that allows for a purely data driven assessment of different parametrization methods.

Our analysis shows that including a suitable equilibrium term is crucial. Omitting the equilibrium term when modeling formation reactions can lead to seemingly negative activation energies. Our tests also show that for formation reactions, the reaction rate decreases much faster towards the equilibrium than theory predicts. We present an empirical modeling approach that can predict the reaction rate of gas-solid reactions, regardless of the shortcomings of theory. In this way, non-parametric modeling offers a powerful tool for applied research and may contribute to the advancement of the thermochemical energy storage technology.

1. Introduction

Thermochemical energy storage (TCES) is one of the prospective technologies that could contribute to covering the future thermal energy storage (TES) demand. Compared to other TES technologies, TCES has the advantage of very high gravimetric and volumetric storage densities, nearly lossless storage at ambient conditions as well as a wide range of operating temperatures, depending on the storage material. In most TCES applications the storage material is a solid that reacts reversibly with a gaseous substance. Redox reactions, where a metal reacts with oxygen, have been proposed for TCES in concentrated solar power plants, because of their high operating temperature at around 1000 °C (see Ref. [1] for a recent review). For lower operating temperatures, such as for district heating or building applications, (de)hydration reactions have been proposed (see Refs. [2,3] for recent reviews).

The process conditions of a TCES reactor must be chosen in a way that the reactor operates energy efficiently, while ensuring sufficiently fast reaction rates. A measure for the exergetic efficiency of thermal storage devices is the temperature spread between the charging and the discharging process. The larger the spread, the lower the exergetic efficiency. In TCES, the spread is caused by the reaction equilibrium, a characteristic feature of reversible gas-solid reactions. Below the equilibrium temperature the formation (discharging) reaction dominates; above, the decomposition (charging) reaction dominates. At the equilibrium temperature, the rates are equal and the net-reaction rate is, thus, zero. Consequently, both the charging and the discharging process need to operate at a certain distance from the equilibrium.

In the charging process heat is consumed by the decomposition reaction. The temperature should be as low as possible to utilize the heat source efficiently, but it must be sufficiently high above the equilibrium temperature to yield acceptable reaction rates. In the discharging process, heat is released by the formation reaction. From the point of view of energy efficiency, the temperature should be as high as possible to maximize the exergy in the heat flow. However,

---

[*] Corresponding author.
E-mail address: felix.birkelbach@tuwien.ac.at (F. Birkelbach).

https://doi.org/10.1016/j.renene.2020.01.033
0960-1481/© 2020 Elsevier Ltd. All rights reserved.

Nomenclature

Acronyms

TCES	thermochemical energy storage
TES	thermal energy storage
TGA	thermogravimetric analysis

Greek Symbols

α	conversion
γ_{v_i}	vector of interpolation coefficients for position v_i
$\Delta^R G$	reaction Gibbs enthalpy in kJ/mol
$\Delta^R H$	reaction enthalpy in kJ/mol
μ_i	chemical potential of species i in kJ/mol
ν_G	stoichiometric coefficient of gas phase
ν_i	stoichiometric coefficient of species i

Roman Symbols

$\mathrm{d}\alpha/\mathrm{d}t$	conversion rate in 1/s
d_k	value of datapoint k
$f(\alpha)$	conversion dependency, reaction model
$f_i(v_i)$	dependency function i
$\boldsymbol{f}_i$	dependency function vector i
$\widehat{f}_i(v_i)$	estimate of dependency function i at v_i
$f_{i,j}$	element j of dependency function vector i
G	Gibbs enthalpy of mixture in kJ/mol
G_z	partial molar Gibbs enthalpy of reaction in kJ/mol
$h(\ldots)$	pressure/equilibrium dependency
$k(T)$	temperature dependency in 1/s
p	partial pressure of gas in Pa
p^*	equilibrium partial pressure of gas in Pa
p_0	standard pressure in Pa
T	temperature in K
t	time in s
v_i	independent variable i
$v_{i,j}$	grid point j in independent variable i
$\widehat{v}_{i,k}$	position of datapoint k in dimension i
z	reaction coordinate

starting from a certain temperature, the reaction rate decreases, as the temperature approaches the equilibrium temperature.

The equilibrium temperature of a gas-solid reaction is determined by the partial pressure of the gaseous reactant. By influencing the partial pressure, e. g. by efficiently removing the product gas from the reaction zone during charging or by increasing the partial pressure during discharging, the temperature spread can be reduced. It has even been shown that thermochemical cycles can be used as heat pumps, if the partial pressure during charging is sufficiently higher than the partial pressure during discharging [4]. Detailed knowledge about the equilibrium position of the reaction and of the kinetics in the vicinity of the equilibrium are required to choose optimal process conditions for maximum efficiency.

The dependency of the reaction rate on temperature, partial pressure and the equilibrium can be determined experimentally with thermal analysis methods. The effect of each variable is generally non-linear and the effects are convoluted in the experimental data. Because of this, advanced modeling methods are required to separate the effect of each variable. The most common formula to describe the conversion rate $\mathrm{d}\alpha/\mathrm{d}t$ is the General Kinetic Equation

$$\frac{\mathrm{d}\alpha}{\mathrm{d}t} = f(\alpha)\, k(T)\, h(p, p^*) \tag{1}$$

Here, α is the conversion, $f(\alpha)$ is the conversion dependency, T is the absolute temperature, $k(T)$ the effect of the temperature, usually expressed by the Arrhenius equation, p is the partial pressure of the gas, p^* the equilibrium pressure and $h(p, p^*)$ the pressure or equilibrium term. Modeling a reaction with this formula is often referred to as the single step approximation, since the main assumption is that the reaction is only limited by the slowest reaction step.

In our recent study of the reaction system Cu_2O/CuO [5] we noticed some inconsistencies in the established modeling approach with the equilibrium term $h(p, p^*) = 1 - p/p^*$. Specifically, that the equilibrium term assumed large negative values when it is applied to formation reactions. Because TCES processes usually operate in the vicinity of the equilibrium, understanding the effect of the reverse reaction is key to obtain a reliable model. Even though our focus lies on empirical data driven modeling, the model should be physically plausible to get more reliable results, instead of just “the best fit”.

We found that other scientists were also struggling with the modeling of the effect of the reverse reaction on formation reactions. Deutsch et al. [6] did not consider the effect of the equilibrium for the oxidation of CuO and obtained negative activation energies. Clayton et al. [7] investigated the kinetics of CuO/Cu_2O. To model the pressure dependency, they somewhat arbitrarily defined a thermodynamic driving force as $p^* - p$. Schaube et al. [8] found that $1 - p/p^*$ does describe the dehydration of $Ca(OH)_2$ well, but does not yield satisfactory results for the hydration reaction, where they identified a negative activation energy in the vicinity of the equilibrium. In hydrogen literature a plethora of models has been employed. Ron [9] published a summary of pressure models in hydrogen literature and proposed a normalized pressure dependency method for the dissociation of hydrogen $|p^* - p|/p^*$. He interpreted the term as an accommodation function for the effect of the reverse reaction in close proximity to the equilibrium for hydrogen desorption, because the term assumes values between 0 and 1. However, he noted that this interpretation is inconsistent for sorption reactions, where the term is unbounded and can assume arbitrarily large values.

In light of these inconsistent and sometimes somewhat arbitrary modeling approaches, we decided to look more closely into modeling approaches for the effect of the equilibrium on the reaction rate of gas-solid reactions. First, we present a short literature review and introduce the most relevant thermodynamic concepts. Then, we evaluate four different parametrization methods for the equilibrium term by applying them to model the hydration of CaC_2O_4, whose viability for thermochemical energy storage has recently been highlighted [10]. Non-parametric modeling with the tensor NPK method [11] is used to analyze the kinetic data, because it does not rely on modeling assumptions besides the General Kinetic Equation. In this way, no additional modeling bias is introduced through the choice of models for the dependencies. Finally, we test the ability of non-parametric models to predict the reaction rate of two very different reactions (hydration of CaC_2O_4 and reduction of CuO) in the vicinity of the equilibrium.

2. Theoretical background

Generally, gas-solid reactions are extremely complex involving a series of different physical and chemical processes. Many widely used modeling concepts, not least the single step approximation in Equation (1), are well known for falling short of accurately describing real chemical reactions. For this reason many applied researchers focus on empirical modeling of gas-solid reactions. Nonetheless, theoretical models are useful, because they provide us with a frame to interpret the behavior of the chemical reaction under consideration and because physically motivated models are often more reliable.

A characteristic feature of reversible reactions is the reaction equilibrium, where the reaction rate of the forward reaction is equal to the rate of the reverse reaction and the net-reaction rate is thus zero. From a thermodynamic perspective the characteristic value to describe a chemical reaction is the partial Gibbs enthalpy of the reaction G_z, i. e. the partial derivative of the Gibbs enthalpy of the mixture G with respect to the reaction coordinate z:

$$G_z(p,T) = \left.\frac{\partial G}{\partial z}\right|_{p,T} = \sum_i \nu_i \mu_i(p,T) \qquad (2)$$

Here, p is the partial pressure of the gaseous component, T is the temperature, ν_i are the stoichiometric coefficients and μ_i are the chemical potentials of the substances. At the equilibrium, the Gibbs energy of the mixture assumes a minimum and the partial Gibbs enthalpy of the reaction, thus, becomes zero.

For a simple reversible gas-solid reaction of the type

$$\nu_A \mathrm{A(s)} + \nu_G \mathrm{G(g)} \rightleftarrows \nu_B \mathrm{B(s)} \qquad (3)$$

the partial molar Gibbs enthalpy of the reaction can be expressed as

$$G_z(T,p) = \Delta^R G(T,p_0) + \nu_G RT \ln\frac{p}{p_0} = \nu_G RT \ln\frac{p}{p^*(T)}. \qquad (4)$$

With the reaction Gibbs enthalpy at standard pressure $\Delta^R G(T, p_0)$, the standard pressure p_0 and the equilibrium pressure at a given temperature $p^*(T)$.

The first studies of the effect of the equilibrium on the reaction rate on heterogeneous reactions date back to the 1950s. In 1952, Burke et al. [12] derived a formula based on the transition state theory to describe the reaction rate of solid state transitions. In 1956, Bradley [13] introduced the vapor gap theory for solid state transitions, which resulted in the same equilibrium term. Bradley's theory found its way into modern kinetic analysis through the works of Šestak [14]. Almost four decades after Burke et al., Reading et al. [15] derived the same expression as them for gas-solid reactions, apparently without knowledge of the 1952 paper.

$$\frac{d\alpha}{dt} = f(\alpha)\, k(T) \left[1 - \exp\left(\frac{G_z(T,p)}{RT}\right)\right] \qquad (5)$$

This formula relates the partial molar Gibbs energy of the reaction G_z at process conditions with the reaction rate. At the equilibrium, G_z is zero and consequently also is the net reaction rate.

Replacing the Gibbs enthalpy in the equilibrium term with the pressure ratio from Eq. (4), results in the well-known formula where the stoichiometric coefficient is usually omitted, since most studies to date dealt with decomposition reactions, where ν_G is 1.

$$h(p,p^*) = 1 - \exp\left(\frac{G_z(T,p)}{RT}\right) = 1 - \left(\frac{p}{p^*}\right)^{\nu_G} \qquad (6)$$

The latter form of the equilibrium term has also been derived based on sorption considerations by Barret [16] and Searcy [17] for decomposition reactions. The stoichiometric coefficient is not included in these derivations and they do not discuss the effect of the equilibrium on formation reactions.

Currently there is no consensus on the validity of the transition state theory for reactions involving solids, as the ongoing academic dispute around the Arrhenius equation shows [18,19]. Notwithstanding, the Arrhenius equation is the most commonly applied formula to describe the temperature dependency of gas-solid reactions and there seems to be no other theory that can interpret the effect of the reaction equilibrium for both formation and decomposition reactions.

The most important implication of the above formula in Equation (6) is that the form of the equilibrium term changes to $1-(p^*/p)^{|\nu_G|}$ for formation reactions, because the sign of the stoichiometric coefficient of the gas phase changes. Despite our extensive literature search, we did not encounter a paper that accounted for the stoichiometric coefficient. In some works the sign of the pressure term was changed for the reverse reaction, so that the value of the pressure term was positive [8,20]. The reciprocal also resolves Ron's [9] issue with the interpretation of his normalized pressure function for sorption reactions: If the stoichiometric coefficient is considered, the value of the accommodation function is between 0 and 1 again.

3. Experimental setup

Simultaneous thermal analysis measurements were performed on a Netzsch STA 449 C Jupiter equipped with a combined TGA-DSC sample holder using open aluminum oxide crucibles containing sample masses around 10 mg. The oven is operable between 25 °C and 1250 °C, regulated by an S-type thermocouple. The gas flow was controlled using red-y smart series mass-flow controller by Voegtlin with an operable range between 2 and 100 ml/min. All reported experiments were conducted at ambient pressure.

Calcium oxalate monohydrate (CAS 5794-28-5) was ordered from Sigma-Aldrich and used as supplied. The anhydrous form was obtained by in-situ dehydration at 300 °C. For the hydration experiments, the system was equipped with a water vapor furnace. The steam was produced in an Adrop water vapor generator and transferred into the furnace via a heated transfer line. To prevent condensation of the water, a carrier gas flow of 50 ml(N_2)/min was used. Setting the steam flow to 2.5 and 5 g/h resulted in partial pressures of 0.66 and 0.79 bar respectively. The protective gas stream was set to 5 ml(N_2)/min.

Copper oxide (CAS 1317-38-0) by Merkur Emsure was grinded using a Retsch planetary ball mill PM 100 and sieved to obtain samples with grain diameters in the range of 1 to 100 µm. Before each experiment, the reactor was purged with nitrogen (99.999 vol %) for a minimum of 30 min to remove oxygen from the reactor. During the experiment the N_2 and O_2 flow rates were set to obtain the target partial pressure in the reactor at a total flow of 100 ml/min.

4. Method

For the kinetic modeling of the experimental data, the tensor NPK method [11], is used. It is based on the observation that the discretization of the General Kinetic Equation in Equation (1) results in a rank-1 tensor. By arranging experimental data in a tensor and applying a suitable algorithm to compute its rank-1 approximation, the effect of each variable can be extracted without any assumption about the model besides the single step approximation.

This data driven approach is often labeled "model-free", in the sense that no sub-models for the effect of each variable have to be chosen. In this way, it allows for the unbiased testing of different parametrization methods, without interference of sub-model choices. To extract information about an effect from experimental data, all the algorithm needs is a variable that the effect is correlated with. Usually, these are the conversion, to find a suitable reaction model, and the temperature, to identify the Arrhenius parameters. To extract information about the effect of the equilibrium on the kinetics, a suitable measure for the distance to the equilibrium is required.

In this paper four different parametrization methods for the equilibrium term are compared. The partial pressure p is used as a reference to check whether meaningful models can be computed, if the equilibrium is not considered. $|p^* - p|$ is used as the most simple way to take the equilibrium into account and $1-(p/p^*)^{\nu_G}$ is used based on the literature study. Additionally we propose to use

$$\frac{G_z}{RT} = \nu_G \ln \frac{p}{p^*} \tag{7}$$

as a generic measure for the distance to the equilibrium. This value can be interpreted as the normalized thermodynamic driving force of the reaction. Like $1-(p/p^*)^{\nu_G}$ it has no unit, becomes zero at the equilibrium and increases monotonically as the distance to the equilibrium increases. In contrast to $1-(p/p^*)^{\nu_G}$ it does not converge to a fixed value at a certain distance to the equilibrium. Because of this, it can capture the effect of the equilibrium at larger distances from the equilibrium than the transition state theory would predict.

In order for the algorithm to recognize the effect of the equilibrium, data points that are at the same distance to the equilibrium must feature the same value of the equilibrium measure. Fig. 1 illustrates the difference between the considered parametrization methods based on the reaction system $CaC_2O_4/CaC_2O_4 \cdot H_2O$. The left most diagram shows the equilibrium diagram of the reaction and the contour lines of the equilibrium terms for the dominant reaction step. I. e. the lines above the equilibrium correspond to the formation reaction, while the lines below correspond to the decomposition. Data points on one contour line are recognized as being at the same distance to the equilibrium. It can be seen that $|p^* - p|$ is no consistent measure for the distance to the equilibrium, even though it includes the equilibrium pressure.

Both $1-(p/p^*)^{\nu_G}$ and G_z/RT result in contour lines, that are "parallel" to the equilibrium. Thus it can be expected that they are capable of modeling the equilibrium effect well. The two diagrams on the right in Fig. 1 show a cross-section of the distance measures in the main diagram at a fixed temperature. At a certain distance, $1-(p/p^*)^{\nu_G}$ converges to 1, while G_z/RT covers the whole p-T range. Because of this, the latter can model the effect of the equilibrium over the whole p-T range.

The tensor NPK algorithm produces the most reliable results if the experimental data is fairly equally distributed on the grid. For data, that has been measured on a $\alpha \times T \times p$ grid, the algorithm works well if the model consists of α, $T$and p as variables. If the data is transformed to include the equilibrium distance, the position of the data points in the data space is distorted and the projection on the tensor may introduce a significant error. To remedy this, the tensor NPK has been adapted to compute the residuals at the data points instead of at the tensor elements (see Appendix A). In this way the projection of the data points on the data tensor can be omitted.

As input for the tensor NPK algorithm, conversion and reaction rate were computed from the mass loss data of the TGA experiments. The temperature and partial pressure values were used to compute the values of the equilibrium terms. G_z and p^* can be calculated with thermodynamic constants from material databases, or, if these constants are not available for the reaction system under consideration, p^* can be determined experimentally in the relevant temperature range and G_z can be calculated with Equation (7).

For each analysis, a grid that fits the data was selected. Then the tensor NPK algorithm [11] was used to extract the effect of each variable on the reaction rate. With the conversion dependency, the best fitting reaction model was identified by fitting 41 reaction models from the literature and a pair-wise F-Test was performed to check whether the performance of the best fitting model was statistically significantly better than the other ones (see Ref. [21] for more details). In the result plots all models are displayed that were not rejected at a 95% confidence level. The Arrhenius parameters were identified from the temperature effect with a non-linear fitting algorithm. The activation energy E_a is displayed with its 95% confidence interval. The frequency factor A is omitted, because it is affected by the choice of the equilibrium term and therefore bears little to no meaning in the context of this analysis.

5. Results and discussion

For the first analysis, a dataset of 18 isothermal hydration reaction runs of CaC_2O_4 is used. The experiments were conducted at two partial pressures (0.66 and 0.79 bar) and five temperatures

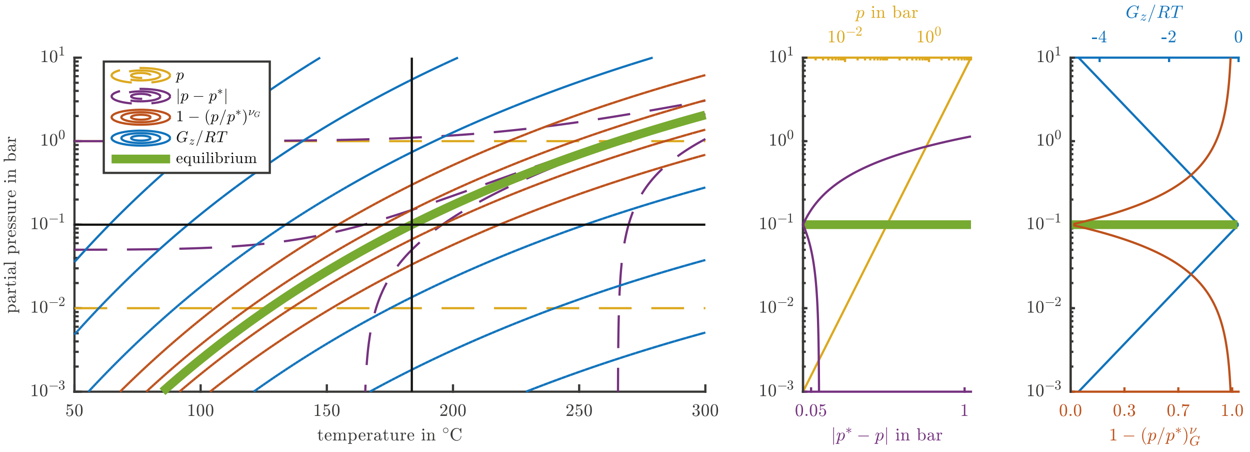

Fig. 1. Contour lines of equilibrium measures in the p-T space (left) with slices at constant temperature (right).

(126, 142, 158, 174 and 190 °C). The reaction can be described by the following formula:

$$CaC_2O_4 + H_2O \rightleftarrows CaC_2O_4 \cdot H_2O + \Delta^R H. \tag{8}$$

Fig. 2 shows the position of the data points in the data space for all considered parametrization methods. The grey lines show the grid that was chosen for the evaluation. In order for the algorithm to identify the effect of the equilibrium, all datapoints at the same distance from the equilibrium must be placed the same value of the equilibrium measure. The leftmost diagram in Fig. 2 shows the undistorted p-T grid. $|p^* - p|$ in the second diagram only introduces a slight shift, while the transformation with $1 - (p/p^*)^{\nu_G}$ completely rearranges the data points. Thus, it can be expected, that the result will differ considerably, even if these parametrization methods seem quite similar. In the third diagram it can be seen, that the data points are squeezed together at values close to 1. To make sure that this does not blur the result, the grid points have been chosen accordingly. G_z/RT rearranges the data points in a similar manner as $1 - (p/p^*)^{\nu_G}$, but it does not squeeze them. Because of this, this variable can capture the effect of the equilibrium at larger distances from the equilibrium. Also, a simple equally spaced grid can be used with this method.

The output of the NPK algorithm for each of the parametrization methods is displayed in Fig. 3. The identified conversion dependency was the same, regardless of the parametrization method. The temperature dependencies of the p and the $|p^* - p|$ model exhibit a decreasing trend. Here, the Arrhenius effect is superimposed by the effect of the reverse reaction. An intent to identify Arrhenius parameters from these curves would result in physically nonsensical negative values for the activation energy.

The temperature dependency of $1 - (p/p^*)^{\nu_G}$ and $G_z/\,RT$ in Fig. 3 show an increasing trend that fits the Arrhenius equation. The identified apparent activation energies are 52.9 kJ/mol ± 18 % and 64 kJ/mol ± 14 % respectively. Even thought the values differ, the confidence intervals overlap. I. e. the difference is within the statistical uncertainty.

If the theoretical model based on transition state theory in Equation (5) was correct, the effect of $1 - (p/p^*)^{\nu_G}$ would be a straight line from 0 to 1. Fig. 3 shows that, the effect approaches zero much faster, specifically at around 0.8. This is consistent with the effect described by Schaube et al. [8] for the hydration of CaO: They found that the reaction rate decelerates much faster close to the equilibrium than predicted by theory and therefore obtained a negative apparent activation energy. By using non-parametric modeling, which allows arbitrary forms of the equilibrium dependency, the temperature dependency can be identified correctly — thus eliminating the need for negative apparent activation energies.

It seems that the available theoretical formulas do not capture the complex behavior of gas-solid reactions in the vicinity of the equilibrium. Recent research on the hydration of salts [22] has found, that the hydration is mediated by a wetting layer and that some salts show a meta-stable zone around the equilibrium, where the reaction is limited by nucleation. In light of these recent findings, the single step approximation, underlying the General Kinetic Equation, has to be assessed thoroughly for these reaction systems. Future research will have to determine the limits of its applicability and find suitable expressions for modeling the rate limiting step.

The NPK method with the G_z/RT parametrization to incorporate the effect of the equilibrium, offers the possibility of modeling the reaction rate regardless of the shortcomings of theory. Neither a theoretical model for the effect of the equilibrium nor a reaction model nor Arrhenius parameters are required. The NPK result vectors (blue dots in Fig. 3) can be used to predict the reaction rate in the parameter range of the dataset. As demonstration, the traces of the experiments have been recreated and compared to the original data. Fig. 4 shows the predicted and measured values of three experimental runs. They are found to be in very good agreement.

To verify this modeling approach with another reaction system and an other type of dataset, the reduction of CuO was investigated. The dataset [5] consists of 7 constant heating rate experiments with 2 K/min at 7 different oxygen partial pressures (10, 20, 50, 80, 100, 150 and 200 mbar). The reaction started, when the temperature exceeded the equilibrium temperature. The starting points of the reaction were found to be in good agreement with thermodynamic predictions. The reaction can be described by the following formula:

$$4\,CuO + \Delta^R H \rightleftarrows 2Cu_2O + O_2 \tag{9}$$

Fig. 5 shows the output of the NPK algorithm. It can be seen, that the effect of the equilibrium decreases continuously towards 0. The fact that the effect of the equilibrium is greater than 0 at the equilibrium can be attributed to the slight deviation of the reaction start temperatures from the theoretical equilibrium temperature. Thus, the theoretical prediction seems to be applicable for this decomposition reaction. This, again, coincides with the findings by Schaube et al. [8], who found the rate of the decomposition reaction could be modeled well with the $1 - (p/p^*)^{\nu_G}$ term (even though they considered a different reaction system). The identified activation energy is 382 kJ/mol ± 24 %, which is an unacceptably large uncertainty. If the goal was to identify kinetic parameters, additional experimental runs with higher heating rates would be required to increase the accuracy of the identified Arrhenius parameters.

For the prediction of the reaction rate, no further identification of the NPK model is required. Only the result vectors (blue dots in Fig. 5) are used. Fig. 6 shows the simulation results for constant

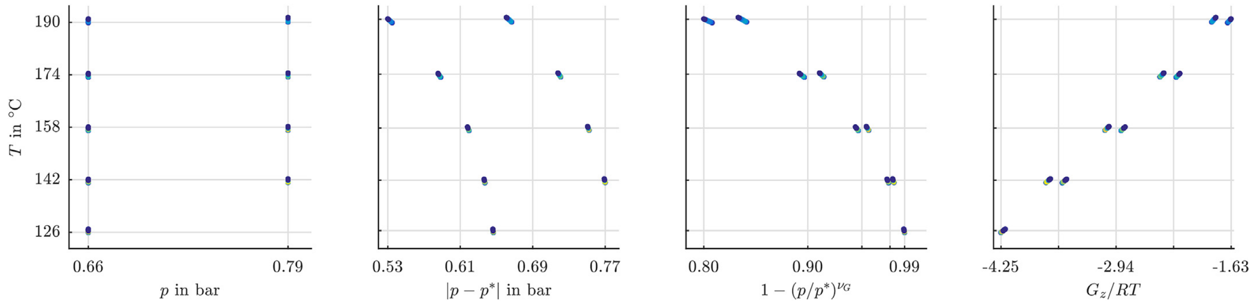

Fig. 2. Distribution of data points in the dataset of the hydration of CaC_2O_4 with the four different parametrization methods.

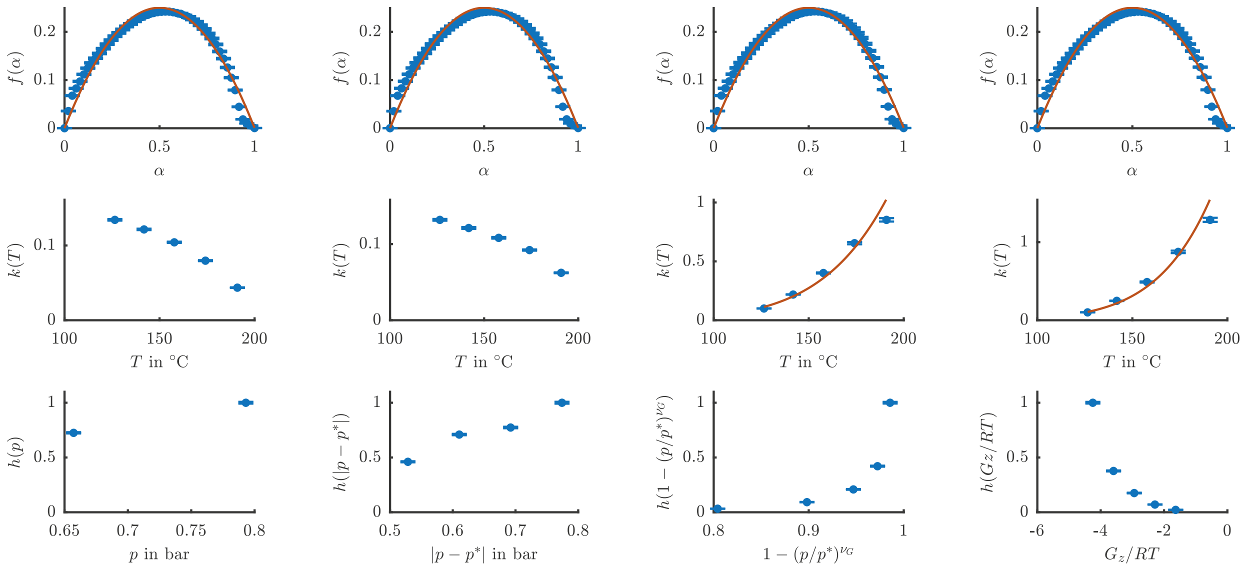

Fig. 3. Output of the NPK algorithm for the hydration of CaC_2O_4 with the four different parametrization methods.

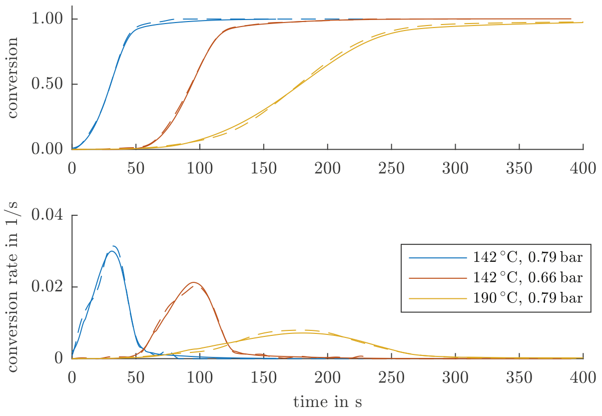

Fig. 4. Simulated reaction trajectories (solid) and experimental data (dashed) for the hydration of CaC_2O_4.

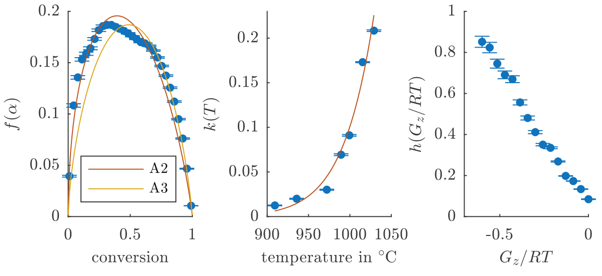

Fig. 5. NPK model of the reduction of CuO.

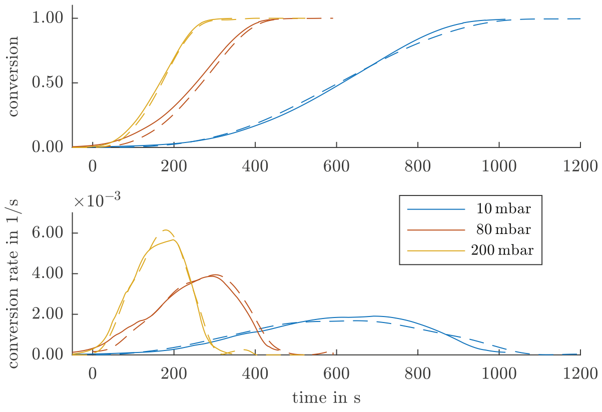

Fig. 6. Simulated reaction trajectories (solid) and experimental data (dashed) for the reduction of CuO.

heating rate experiments at different partial pressures. The predicted trajectories are in very good agreement with the experimental values. Thus, non-parametric modeling can be used as a generic approach to predict the reaction rate of gas-solid reactions in absence of detailed theoretical models. Only sufficient data and variables that the main effects are correlated with are required.

6. Conclusion

A review of the literature about the effect of the reaction equilibrium on the reaction rate of gas-solid reactions has been presented and four different parametrization methods have been compared by non-parametric modeling of kinetic data of the hydration of CaC_2O_4. Our results show that taking the effect of the reverse reaction into account is essential for modeling the reaction rate in the vicinity of the equilibrium. Of the four parametrization methods, only $1-(p/p^*)^{\nu_G}$ and G_z/RT were capable of capturing the effect of the reaction equilibrium correctly. However, G_z/RT is a better match for non-parametric modeling, as it is an unbounded value that allows to identify the effect of the equilibrium at any distance from the equilibrium.

Our analysis has shown that the effect of the equilibrium, derived from experimental data of the hydration of CaC_2O_4, does not match the theoretical formula based on transition state theory. Since this finding is consistent with observations of other researchers, it can be expected that this formula will fall short of describing the effect of the equilibrium for formation reactions in general. More sophisticated theories to describe the effects in close vicinity of the reaction equilibrium will have to be developed. Considering the complexity of hydration reactions and gas-solid reactions in general, the possibility of a physical process being the rate limiting step has to be considered and also the single step assumption has to be assessed critically.

One of the main advantages of non-parametric modeling is that it does not require explicit models to predict the reaction rate of gas-solid reactions. As demonstration, the hydration of CaC_2O_4 and the reduction of CuO have been modeled and the reaction trajectories have been simulated. The simulated trajectories have been found to be in good agreement with experimental data. This generic data-driven modeling approach can be used regardless of the shortcomings of theory, for reactions as diverse as the two considered in this paper. In this way, non-parametric modeling offers a powerful tool for applied research in the field of thermochemical energy storage to predict the kinetics of gas-solid reactions for reactor and process design.

Author contributions section

Felix Birkelbach: Conceptualization, Methodology, Software, Formal analysis, Writing - Original Draft. Markus Deutsch: Methodology, Writing - Review & Editing. Andreas Werner: Supervision, Project administration, Funding acquisition.

Declaration of competing interest

The authors declare that they have no known competing financial interests or personal relationships that could have appeared to influence the work reported in this paper.

Acknowledgements

The authors would like to thank Christian Knoll and Saman Setoodeh Jahromy for providing us with the raw data of their measurements for our analysis as well as the Austrian Research Promotion Agency (FFG) for their financial support of the project SolidHeat Pressure (#853593).

Appendix A. Adaptation of the modeling algorithm

For this work the non-linear least squares algorithm that we published in Ref. [11] was adapted. Now the residuals are computed at the data points instead of at the tensor elements. In this way, the error introduced by projecting the data points onto the data tensor can be avoided, which improves the results on unequally distributed data sets like in this study considerably.

To compute the residuals at the datapoints, the value of the unknown functions $f_i(v_i)$ inbetween two grid points $v_{i,j^*} < v_i < v_{i,j^*+1}$ needs to be estimated. Starting from Equation (4) in Ref. [11], the value of $f_i(v_i)$ can be approximated with local linear interpolation

$$f_i(v_i) \approx \widehat{f}_i(v_i) = \begin{bmatrix} 1 & v_i \end{bmatrix} \begin{bmatrix} 1 & v_{i,j^*} \\ 1 & v_{i,j^*+1} \end{bmatrix}^{-1} \begin{bmatrix} f_{i,j^*} \\ f_{i,j^*+1} \end{bmatrix} = \boldsymbol{\gamma}_{v_i} \boldsymbol{f}_i. \tag{A.1}$$

Here, $\boldsymbol{\gamma}_{v_i}$ is a row vector containing the interpolation coefficients at the positions corresponding to v_{i,j^*} and v_{i,j^*+1} and zero otherwise. The interpolation can always be computed as a matrix multiplication, regardless of the polynomial order, so higher order interpolation polynomials would also be possible.

Given a data set $[d_k,\ \widehat{v}_{1,k},\ \ldots,\ \widehat{v}_{D,k}]$, where

$$d_k = \frac{\mathrm{d}\alpha}{\mathrm{d}t}\left(\widehat{v}_{1,k}, \ldots, \widehat{v}_{D,k}\right) \tag{A.2}$$

from experiments, the residuals can be computed with

$$r_k = \prod_{i=1}^{D} \boldsymbol{\gamma}_{\widehat{v}_{i,k}} \boldsymbol{f}_i - d_k. \tag{A.3}$$

Since neither the position of the data points nor of the grid points changes during the optimization, all $\boldsymbol{\gamma}_{\widehat{v}_{i,k}}$ can be computed beforehand.

To solve the optimization problem efficiently, the model needs to be reduced as shown in Equation (14) and the Jacobian can be derived analytically in analogy to Equation (15) and Equation (16) in Ref. [11].

We provide a Matlab implementation of this algorithm as supplementary material.

Appendix B. Supplementary data

Supplementary data to this article can be found online at https://doi.org/10.1016/j.renene.2020.01.033.

References

[1] C. Agrafiotis, M. Roeb, M. Schmücker, C. Sattler, Exploitation of thermochemical cycles based on solid oxide redox systems for thermochemical storage of solar heat. Part 1: Testing of cobalt oxide-based powders, Sol. Energy 102 (2014) 189–211, https://doi.org/10.1016/j.solener.2013.12.032.

[2] A. Solé, I. Martorell, L.F. Cabeza, State of the art on gas–solid thermochemical energy storage systems and reactors for building applications, Renew. Sustain. Energy Rev. 47 (2015) 386–398, https://doi.org/10.1016/j.rser.2015.03.077.

[3] P. Donkers, L.C. Sögütoglu, H.P. Huinink, H.R. Fischer, O. Adan, A review of salt hydrates for seasonal heat storage in domestic applications, Appl. Energy 199 (2017) 45–68, https://doi.org/10.1016/j.apenergy.2017.04.080.

[4] Y. Kato, Y. Sasaki, Y. Yoshizawa, Magnesium oxide/water chemical heat pump to enhance energy utilization of a cogeneration system, Energy 30 (11–12) (2005) 2144–2155, https://doi.org/10.1016/j.energy.2004.08.019.

[5] S. Setoodeh Jahromy, F. Birkelbach, C. Jordan, C. Huber, M. Harasek, A. Werner, F. Winter, Impact of partial pressure, conversion, and temperature on the oxidation reaction kinetics of Cu_2O to CuO in thermochemical energy storage, Energies 12 (3) (2019) 508, https://doi.org/10.3390/en12030508.

[6] M. Deutsch, F. Horvath, C. Knoll, D. Lager, C. Gierl-Mayer, P. Weinberger, F. Winter, High-temperature energy storage: kinetic investigations of the CuO/Cu_2O reaction cycle, Energy Fuels 31 (3) (2017) 2324–2334, https://doi.org/10.1021/acs.energyfuels.6b02343.

[7] C.K. Clayton, K.J. Whitty, Measurement and modeling of decomposition kinetics for copper oxide-based chemical looping with oxygen uncoupling, Appl. Energy 116 (2014) 416–423, https://doi.org/10.1016/j.apenergy.2013.10.032.

[8] F. Schaube, L. Koch, A. Wörner, H. Müller-Steinhagen, A thermodynamic and kinetic study of the de- and rehydration of $Ca(OH)_2$ at high H_2O partial pressures for thermo-chemical heat storage, Thermochim. Acta 538 (2012) 9–20, https://doi.org/10.1016/j.tca.2012.03.003.

[9] M. Ron, The normalized pressure dependence method for the evaluation of kinetic rates of metal hydride formation/decomposition, J. Alloy. Comp. 283 (1–2) (1999) 178–191, https://doi.org/10.1016/S0925-8388(98)00859-7.

[10] C. Knoll, D. Müller, W. Artner, J. Welch, A. Werner, M. Harasek, P. Weinberger, Probing cycle stability and reversibility in thermochemical energy storage - CaC_2O_4–H_2O as perfect match? Appl. Energy 187 (2017) 1–9, https://doi.org/10.1016/j.apenergy.2016.11.053.

[11] F. Birkelbach, M. Deutsch, S. Flegkas, F. Winter, A. Werner, NPK 2.0: introducing tensor decompositions to the kinetic analysis of gas-solid reactions, Int. J. Chem. Kinet. 51 (4) (2019) 280–290, https://doi.org/10.1002/kin.21251.

[12] J.E. Burke, D. Turnbull, Recrystallization and grain growth, Prog. Met. Phys. 3 (1952) 220–292, https://doi.org/10.1016/0502-8205(52)90009-9.

[13] R.S. Bradley, The energetics and statistical mechanics of the kinetics of solid–>solid reactions, J. Phys. Chem. 60 (10) (1956) 1347–1354, https://doi.org/10.1021/j150544a002.

[14] J. Sestak (Ed.), Science of Heat and Thermophysical Studies: A Generalized Approach to Thermal Analysis, first ed., Elsevier Science, 2005.

[15] M. Reading, D. Dollimore, R. Whitehead, The measurement of meaningful kinetic parameters for solid state decomposition reactions, J. Therm. Anal. 37 (9) (1991) 2165–2188, https://doi.org/10.1007/BF01905585.

[16] P.M. Barret, Expression théorique en fonction de la pression de la loi de vitesse de croissance d'une solide, Comptes rendus hebdomadaires des séances de l'Académie des sciences, Série C Sc. Chim. 266 (1968) 856–859.

[17] A.W. Searcy, D. Beruto, Kinetics of endothermic decomposition reactions: 2. Effects of the solid and gaseous products, J. Phys. Chem. 82 (2) (1978) 163–167, https://doi.org/10.1021/j100491a008.

[18] A. Galwey, M. Brown, Application of the Arrhenius equation to solid state kinetics: Can this be justified? Thermochim. Acta 386 (2002) 91–98.

[19] P. Šimon, Considerations on the single-step kinetics approximation, J. Therm. Anal. Calorim. 82 (3) (2005) 651–657, https://doi.org/10.1007/s10973-005-0945-6.

[20] V. Goetz, A. Marty, A model for reversible solid-gas reactions submitted to temperature and pressure constraints: simulation of the rate of reaction in solid-gas reactor used as chemical heat pump, Chem. Eng. Sci. 47 (17–18) (1992) 4445–4454, https://doi.org/10.1016/0009-2509(92)85122-R.

[21] M. Deutsch, F. Birkelbach, C. Knoll, M. Harasek, A. Werner, F. Winter, An extension of the NPK method to include the pressure dependency of solid state reactions, Thermochim. Acta 654 (2017) 168–178, https://doi.org/10.1016/j.tca.2017.05.019.

[22] L.-C. Sögütoglu, M. Steiger, J. Houben, D. Biemans, H.R. Fischer, P. Donkers, H. Huinink, O.C.G. Adan, Understanding the hydration process of salts: the impact of a nucleation barrier, Cryst. Growth Des. 19 (4) (2019) 2279–2288, https://doi.org/10.1021/acs.cgd.8b01908.

Relevant publications as co-author

While doing the research for this thesis I got to collaborate with colleagues who were working on similar topics. Here, I briefly present our joint papers and highlight the most important findings in the context of this theses.

Paper 4 An extension of the NPK method to include the pressure dependency of solid state reactions

by Markus Deutsch, Felix Birkelbach, Christian Knoll, Daniel Lager, Christian Gierl-Mayer, Peter Weinberger und Franz Winter; published in Thermochimica Acta.

In this paper, the original NPK method was extended, so that it could also be used to model the pressure dependency of gas-solid reactions. The algorithm was limited to two dimensions. The pressure dependency was included by applying it twice: once on a conversion-temperature plane, once on a conversion-pressure plane. The full three-dimensional model was obtained by combining the two two-dimensional models by considering the intersection of the two planes. The method was demonstrated by applying it to a simulated dataset and to model the decomposition of $CdCO_3$ (cadmium carbonate).

The research in this paper showed the potential of data-driven modeling in more than two variables. However, the limitation to two panes limited the type of data that could be used and consequently the scope of the kinetic study.

My contribuion: Presenting the underlying mathematics. Implementation of statistical hypothesis testing for model-fitting. Editing of the manuscript and handling the revision process.

M. Deutsch, F. Birkelbach, C. Knoll, M. Harasek, A. Werner, and F. Winter (2017). "An extension of the NPK method to include the pressure dependency of solid state reactions". In: Thermochimica Acta *654, pp. 168–178.* ISSN*: 00406031.*
DOI*: `10.1016/j.tca.2017.05.019`*

Abstract

An novel method to identify the pressure dependency for reactions of the type $A(s) \rightleftarrows B(s) + C(g)$ is proposed. It is an extension of the non-parametric kinetic analysis (NPK) method as it identifies the pressure dependency in addition to the temperature and conversion dependency of the reaction. This is done by analyzing kinetic data in a three-dimensional data space (conversion, temperature, pressure) and attributing the variation of the conversion rate to these independent variables. Thus a reduction from a three-dimensional problem to three one-dimensional problems is achieved. The derivation of a kinetic model can then be performed for each dependency independently, which is easier than deriving a model directly from the data.

This work presents the basic approach of the identification and combination of the three dependencies to build a full kinetic model. Also, the interpretation of the model to achieve a physically motivated model is illustrated.

Then the method is applied to identify the complex reaction kinetics of the decomposition of $CdCO_3$ based on a set of thermogravimetric measurements. It is shown that it is possible to identify interaction terms between the dependency terms.

Paper 5 Impact of Partial Pressure, Conversion, and Temperature on the Oxidation Reaction Kinetics of Cu_2O to CuO in Thermochemical Energy Storage

by Saman Setoodeh Jahromy, Felix Birkelbach, Christian Jordan, Clemens Huber, Michael Harasek, Andreas Werner and Franz Winter; published in Energies.

The REDOX (reduction-oxidation) system Cu_2O/CuO (cuprous oxide/cupric oxide) is one of the potential reaction systems for thermochemical energy storage in concentrated solar power plants. In this paper, the material was analyzed with various methods and the oxidation kinetics were studied. For the kinetic analysis a large dataset with measurements at four different temperature and partial pressure levels was used. From this dataset a kinetic model that included the effect of the equilibrium/driving force was derived with the TensorNPK method and interpreted in terms of the chemical reaction.

This was the first application of the newly developed TensorNPK method. The method proved very useful — especially because this type of analysis, with an equilibrium term but without specific its shape, would not have been possible with any other method. The analysis of the oxidation data revealed two things: First, that the effect of the equilibrium has to be taken into account to get a consistent model. Second, that the reaction rate decreases much faster towards the equilibrium than theory would suggest.

During the modeling I noticed an inconsistency with the standard equilibrium term $1-p/p_{\mathrm{eq}}$. It assumed large negative values, which could not be interpreted in a meaningful way. Also, the transformation from the temperature-pressure grid, where the experimental data was collected, to the temperature-equilibrium distance grid that was used for the kinetic modeling, introduced an significant error. Both aspects were identified as open questions that needed to be addressed as soon as possible (see Paper 3).

My contribuion: Processing the kinetic data with specialized algorithms. Kinetic modeling of the oxidation data.

S. Setoodeh Jahromy, F. Birkelbach, C. Jordan, C. Huber, M. Harasek, A. Werner, and F. Winter (2019). "Impact of Partial Pressure, Conversion, and Temperature on the Oxidation Reaction Kinetics of Cu_2O to CuO in Thermochemical Energy Storage". In: Energies *12.3, p. 508.* ISSN*: 1996-1073.*
DOI*:* `10.3390/en12030508`

Abstract

Metal oxides are promising potential candidates for thermochemical energy storage in concentrated solar power plants. In particular, the Cu_2O/CuO system is suitable because of its high energy density, applied temperature interval, and reduced cost compared to the CoO/Co_3O_4 system. In heterogenous gas-solid reactions, the pressure affects the

kinetics significantly. To quantify this effect for oxidation of Cu_2O to CuO, isothermal runs between 800 °C and 930 °C at different oxygen partial pressures (0.1, 0.2, 0.5, and 1.0 bar) were conducted with thermogravimetric analysis (TGA). Defined fractions of CuO samples (1–100 µm) were analyzed with X-ray diffraction (XRD), Brunauer-Emmett-Teller (BET) analysis, and scanning electron microscopy (SEM) analysis. The kinetic analyses were performed with extended non-parametric kinetics (NPK), which is applied for the first time to consider the pressure term in the general kinetic equation in addition to the conversion and the temperature term.

The results show how the oxygen partial pressure impacts the kinetics and how reparameterization of the pressure term affects the kinetic analysis of the oxidation reaction of Cu_2O to CuO. The best conversion model is a two-dimensional Avrami-Erofeev model with an activation energy of 233 kJ/mol. The kinetic models for conversion, temperature, and pressure presented in this work provide one of the most important requirements for reactor designs.

Paper 6 The multistep decomposition of Boric Acid

by Clemens Huber, Saman Setoodeh Jahromy, Felix Birkelbach, Jakob Weber, Christian Jordan, Manfred Schreiner, Michael Harasek and Franz Winter; published in Energy Science & Engineering.

The reaction system H_3BO_3/B_2O_3 (boric acid/boron oxide) has been proposed as thermochemical heat storage system for low temperature applications such as household and district heating. Compared to other systems that we analyzed, the dehydration of H_3BO_3 is much more complex. Its decomposition consists of various steps — the exact number of steps was not agreed upon. This paper seeks to clarify this open question and to get insight into the reaction kinetics.

Due to the multi-step nature of the decomposition, kinetic modeling was quite challenging. First, the reaction steps were deconvoluted with a peak-fitting procedure to make the tensor NPK method applicable. Then a kinetic model of each reaction step was derived. Due to the narrow temperature ranges, where data was available for each reaction step, and uncertainties introduced by the deconvolution procedure, it was hard to interpret the resulting kinetic models mechanistically. Nevertheless the models provided an insight into the reaction steps of the decomposition of H_3BO_3.

My contribuion: Devising a kinetic modeling strategy and assisting with kinetic modeling.

C. Huber, S. S. Jahromy, F. Birkelbach, J. Weber, C. Jordan, M. Schreiner, M. Harasek, and F. Winter (2020). “The multistep decomposition of boric acid”. In: Energy Science & Engineering *35, p. 143.* ISSN*: 2050-0505.*
DOI*: `10.1002/ese3.622`*

Abstract

Due to its high potential for thermal energy storage systems the decomposition of boric acid is of particular interest in the field of applied research. The complexity of the reaction mechanism, with its multiple partially-overlapping reaction steps, hitherto prevented a clear identification and analysis of each stoichiometric reaction step. So far, various research teams performed different kinetic analyses of boric acid, which led to various reaction mechanisms and stoichiometric reaction steps with yet inconclusive results for process modeling. Thus, a deeper examination of the process was desirable, to validate whether a proposed reaction is reasonable or not. For this purpose, experimental data were used for a deconvolution of the reaction sequence, using the Fraser-Suzuki function, which clearly revealed the respective single reactions. The results of the deconvolution were compared with the proposed reaction steps in consideration of the stoichiometric ratio and thereby illustrated that the decomposition of polycrystalline boric acid more likely consists of three reaction steps. In contrary to the two-step mechanism, the three-step mechanism showed a very good correlation ($r > 99\,\%$).

Based on these outcomes, kinetic analyses were performed for each reaction step, by means of the non-parametric kinetics 2 (NPK2) method with subsequent determination of kinetic parameters. Additionally, for a deeper insight into the reaction, analyzing techniques like X-ray diffraction (XRD), scanning electron microscopy (SEM) and simultaneous thermal analysis (STA) were applied.

Paper 7 Hydration of salts as a two-step process: Water adsorption and hydrate precipitation

by Leyla-Cann Söğütoğlu, Felix Birkelbach, Andreas Werner and Henk Huinink; submitted to Thermochimica Acta.

In collaboration with the TU Eindhoven an in-depth kinetic study of the hydration of salts was conducted. The focus lay on K_2CO_3 (potassium carbonate) and the results were confirmed with LiCl (lithium chloride), $MgCl_2$ (magnesium chloride) and $CuCl_2$ (copper chloride). Some of these salts show a metastable zone around the reaction equilibrium, where the reaction is kinetically inhibited and rapidly increasing kinetics outside this zone. The TensorNPK method was used extensively to model the kinetics in various ways to understand the rate limiting processes during hydration.

We were able to show that the reaction is inhibited by nucleation inside the metastable zone and limited by diffusion to the wetting layer outside the metastable zone. The TensorNPK method proved a versatile tool to test hypothesis against the data and to separate the effects of different variables.

My contribuion: Kinetic modeling of the hydration data. Drafting the paper.

Currently submitted to Thermochimica Acta.

Abstract

K_2CO_3 is a promising salt for thermochemical heat storage. For a high performance, the thermochemical reaction must take place as close as possible to the equilibrium, while ensuring sufficient reaction rates. In this work, we studied the near-equilibrium hydration kinetics of K_2CO_3 and other salts ($CuCl_2$, $MgCl_2$ and LiCl). We proposed a generic two-step mechanism for the hydration of salts, consisting of (1): adsorption of water

vapour and dissolution of ions from the initial phase (a wetting film) and (2): formation of the hydrate crystal. The two steps are assumed to be in momentarious balance during the hydration process. As a result, nucleation is rate limiting at low supersaturations of water vapour (inside the metastable zone), and water diffusion to the wetting film is rate limiting at high supersaturations (outside the metastable zone). We have seen that the vapour pressure of the wetting film stabilises at the metastable zone boundary p^*. The driving force for hydration outside the metastable zone is therefore the pressure difference between the atmospheric vapour pressure and the vapour pressure of the wetting film, $p - p^*$. As expected, the diffusion limited process at high supersaturations hardly depends on the temperature, but mainly on the pressure difference. Experimental data were found consistent with models of nucleation/growth inside the metastable zone. Models outside the metastable zone suggest a reaction interface which does not contract throughout the conversion. It is further shown that the diffusion limited process can be characterised with an apparent activation energy. However, this apparent activation energy is in fact the hydration enthalpy and does not refer to a real energy barrier.

Contributions to international conferences

Paper 8 The effect of the reaction equilibrium on the kinetics of gas-solid reactions — A non-parametric modeling study

by Felix Birkelbach, Markus Deutsch and Andreas Werner; oral presentation at the EuroTherm Seminar #122 in Lleida.

This conference paper was selected to be published in a Special Issue of the Renewable Energy journal. The journal paper is included as Paper 3 in this thesis. A comment on the research that is presented in this paper can be found there.

F. Birkelbach, M. Deutsch, and A. Werner (2019b). "The effect of the reaction equilibrium on the kinetics of gas-solid reactions — A non-parametric modeling study". In: Advances in Thermal Energy Storage. *Ed. by Universitat de Lleida. Edicions de la Universitat de Lleida, pp. 161–171.* ISBN*: 978-84-9144-155-7.*

Abstract

Thermochemical energy storage has great potential to contribute to covering future thermal storage demand, mostly due to its high volumetric and gravimetric energy densities, nearly lossless storage, as well as the wide range of operating temperature levels. Most thermochemical energy storage concepts are based on gas-solid reactions, whose viability for a given application is often determined by the reaction kinetics under process conditions. From a thermodynamic perspective, the two most important variables determining the reaction rate are the temperature and the partial pressure of the reactant gas. In kinetic modeling, the effect of the temperature is usually modeled with the Arrhenius equation and the partial pressure is commonly used as a measure of the distance to the reaction equilibrium.

In the present work, different parametrization methods are compared, that are available

in the literature to quantify the distance to the equilibrium. Their viability is evaluated by modeling the kinetics of two reaction systems, relevant for thermochemical energy storage, from experimental (TGA) data. For the derivation of kinetic models from experimental data, a non-parametric modeling method based on tensor decompositions is used. The main advantage of this method is that it is model-free, i.e. that it does not rely on an a-priori assumption about the functions in the general kinetic equation. In this way, it allows for the unbiased, purely data driven, assessment of different parametrization methods, without interference of the model choice. Additionally, an adaptation of the method is presented to facilitate the utilization of experimental data from a p-T grid for modeling with an equilibrium term.

Our tests on experimental data in the vicinity of the equilibrium show that the derived models fit the data well, if a suitable equilibrium term is included. It is especially important to take the distance to the equilibrium into account when modeling formation reactions, because the effect of the equilibrium distance counteracts the Arrhenius term, leading to seemingly negative activation energies if the equilibrium term was omitted. Our tests also show that for formation reactions, the reaction rate decreases much faster towards the equilibrium than theory predicts. We present an empirical modeling approach that can predict the reaction rates of gas-solid reactions in the vicinity of the equilibrium irrespective of the shortcomings of theory. In this way, the non-parametric modeling framework offers a powerful tool for applied research.

Appendices

A Practical aspects of non-parametric kinetic modeling

Non-parametric modeling is a versatile tool to interpret reaction rate data according to the General Kinetic Equation. Compared to other kinetic modeling methods, it is more flexible and it requires fewer a-priori assumptions about the reaction. Initially, the main issue with non-parametric modeling was that the algorithms were too complicated to make it a viable option for most research groups. With the new algorithm that I developed in this thesis, the modeling process is much easier and less prone to errors. Further, the extension to more than two variables allows to model more complex effects. A Matlab implementation of the TensorNPK method is available in the supplementary material of Paper 3.

I am convinced that the TensorNPK method is a good choice for various kinetic modeling tasks and I hope that it will be used by other research groups. For this reason, I added this chapter to discuss the practical aspects and the work-flow of generating reliable models with the TensorNPK method. Additionally, I will present some best-practice approaches that have proven viable in the last three years.

The starting point for this discussion is a data set with mass, heat, temperature, . . . traces at different reaction conditions. We will assume that the experiments have been conducted meticulously and measurement artifacts have been compensated. Also, the decision which variables will be used for the model has already been made. Starting from this data set, the work-flow for deriving a kinetic model is the following:

1. Screening of the data set: Consistency checks, range of variables, correlations, etc. .
2. Pre-processing of experimental data: smoothing, calculation of conversion, etc. .
3. Selecting a modeling grid and smoothing parameters.
- Decomposing the experimental data into the contributions of each variable with the TensorNPK method.
4. Evaluation of the output: Numerical accuracy, viability of single step approximation, consistency with theory, comparison with results from other methods,. . .
5. Post processing: Fitting of reaction models, determining Arrhenius parameters, etc. .

In the following sections, each of these steps will be discussed in detail.

A.1 Screening of the data set

The most important requirement on the data is that it be representative of the reaction under consideration and that interference of other processes is negligible. This is, of course, easier said than done, considering that a multitude of processes are taking place at the same time during a gas-solid reaction. A discussion of how to conduct experiments is beyond the scope of this work. In Section 2.3 some references to relevant publications on the topic are provided.

The range of each variable, where experimental data is available, determines the validity range of the model. Consequently, experiments have to cover the variable range that is required by the application that the model is intended for. Since gas-solid reactions show

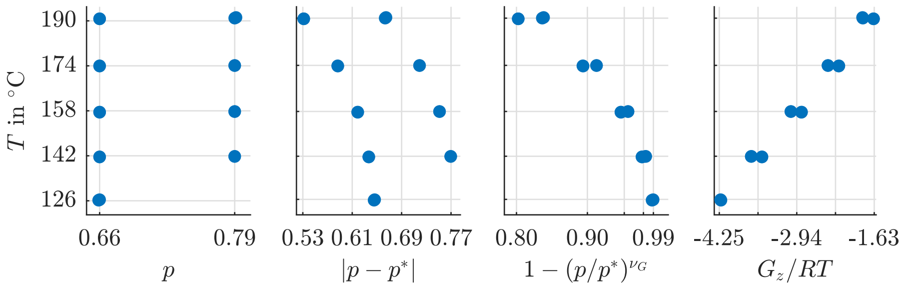

Figure A.1: *Kinetic dataset of the hydration of* CaC_2O_4 *with different pressure/driving force terms.*

highly non-linear behavior and even discontinuities, extrapolation of kinetic models is generally unreliable.

One of the main advantages of the TensorNPK method is, that it can process arbitrarily distributed data sets. Because of this, transformation of the data (e.g. by considering different driving force terms) is not an issue. Though, in order for the algorithm to determine the effect of each variable accurately, kinetic data must be distributed fairly equally over the whole variable range. If data is correlated between two variables, the algorithm does not know which variable to attribute the change of conversion rate to. This happens for example, when data of a formation reaction was collected on, say, five pressure levels at various temperatures (see Figure A.1). The left most diagram shows the p-T-grid were the data has been collected. Here, the data shows no correlation. Though, after transformation to a G_z/RT-T-grid, the data points show considerable correlation. The higher the temperature, the smaller the distance to the equilibrium. The correlation of the data points can affect the reliability of the model that is derived from such a data set. This should be kept in mind when drawing up the experimental schedule.

A.2 Pre-processing of experimental data

If experimental data is noisy, it should be smoothed before doing any further computations on it. For this task, locally estimated scatterplot smoothing (LOESS) methods, which are closely related to Savitzky-Golay filters, have been found to perform very well — especially, if the noisy signal has to be differentiated to obtain the conversion rate (such as with TGA or XRD data). The main advantage is that these methods can smooth and differentiate the signal at the same time (see Figure A.2). For this reason they yield better results than methods where the signal is first smoothed and then differentiated.

The amount of smoothing in LOESS is determined by two parameters: the polynomial order and the window size. If the signal is only smoothed, second order polynomials were found to perform well. If the differentiated signal is also computed, third order polynomials generally were the better choice. The optimal window size was determined with a leave-one-out cross-validation algorithm.

In some cases, the numerical differentiation with LOESS does not preserve the final value of the integral, i.e. the integral over the differentiated signal does not give the final

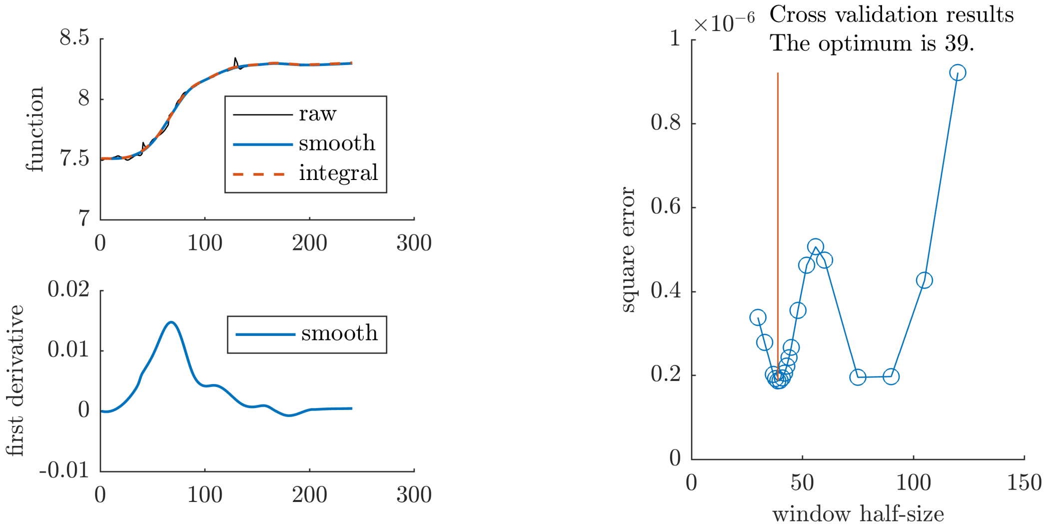

(a) *Smoothed mass trace (top) and mass change (bottom).*

(b) *Cross validation output to determine the optimal window size.*

Figure A.2: *Output of LOESS smoothing algorithm applied to a mass trace.*

value of the original signal. To prevent this, the differentiated data can be normalized so that the integral matches the end value of the original trace. This problem may arise if the sampling rate is low compared to the reaction duration. Because it may result in errors that are hard to track down, the consistency of the smooth signal and the integral over the differentiated signal should be checked routinely.

The next step in pre-processing usually is to perform the thermodynamic calculations to obtain the equilibrium partial pressure, driving force, etc. from the temperature and partial pressure of the sample. For these calculations, we usually rely on thermodynamic constants from material databases. Here, the usual caveats apply: Does the behavior of my sample match the predictions of the database constants? It might be worth confirming this experimentally.

A.3 Selecting the grid and penalty parameters

While the previous two sections are also valid for all other kinetic modeling methods, this section is specific to the non-parametric modeling. The TensorNPK method requires a modeling grid, on which it performs its calculations. The grid is defined by specifying an “axis” for each variable, i.e. a set of discrete values of this variable. Generally speaking, the range and number of grid points for each variable should match the range and density of data points. In regions where a lot of data is available, many grid points can be placed. In regions where no data is available, no grid points should be placed.

If not enough grid points are used, important features of the effect of this variable might not be identified. Using too many grid points might result in over-fitting, where the output not only reflects the “true” effect but also random noise in the data.

If the experimental data has been recorded with a high sample rate, an equally spaced grid with 30–50 grid points is usually a good choice for the conversion axis. If the data set consists of isothermal measurements, the temperature grid should match the temperature values, where the experiments have been conducted. For constant-heating-rate measurements, equally spaced grids can be used.

To alleviate some of the burden of selecting the correct number of grid points and placing them correctly, ridge regression with a smoothness penalty was implemented. With this method, grid points can be used generously and the smoothness penalty counteracts over-fitting if necessary. For this to work as intended the penalty parameter has to be chosen correctly. The penalty parameter essentially controls the weighting of numeric error vs. smoothness. I.e. the larger the penalty parameter, the smoother the output, at the cost of larger deviations between model and data. In the extreme case of exceedingly large penalty parameters, the effects of all variables would be straight lines (the best fit to the data with no curvature).

Generally, the smoothing parameter should be as small as possible, but large enough to produce a reliable model. To choose the penalty parameter automatically, k-fold cross validation was implemented. It works well on “well behaved” data sets, but sometimes fails on sparse data sets or if only few grid points are used. In these cases appropriate penalty parameters have to be selected by hand.[6]

A.4 Evaluation of the output

When the model has been computed, the first question that arises is “Is it any good?”. We found that goodness of fit tests are not really meaningful, because kinetic data sets are so large that the power of the test becomes so high that even insignificant deviations are identified as a lack of fit. Also, one single test could hardly catch the complexity of a kinetic model.

To evaluate whether the algorithm could identify significant effects, the effect plot can be evaluated. The error bars show the confidence interval of each value and provide information on the uncertainty. An effect can be considered significant, if at least some of its elements are significantly different from zero, i.e. if the error bars do not intersect with the x-axis, and if at least some elements are significantly different from each other, i.e. if they do have non-overlapping confidence intervals.

If the effect of a variable is found to be insignificant, the variable can usually be removed from the model. If the variable should have a significant effect, but the algorithm does not find it, this can have two reasons: One, another important effect is omitted in the model, which is superimposing the effect that we are looking for. E.g. when omitting the equilibrium distance/driving force in formation reactions, the effect of temperature can be superimposed with the effect of the equilibrium/driving force. Second, if the variable of the effect is correlated with another variable, it could be that the algorithm attributed the effect to the other variable. In this case, additional experiments should be conducted

---

[6] More sophisticated algorithms for choosing optimal penalty parameters would also be an option, but I did not find the time to develop them.

to alleviate the correlation of the two variables. Sometimes, imputing additional data points that enforce consistency with theory can help the algorithm to identify the effects correctly. An example would be adding data-points with zero conversion rate at the reaction equilibrium, if the data set does not include experimental data at the equilibrium.

To evaluate whether the model is accurate, the residuals should be analyzed. The residuals should be equally distributed across the range of all variables. Larger residuals in some regions might point to inadequacies of the model, i.e. deviations from the single-step assumption. To identify regions with exceptionally large residuals, the residuals can be plotted over each variable. The more variables are considered in the model, the harder it is to identify regions with larger residuals.

Another way to look at the residuals is to project the experimental conversion rate values on the effect of each dimension by eliminating the effect of the other variables. The formulas for this are given in Equation (B.26).

A good way to evaluate the model is to check whether the model is capable of reproducing the experimental trajectories, which were used as input to the TensorNPK algorithm. To get the simulated trajectories, the model and the reaction conditions of the experiment are fed into an ODE solver. Then the experimental and simulated trajectories are compared qualitatively. This evaluation is only meaningful, if reaction trajectories are simulated that have not been used to derive the model. A bootstrapping procedure, where all but one experiment are used to derive the model and the model is then used to simulate the trajectory of the left-out experiment may help identifying experimental runs that diverge from the others.

Generally, splitting the data-set can be used to detect deviations from the single rate-limiting step assumption. By splitting the dataset into conversion intervals, the single step approximation can be tested similarly to how isoconversional methods do it. Also, the dataset can be split into different regions by reaction conditions to check if the rate limiting step changes.

A.5 Post-processing

The only two types of post-processing that we did regularly were fitting reaction models from literature to determine the best-fitting one and fitting the Arrhenius equation to determine the Arrhenius parameters. For both these fitting operations, weighting the output with the inverses of the variance increased the quality of the fit considerably. Especially values at the lower and the upper end of the range of each variable can often only be determined with lower accuracy than values in the center. The variance of these values is then considerably larger and weighting with the inverse of the variances makes sure that these values do not affect the fit adversely.

To identify the best fitting reaction model, pair-wise F-testing has proven to be useful. For the Arrhenius parameters, the confidence intervals should be evaluated.

An issue with using the values of the effect vectors for the model fitting is that the confidence interval of the identified parameters will depend on the number of grid points that were used in that dimension. This is of course an unwanted property. To resolve this issue, the data points can be projected onto the dimension (Equation (B.26)) and model fitting can be done with these values as input. Whether using the values of the effect vector or the projected values is correct from a mathematical perspective, I do not know. Since typical data sets contain many more data points than there are grid points in a NPK model, the confidence intervals are much more narrow with the second approach.

A.6 Concluding remarks

Regarding the "correctness" of kinetic models, some degree of uncertainty will always remain, since an independent validation of the kinetic model is usually not possible. The effects that the TensorNPK method identifies are first and foremost correlations of the reaction rate data with the selected variables, and the connection between correlation and causality should be well known.

In a gas-solid reaction a vast number of processes interact with each other. With today's experimental methods, only the combined effect of all these processes (e.g. heat release or mass change) can be measured. Conclusions on reaction mechanism should not be based on thermal analysis alone but always be backed up with data from other complementary analysis methods. The results of the NPK analysis could for example be compared with the results of optical and electron microscopy images or crystallographic analyses to back up the findings.

Empirical models that are used for predicting the reaction rate should always be treated as contingent on the reaction conditions in the experiment and the configuration of the solid reactant.

B Mathematics of the TensorNPK method

Most of the math that the TensorNPK method is based on has already been presented in Paper 2 “NPK 2.0: Introducing tensor decompositions to the kinetic analysis of gas-solid reactions” and the change of how the residuals are calculated has been presented in Paper 3 “The effect of the reaction equilibrium on the kinetics of gas-solid reactions — A non-parametric modeling study”. The formulas for the penalized regression are fairly standard formulas and have not yet been included in any of my publications. Regardless, it might be useful to have all the equations in one place. (A Matlab implementation of the TensorNPK method is available in the supplementary material of Paper 3.)

The starting point is the General Kinetic Equation (GKE) for gas-solid reactions that models the conversion rate $\mathrm{d}\alpha/\mathrm{d}t$ as

$$\frac{\mathrm{d}\alpha}{\mathrm{d}t} = f(\alpha)\, k(T)\, h(p)\,. \tag{B.1}$$

Here, $f(\alpha)$ is the effect of conversion, $k(T)$ the effect of temperature and $h(p)$ the effect of the driving force — in this case pressure. The GKE is discussed at length in Section 2.2.

More generally, the conversion rate is assumed to be the multiplication of D independent effects:

$$\frac{\mathrm{d}\alpha}{\mathrm{d}t} = \prod_{i=1}^{D} f_i(v_i)\,. \tag{B.2}$$

Here, $f_i(v_i)$ are the unknown effects of the variables v_i. Typically these would be $f(\alpha)$, $k(T)$ and $h(p)$ from Equation (B.1). In other words: Equation (B.2) is a generalization of the GKE for an arbitrary number of effects. The goal of the TensorNPK algorithm is to derive these unknown effects $f_i(v_i)$ from experimental data.

A dataset contains various data points k, were each data point consists of the values of the D variables considered in the model and the corresponding value of the conversion rate R_k. The formal definition of a dataset with N_{data} elements is

$$[v_{k,1},\, \ldots,\, v_{k,D},\, R_k] \quad \text{with} \quad k \in [1, N_{\mathrm{data}}]\,. \tag{B.3}$$

So this is the starting point for the TensorNPK algorithm: The model in Equation (B.2) and a data set as defined in Equation (B.3). The goal of the algorithm is to calibrate the model, so that it matches the data. In mathematical terms, the goal is to minimize the deviation between the model estimate and the measured conversion rate:

$$\min \sum_k \left[\left.\frac{\mathrm{d}\alpha}{\mathrm{d}t}\right|_{v_{k,1},\, \ldots,\, v_{k,D}} - R_k \right]^2 . \tag{B.4}$$

In the following section, the “core” math will be covered. In Appendix B.2, I will try to illustrate the working principle of the TensorNPK method in a way that is easier to comprehend than plain math. The other two sections in this chapter address variance estimation and penalized regression.

Throughout this chapter the following formalism is used: Vectors are written in bold lower-case letters $\boldsymbol{v}$, tensors in calligraphic letters $\mathcal{T}$. The index k is used to refer to data points or symbols related to data points. The index i is used to refer to dimensions, j is used to refer to elements of vectors or tensors. Consequently j_i is the element index in dimension i.

B.1 Discretization and rank-1 approximation

Let's consider the model in Equation (B.2). First, the interval of each variable v_i is discretized into N_i elements with the index $j_i \in [1, N_i]$. We define the

- variable vectors $\boldsymbol{v}_i = [v_{i,1}, \dots, v_{i,N_i}]^T$ and the
- effect vectors $\boldsymbol{f}_i = [f_i(v_{i,1}), \dots, f_i(v_{i,N_i})]^T = [f_{i,1}, \dots, f_{i,N_i}]^T$.

The first and last element of each variable vector should match the range of the variable, where experimental data is available. The effect vectors are the values of the unknown effects $f_i(v_i)$ evaluated at the elements of the variable vector $\boldsymbol{v}_i$.

The variable vectors make up the grid $(\boldsymbol{v}_1 \times \cdots \times \boldsymbol{v}_D)$. Evaluating Equation (B.2) on the grid and arranging the values in the model tensor $\mathcal{T}$ yields

$$\mathcal{T} = \left.\frac{\mathrm{d}\alpha}{\mathrm{d}t}\right|_{\boldsymbol{v}_1 \times \cdots \times \boldsymbol{v}_D} = \boldsymbol{f}_1 \otimes \cdots \otimes \boldsymbol{f}_D \,. \tag{B.5}$$

Because of the multiplication of the effects in Equation (B.2), the model tensor $\mathcal{T}$ can be expressed as the outer product $\otimes$ of the effect vectors.

A D-dimensional tensor is rank-1 if it can be written as the outer product of D vectors. Consequently, $\mathcal{T}$ is by definition rank-1. This rank-1 structure can be exploited to find the unknown effects $f_i(v_i)$. In Paper 2 we proposed to use the dataset from Equation (B.3) to populate a data tensor. Then, the rank-1 approximation of this data tensor can be computed with a non-linear optimization algorithm that minimizes the deviation between the model tensor and the data tensor. The result are the effect vectors $\boldsymbol{f}_i$, which correspond to the effects $f_i(v_i)$ and can be interpreted in terms of the kinetic model.

In the first study where we applied the TensorNPK method (Paper 5) we found that the projection of the dataset onto the data tensor introduces a significant error if data points lie in-between the grid points $(\boldsymbol{v}_1 \times \cdots \times \boldsymbol{v}_D)$, which happens frequently in real world datasets. To prevent the error introduced by the projection of the data onto the data tensor, the projection step has to be eliminated (Paper 3). Consequently, there is no data tensor, which means that no deviation between tensor elements can be calculated. Instead, the deviation must be calculated at the data points. To do that, the value of the unknown effects $f_i(v_i)$ at the position of the data points $v_{k,i}$ must be approximated by interpolation of the effect vectors.

For the interpolation, polynomials of any order p can be used. To compute the interpolation coefficients $p+1$ elements of the variable vector $\boldsymbol{v}_i$ around $v_{k,i}$ need to be selected. The indices of these grid points are denoted $j_i^{\ddagger}, \dots, j_i^{\ddagger} + p$. Using the

Vandermonde matrix $\boldsymbol{V}$ the interpolation can formally be written as

$$\begin{aligned} f_i(v_{k,i}) &\approx \begin{bmatrix} 1 & v_{k,i} & \dots & v_{k,i}^p \end{bmatrix} \boldsymbol{V}(v_{i,j_i^\ddagger}, \dots, v_{i,j_i^\ddagger+p})^{-1} \begin{bmatrix} f_{i,j_i^\ddagger} \\ \vdots \\ f_{i,j_i^\ddagger+p} \end{bmatrix} = \\ &= \begin{bmatrix} \gamma_{k,i,j_i^\ddagger} & \cdots & \gamma_{k,i,j_i^\ddagger+p} \end{bmatrix} \begin{bmatrix} f_{i,j_i^\ddagger} \\ \vdots \\ f_{i,j_i^\ddagger+p} \end{bmatrix} = \boldsymbol{\gamma}_{k,i}^T \boldsymbol{f}_i \,, \end{aligned} \tag{B.6}$$

where $\boldsymbol{\gamma}_{k,i}$ is the interpolation vector that contains the interpolation coefficients γ_{k,i,j_i} at the positions corresponding to $j_i^\ddagger, \dots, j_i^\ddagger + p$ and zero otherwise. The interpolation operation is a linear operation regardless of the polynomial order.

Even though higher order polynomials could be used for the interpolation, I do not think that higher order polynomials would have an advantage over linear interpolation ($p = 1$). Nearest-neighbor extrapolation for data points outside the model grid might be useful to avoid negative values in some cases.

With the interpolation set up, the value of the conversion rate at the position of a data point can be approximated with

$$\left.\frac{\mathrm{d}\alpha}{\mathrm{d}t}\right|_{v_{k,1},\,\dots,\,v_{k,D}} = \prod_{i=1}^{D} f_i(v_{k,i}) \approx \prod_{i=1}^{D} \boldsymbol{\gamma}_{k,i}^T \boldsymbol{f}_i \,. \tag{B.7}$$

The goal of the optimization problem is to minimize the distance between the measured conversion rate R_k and the approximation in Equation (B.7) by selecting the values of the effect vectors $\boldsymbol{f}_i$ accordingly:

$$\underset{\boldsymbol{f}_1,\dots,\boldsymbol{f}_D}{\arg\min} \sum_k \left[\prod_{i=1}^{D} \boldsymbol{\gamma}_{k,i}^T \boldsymbol{f}_i - R_k \right]^2 \,. \tag{B.8}$$

This optimization problem has $\sum_{i=1}^{D} N_i$ unknown parameters. Strictly speaking, this is not a rank-1 approximation problem because the data tensor is not formed explicitly. Nonetheless, the goal is to find the rank-1 tensor that best approximates the data. Notice that the $\boldsymbol{\gamma}_{k,i}$ only depend on the position of the grid points and the data points (see Equation (B.6)). Because of this, they are constant throughout the optimization and can be pre-calculated to improve the performance.

Unfortunately, the scaling indeterminacy makes the optimization problem in Equation (B.8) ill-posed. If one $\boldsymbol{f}_i$ is multiplied by a factor and another $\boldsymbol{f}_i$ is divided by that factor, the deviation does not change. This optimization problem is singular with $D - 1$ degrees of freedom. One way to deal with this, is to use Tikhonov regularization, but that would require devising an algorithm for choosing the penalty parameter and also the solution might be distorted. Alternatively, a (soft) constraint could be used to link the $\boldsymbol{f}_i$ in some way. In this particular case, the surplus degrees of freedom can also be eliminated analytically. This is the approach that was employed in the TensorNPK algorithm.

By choosing a reference grid point $(j_1^*, \dots, j_D^*)$, the approximation in Equation (B.7) is changed to

$$\left.\frac{\mathrm{d}\alpha}{\mathrm{d}t}\right|_{v_{k,1},\,\dots,\,v_{k,D}} \approx \prod_{i=1}^{D} f_{i,j_i^*} \boldsymbol{\gamma}_{k,i}^T \frac{\boldsymbol{f}_i}{f_{i,j_i^*}} = K \prod_{i=1}^{D} \boldsymbol{\gamma}_{k,i}^T \boldsymbol{f}_i' \,. \tag{B.9}$$

Here, $K = \prod_{i=1}^{D} f_{i,j_i^*}$ is the global scaling factor and $\boldsymbol{f}_i' = \boldsymbol{f}_i / f_{i,j_i^*}$ are the normalized effect vectors. Now, the parameters for the optimization are the scaling factor K and the values of the normalized effect vectors f_{i,j_i}' except for the f_{i,j_i^*}', which are equal to 1 by definition. This optimization problem, the reduced problem, has $\sum_{i=1}^{D} N_i - D + 1$ unknowns and is well-posed.

The reduced optimization problem can be solved with any non-linear least squares algorithm. Most of these algorithms need the residuals and the Jacobian matrix as input, to solve the problem efficiently. The residuals are given by

$$\begin{aligned} \boldsymbol{r} &= [r_1, \dots, r_{N_{\mathrm{data}}}]^T \quad \text{with} \\ r_k &= K \prod_{i=1}^{D} \boldsymbol{\gamma}_{k,i}^T \boldsymbol{f}_i' - R_k \quad \text{and} \quad k \in [1, N_{\mathrm{data}}] \,. \end{aligned} \tag{B.10}$$

The Jacobian contains the partial derivatives of the residuals with respect to each optimization parameter:

$$\boldsymbol{J} = (\nabla \boldsymbol{r})^T \tag{B.11}$$

with

$$\frac{\partial r_k}{\partial f_{i,j_i}'} = \gamma_{k,i,j_i} \, K \prod_{\substack{i'=1 \\ i' \neq i}}^{D} \boldsymbol{\gamma}_{k,i'}^T \boldsymbol{f}_{i'}' \qquad \forall j_i \neq j_i^* \tag{B.12}$$

$$\frac{\partial r_k}{\partial K} = \prod_{i'=1}^{D} \boldsymbol{\gamma}_{k,i'}^T \boldsymbol{f}_{i'}' \,. \tag{B.13}$$

The Jacobian can typically get quite large. Specifically it has $(\sum_{i=1}^{D} N_i - D + 1) \times N_{\mathrm{data}}$ elements. Though, its very sparse and only contains $(D(p+1)+1)N_{\mathrm{data}}$ non-zero elements.

After the optimal parameters of the reduced problem are computed, the effect vectors must be found. For this, the value of K must be attributed to the f_{i,j_i^*}. In absence of a strict rule for how to divide K, it can simply be split equally $f_{i,j_i^*} = \sqrt[D]{K}$. The effect vectors are then given by

$$\boldsymbol{f}_i = f_{i,j_i^*} \boldsymbol{f}_i' \,. \tag{B.14}$$

If the model converged sufficiently well, the effect vectors $\boldsymbol{f}_i$ on the grid $\boldsymbol{v}_i$ can now be interpreted in terms of the effects $f_i(v_i)$.

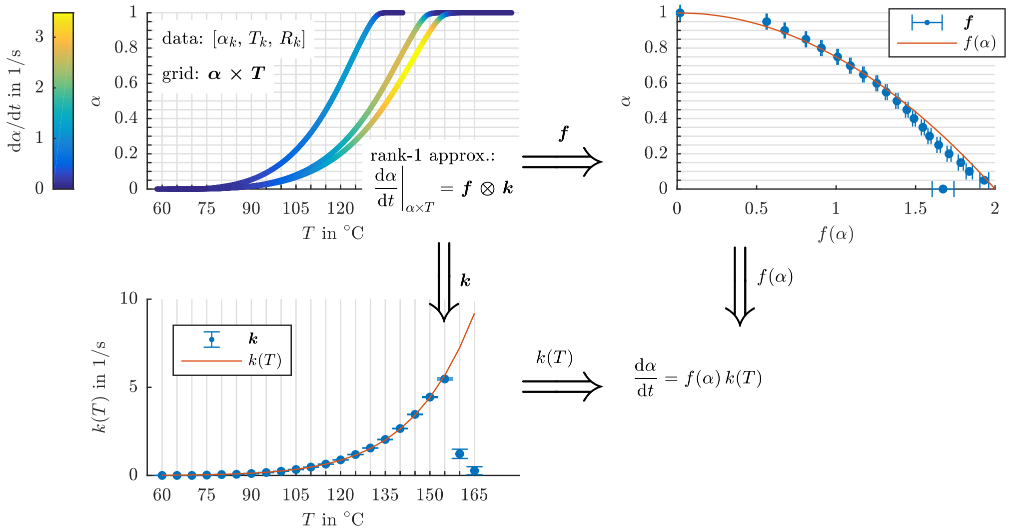

Figure B.1: *Illustration of the TensorNPK method for a 2-D model. Experimental data (top left) is used to identify the effect of conversion α (top right) and temperature T (bottom).*

B.2 Illustration of working principle in two dimensions

In this section I will try to present the TensorNPK method in a way that is easier to comprehend than the plain math in the previous section. To illustrate how the TensorNPK method works, I will use a simple two-dimensional example where the conversion rate is modeled with the General Kinetic Equation (GKE) as a function of conversion α and temperature T.

For this example I will use a data set with three constant-heating-rate measurements of a decomposition reaction. The data set consists of various data points k with conversion, temperature and conversion rate values. Formally, the data set can be expressed as

$$[\alpha_k,\, T_k,\, R_k] \quad \text{with} \quad k \in [1, N_{\text{data}}]\,. \tag{B.15}$$

To wrap your head around how the algorithm works, it might help to interpret everything geometrically. Imagine that each independent variable in the GKE is a direction in D-dimensional space. In this example we have two dimensions: α and T. Then $[\alpha_k,\, T_k]$ are the "coordinates", where the conversion rate values R_k have been measured. This point cloud is illustrated in the top left diagram in Figure B.1, where the conversion rate is plotted at the corresponding conversion and temperature values. The data points in this data set are so close together that they appear as lines and the reaction trajectories of each of the three measurements are clearly visible.

The model that we are going to employ is the GKE with a conversion and a temperature term

$$\frac{d\alpha}{dt} = f(\alpha)\,k(T)\,, \tag{B.16}$$

where the effects of conversion $f(\alpha)$ and temperature $k(T)$ are unknown. We want to find the model that best fits the data, i.e. the model with the smallest deviation between the predicted and the measured conversion rate. This condition can be written as

$$\min \sum_k \left[\, f(\alpha_k)\, k(T_k) - R_k \right]^2 . \tag{B.17}$$

Because $f(\alpha)$ and $k(T)$ are unknown (and we do not want to make any wild assumptions), they need to be approximated.

The TensorNPK method needs a grid, on which the calculations are performed. So the next step is to select an “axis” for each dimension. Formally we write

- $\boldsymbol{\alpha} = [\alpha_1, \alpha_2, \dots]^T$ with the corresponding effect vector $\boldsymbol{f} = [f(\alpha_1), f(\alpha_2), \dots]^T$ and
- $\boldsymbol{T} = [T_1, T_2, \dots]^T$ with the corresponding $\boldsymbol{k} = [k(T_1), k(T_2), \dots]^T$.

The grid must match the range where experimental data is available. Here, I selected $\boldsymbol{\alpha} = [0, 0.05, 0.1, \dots, 1]^T$ and $\boldsymbol{T} = [60, 65, 70, \dots, 165\,°\mathrm{C}]^T$. In Figure B.1 this grid is illustrated with grey grid lines.

On this $\boldsymbol{\alpha} \times \boldsymbol{T}$ grid, we evaluate Equation (B.16)

$$\begin{aligned} \left.\frac{\mathrm{d}\alpha}{\mathrm{d}t}\right|_{\boldsymbol{\alpha}\times\boldsymbol{T}} &= \begin{array}{c|ccc} & T_1 & T_2 & \cdots \\ \hline \alpha_1 & f(\alpha_1)\,k(T_1) & f(\alpha_1)\,k(T_2) & \cdots \\ \alpha_2 & f(\alpha_2)\,k(T_1) & f(\alpha_2)\,k(T_2) & \cdots \\ \vdots & \vdots & \vdots & \ddots \end{array} = \\ &= \begin{bmatrix} f(\alpha_1) \\ f(\alpha_2) \\ \vdots \end{bmatrix} \begin{bmatrix} k(T_1) & k(T_2) & \cdots \end{bmatrix} = \boldsymbol{f} \otimes \boldsymbol{k} \end{aligned} \tag{B.18}$$

In this two-dimensional example it is easy to see that the model matrix can be expressed as the outer product of the effect vectors, i.e. that the model matrix is rank-1 by definition. In non-parametric modeling, this rank-1 structure is exploited to identify the effect vectors $\boldsymbol{f}$ and $\boldsymbol{k}$ without any assumptions about the unknown effects $f(\alpha)$ and $k(T)$. Basically, the algorithm correlates the change of conversion rate with the axes that it received as input.

The effect vectors are shown in the right and the bottom diagram in Figure B.1. They can be used to compute kinetic predictions without any further post-processing or they can be interpreted in terms of the kinetic model. The most common analysis are to identify the most likely reaction model $f(\alpha)$ from $\boldsymbol{f}$ over $\boldsymbol{\alpha}$ and to fit the Arrhenius equation to $\boldsymbol{k}$ over $\boldsymbol{T}$. This is illustrated in the right and the bottom diagram of Figure B.1 and in the bottom right quadrant.

B.3 Residuals and variances

Once the model has been derived from the data set, i.e. once the solution of the optimization problem has been computed, the output must be evaluated in some way. In model fitting, this is usually done by evaluating the residuals and the variances of the parameters. Here, some aspects of interpreting residuals in the context of the TensorNPK method are discussed and formulas for estimating various variances are presented. These variances are not only useful for evaluating the model, they can also be used as weights for model fitting during post processing.

The basis for the equations presented here, are the equations in Appendix B.1. The optimization problem outlined in that section can be solved with any non-linear optimization algorithm by using the residuals $\boldsymbol{r}$ in Equation (B.10) and the Jacobian $\boldsymbol{J}$ in Equation (B.11). In addition we consider a weight matrix $\boldsymbol{W}$ for the data points. If no weighting is required, $\boldsymbol{W}$ can be set equal to the identity matrix.

After computing the solution of the optimization problem, the variance-covariance matrix $\boldsymbol{D}$ of the parameters at the solution can be estimated with

$$MSE = \frac{\boldsymbol{r}^T \boldsymbol{W} \boldsymbol{r}}{N_{\text{data}} - \left(\sum_{i=1}^{D} N_i - D + 1\right)} \tag{B.19}$$

and

$$\boldsymbol{D} = MSE \left(\boldsymbol{J}^T \boldsymbol{W} \boldsymbol{J}\right)^{-1} . \tag{B.20}$$

The main diagonal of $\boldsymbol{D}$ contains the variances of the parameters $\mathrm{Var}(f'_{i,j_i})$ for all $j_i \neq j_i^*$ and $\mathrm{Var}(K)$.[7] The column corresponding to K also contains the covariances $\mathrm{Cov}(f'_{i,j_i}, K)$. These values can be used to estimate the variance of the effect vector values by assuming linear error propagation:

$$\frac{\mathrm{Var}(f_{i,j_i})}{f_{i,j_i}^2} = \begin{cases} \dfrac{\mathrm{Var}(K)}{K^2} & \text{for } j_i = j_i^* \\ \dfrac{\mathrm{Var}(K)}{K^2} + \dfrac{\mathrm{Var}(f'_{i,j_i})}{f'^2_{i,j_i}} + 2\dfrac{\mathrm{Cov}(f'_{i,j_i}, K)}{f'_{i,j_i} K} & \text{for } j_i \neq j_i^* \end{cases} . \tag{B.21}$$

Since this equation is prone to division by zero, the following form that exploits Equation (B.14) should be used to perform the calculations.

$$\mathrm{Var}(f_{i,j_i}) = \begin{cases} \dfrac{f_{i,j_i}^2}{K^2} \mathrm{Var}(K) & \text{for } j_i = j_i^* \\ \dfrac{f_{i,j_i}^2}{K^2} \mathrm{Var}(K) + {f_{i,j_i^*}}^2 \mathrm{Var}(f'_{i,j_i}) + 2\dfrac{f_{i,j_i} f_{i,j_i^*}}{K} \mathrm{Cov}(f'_{i,j_i}, K) & \text{for } j_i \neq j_i^* \end{cases} . \tag{B.22}$$

These variances convey important information about the quality of the model. An effect is significant if the values of the corresponding effect vector are significantly different from each other, i.e. if their confidence intervals do not overlap. Values, where the confidence interval intersects with zero, are very unreliable and the model should not be

---

[7] The estimated variances can get quite small — probably because of the large number of data points in a typical data set. A possible solution to these unrealistically small variances would be to consider Effective Degrees of Freedom or to incorporate the correlation of data points by using Generalized Least Squares. Unfortunately I did not get around to look into this.

evaluated in this variable range. If this variable range is relevant for the application of the model, additional experimental data is required. In case of scattering values with small confidence intervals over-fitting or an inconsistent data set might be the issue.

Another important indicator of the model quality are the residuals, which are the difference between the conversion rate R_k and the model estimate for this data point

$$\hat{R}_k = \prod_{i=1}^{D} \boldsymbol{\gamma}_{k,i}^T \boldsymbol{f}_i \,. \tag{B.23}$$

The residuals should be normally distributed and they should scatter similarly in each dimension. Systematic deviations in any dimension might point toward deviations of the experimental data from the General Kinetic Equation.

The variance of the conversion rate estimate can be estimated with

$$\mathrm{Var}(\hat{R}_k) = \sum_{i=1}^{D} \left(\hat{R}_k^{\setminus i}\right)^2 \boldsymbol{\gamma}_{k,i}^T \,\mathrm{diag}\left(\mathrm{Var}(\boldsymbol{f}_i)\right) \boldsymbol{\gamma}_{k,i} \,, \tag{B.24}$$

where $\mathrm{Var}(\boldsymbol{f}_i)$ is the vector $[\mathrm{Var}(f_{i,1}), \cdots, \mathrm{Var}(f_{i,N_i})]^T$ according to Equation (B.21) and $\hat{R}_k^{\setminus i}$ is the estimate for the data point k excluding the effect of variable i (symbolized by the set-difference operator $\setminus$)

$$\hat{R}_k^{\setminus i} = \prod_{\substack{i'=1 \\ i' \neq i}}^{D} \boldsymbol{\gamma}_{k,i'}^T \boldsymbol{f}_{i'} \,. \tag{B.25}$$

When an effect vector is used in post-processing to perform model fitting — e.g. to determine the Arrhenius parameters from the temperature effect vector — an issue that I came across was that the confidence interval of the estimated parameters depended on the number of grid points in that dimension. This is, of course, an undesired property. A way to work around this issue is to project the experimental conversion rate values into dimension i and to use these values instead of the effect vector $\boldsymbol{f}_i$. These projected values can be calculated by using the model estimate excluding the effect of variable i

$$\hat{f}_{k,i} = \frac{R_k}{\hat{R}_k^{\setminus i}} \,. \tag{B.26}$$

The variance of $\hat{f}_{k,i}$ can be estimated with

$$\mathrm{Var}(\hat{f}_{k,i}) = \left(\frac{1}{\hat{R}_k^{\setminus i}}\right)^2 \left[\mathrm{Var}(R_k) + (\hat{f}_{k,i})^2 \,\mathrm{Var}(\hat{R}_k^{\setminus i})\right] , \tag{B.27}$$

where

$$\mathrm{Var}(\hat{R}_k^{\setminus i}) = \sum_{\substack{i'=1 \\ i' \neq i}}^{D} \left(\hat{R}_k^{\setminus i,i'}\right)^2 \boldsymbol{\gamma}_{k,i'}^T \,\mathrm{diag}\left(\mathrm{Var}(\boldsymbol{f}_{i'})\right) \boldsymbol{\gamma}_{k,i'} \,. \tag{B.28}$$

B.4 Counteracting over-fitting with penalized regression

On some sparse, unequally distributed data sets, the TensorNPK method turned out to be sensitive to the placement of the grid points $\boldsymbol{v_i}$. Instead of deciding where exactly to place the grid points, it would be much more convenient to just place many grid points and let the algorithm figure out the rest. Unfortunately, placing too many grid points leads to over-fitting and consequently poor results.

To counteract over-fitting and improve the TensorNPK method's performance on certain data sets, penalized regression seems to be a good solution. With penalized regression, the minimization problem of fitting the model to the data is extended by a penalty term that enforces certain characteristics of the solution.

$$\min \sum_k \left(\hat{R}_k - R_k \right)^2 + \sum_i \lambda_i^2 \|\boldsymbol{\Gamma}_i \boldsymbol{f}_i\|^2 . \tag{B.29}$$

Here, the first sum is the deviation between the model estimate and the conversion rate data and the second sum is the penalty. $\boldsymbol{\Gamma}_i$ is the penalty matrix. It determines, which feature of the solution is penalized. Here, a second-order finite-difference matrix is used to penalize the curvature of the solution. λ_i is a penalty parameter that determines the relative weight of model deviation and the penalty term. The larger λ_i the more the algorithm prioritizes smoothness over goodness of fit.

The main challenge is to choose the λ_i correctly. If they are too small, the model performance is poor because of over-fitting. If they are too large, the model will fit the data poorly. Also, it will lead the algorithm to underestimate the variance of the solution values, which may cause the impression that the model is fitting the data better than it actually does. Cross validation can be used to select optimal λ_i.

Penalized regression can be thought of as helping the optimization algorithm to find the "correct" solution instead of just the numerically best fit to the data. With the right strategy, penalized regression has a lot of potential to improve the performance of the TensorNPK method by enforcing certain features of the solution such as smoothness. Though, these strategies have yet to be developed.

About the author

Felix Birkelbach was born in Vienna, Austria in 1989. After finishing the high-school for electrical engineering (HTL) in Wr. Neustadt in 2009 he started working at Ac^{2}t research GmbH as a technician in the research group for electrical contacts. Soon after, in 2010 he entered the TU Wien to study Mechanical Engineering – Management, specializing in Advanced Energy Systems and Risk Management. He continued working part-time at Ac^{2}t research GmbH as Junior Scientist until 2015. During his studies he did exchange semesters at the Northeastern University in Boston, MA and the Universidad Polytécnica de Madrid in Spain. In 2016 he graduated with distinction.

His interest in energy technology led him to pursue a PhD at the Institute for Thermodynamics and Energy Systems at TU Wien, where he did research on thermochemical energy storage in the research projects SolidHeat Kinetics, Tes4seT and SolidHeat Pressure. This thesis is based on that research.

A list of his publications can be found at https://orcid.org/0000-0003-4928-6209.